

**Dynamics of Mixed *Pseudomonas putida* Populations  
under Neutral and Selective Growth Conditions**



**Dissertation**

**Felix Becker**

**2018**

# **Dynamics of Mixed *Pseudomonas putida* Populations under Neutral and Selective Growth Conditions**



## **Dissertation**

der Fakultät für Biologie

der Ludwig-Maximilians-Universität München

vorgelegt von

**Felix Becker**

**München, September 2018**

Diese Dissertation wurde angefertigt  
unter der Leitung von Herrn Prof. Dr. Heinrich Jung  
im Bereich der Mikrobiologie  
an der Ludwig-Maximilians-Universität München

Erstgutachter: Prof. Dr. Heinrich Jung

Zweitgutachter: Prof. Dr. Marc Bramkamp

Tag der Abgabe: 20.09.2018

Tag der mündlichen Prüfung: 06.12.2018

## **Eidesstattliche Versicherung und Erklärung**

Hiermit versichere ich an Eides statt, dass die vorliegende Dissertation von mir selbständig und ohne unerlaubte Hilfe angefertigt wurde. Zudem wurden keine anderen als die angegebenen Quellen verwendet.

Außerdem versichere ich, dass die Dissertation keiner anderen Prüfungskommission vorgelegt wurde und ich mich nicht anderweitig einer Doktorprüfung ohne Erfolg unterzogen habe.

München, 20.09.2018

Felix Becker

## **Statutory declaration and statement**

I declare that I have authored this thesis independently, that I have not used other than the declared sources/resources. As well I declare that I have not submitted a dissertation without success and not passed the oral exam. The present dissertation (neither the entire dissertation nor parts) has not been presented to another examination board.

München, 20.09.2018

Felix Becker

---

## Table of contents

<b>Abbreviations.....</b>	<b>I</b>
<b>List of publications.....</b>	<b>II</b>
<b>Contributions to publications presented in this thesis.....</b>	<b>III</b>
<b>Declaration of contributions about shared co-authorship in Chapter III.....</b>	<b>IV</b>
<b>Summary.....</b>	<b>V</b>
<b>Zusammenfassung.....</b>	<b>VII</b>
<b>Chapter I — Introduction.....</b>	<b>1</b>
1.1. Theoretical aspects about cooperation and its dilemma.....	2
1.2. Cooperative interactions in microbial systems.....	4
1.3. Uptake of the essential element iron by public good-siderophores.....	6
1.4. Social interactions mediated via siderophores might overcome the dilemma of cooperators.....	12
1.5. Simpson’s paradox and theoretical cooperation models of growing populations.....	15
1.6. Thesis objective.....	18
<b>Chapter II.....</b>	<b>20</b>
Non-Selective Evolution of Growing Populations	
<b>Chapter III.....</b>	<b>34</b>
Interactions mediated by a public good transiently increase cooperativity in growing <i>Pseudomonas putida</i> metapopulations	
<b>Chapter IV — Concluding Discussion.....</b>	<b>56</b>
4.1. Important features for the metapopulation studies.....	57
4.2. Non-selective growth of the metapopulation.....	58
4.3. The importance of initial cell number.....	59
4.4. Choice of constitutive cooperator to simplify social interactions mediated by pyoverdine.....	60
4.5. Selective growth and the development of cooperative interactions.....	62
4.6. Impact of environmental conditions on public good mediated interactions.....	65
4.7. Pyoverdine-mediated social interactions in nature and their practical usage.....	69
4.8. Outlook.....	71
<b>References of Chapter I and Chapter VI.....</b>	<b>74</b>
<b>Acknowledgments.....</b>	<b>83</b>
<b>Curriculum Vitae.....</b>	<b>84</b>

---

## Abbreviations

ABC	ATP-binding cassette
AHL	N-acylated homoserine lactone
C	Cooperator
CAA	Casamino acids
cfu	Colony forming units
CM	Cytoplasmic membrane
D	Defector
DNA	Deoxyribonucleic acid
DP	2,2'-dipyridyl
ECF	Extracytoplasmic function
Fur	Ferric uptake regulator
IM	Inner membrane
$K_a$	Affinity coefficient
KB	King's B
M	Molarity ( $\text{mol} \cdot \text{L}^{-1}$ )
$\mu$	Growth rate
N	Cell number
NRPS	Nonribosomal peptide-synthetases
$\text{OD}_x$	Optical density at the wavelength of x nm
OM	Outer membrane
P	Promoter
PCR	Polymerase chain reaction
PVD	Pyoverdine
RNA	Ribonucleic acid
t	Time
V	Volume
x	Cooperator/producer fraction
$\bar{x}$	Global cooperator/producer fraction

## List of publications

### Publications presented in this thesis:

#### Chapter II

Wienand, K.\*, Lechner, M.\*, **Becker, F.\***, Jung, H., Frey, E. (2015) Non-Selective Evolution of Growing Populations. *PLoS ONE* **10**(8): e0134300. doi:10.1371/journal.pone.0134300

\* These authors contributed equally to this work

#### Chapter III

**Becker, F. \***, Wienand, K. \*, Lechner, M., Frey, E., and Jung, H. (2018) Interactions mediated by a public good transiently increase cooperativity in growing *Pseudomonas putida* metapopulations. *Scientific Reports* **8**: 4093.

\* These authors contributed equally to this work

## Contributions to publications presented in this thesis

### Chapter II

Heinrich Jung and Felix Becker conceived, designed and performed the experiments (Felix Becker designed and performed non-selective growth experiments and experiments for supplementary information). Felix Becker, Heinrich Jung, Matthias Lechner, Karl Wienand and Erwin Frey analyzed the data (Felix Becker analyzed data of biological experiments). Erwin Frey, Matthias Lechner and Karl Wienand contributed reagents, materials and analysis tools and designed theoretical analysis. Matthias Lechner and Karl Wienand performed theoretical analysis. Erwin Frey, Heinrich Jung, Matthias Lechner and Karl Wienand wrote the paper.

### Chapter III

Felix Becker and Heinrich Jung designed and performed the experiments (Felix Becker constructed the strain KP1 and designed and performed metapopulation experiments under selective conditions and the experiments examining the basics of the public good system). Karl Wienand, Matthias Lechner and Erwin Frey designed and performed theoretical analysis. Felix Becker, Karl Wienand, Matthias Lechner, Erwin Frey and Heinrich Jung analyzed the experimental and computational data (Felix Becker analyzed results of the lab results). Karl Wienand, Matthias Lechner, Erwin Frey, Felix Becker and Heinrich Jung wrote the paper (Felix Becker wrote Material and Methods of biological experiments and helped with biological part of introduction, result and discussion).

Felix Becker

Prof. Dr. Heinrich Jung

## Declaration of contributions about shared co-authorship in Chapter III

Felix Becker:

Felix Becker constructed the strain KP1 (procedure see Material and Methods), designed and performed the metapopulation experiments under selective conditions (**Fig. 5** and experimental results of **Fig. 6**; initial conditions see **Fig. S3**) and the experiments examining the basics of the public good system (**Fig. 2b**, **Fig. 3**, **Fig S1**, **Fig S2** and **Table S1**). He analyzed the experimental results and made the biological results. He wrote Material and Methods of biological experiments and helped with biological part of Introduction, Results and Discussion.

Karl Wienand:

Karl Wienand designed and performed theoretical analysis and analyzed the computational data (outcomes of simulations see **Fig. 4** and **Fig. 6**; equations and assumptions of the theoretical model are found in Results and Supplementary text). He was the major writer of Introduction, Result, Discussion and Supplementary text and included and formatted all corrections, additions and suggestions from the other authors.

Felix Becker

Dr. Karl Wienand

## Summary

In nature, bacteria live together in complex populations. There, it can have either neutral effects as genetic drift under non-selective conditions or social interactions, e.g cooperativity, under selective conditions. Under selective conditions some bacteria invest into a cooperative trait. This investment is costly but is of benefit for the whole population including defectors, which do not have this cooperative trait. The cooperators are in a dilemma, because the defectors have a selection advantage, but this cooperative trait is also essential for the whole population. In order to prevent an extinction of these essential cooperative bacteria and following collapse of the whole population, cooperative interactions are indispensable. One microbial system to analyze the development of cooperativity is the production of a common good. Here, cooperative bacteria produce extracellular compounds and an example is siderophores, a group of iron scavenging molecules including pyoverdine, the primary siderophore of fluorescent pseudomonads. These are needed for growth under iron limitation and are stable over long time periods. Pyoverdine production can be regulated according to pyoverdine or iron concentrations in the environment. The cooperativity can be examined in a metapopulation approach containing of many subpopulations. This leads to multi-level selection, where inside subpopulations defectors have a selection advantage and will increase in ratio over time. But, there is also selection between subpopulations, where subpopulations with higher initial cooperator fractions grow to higher cell densities in the same time period. The interplay of both selections could result into an increase of the cooperator fraction of the metapopulation. This increase would be in agreement with the statistical phenomenon Simpson's paradox, observing a reversed trend between subpopulations and the metapopulation consisting of all subpopulations. To obtain such a scenario, a stochastic distribution of initial cooperator fraction between subpopulations is necessary.

The focus of the first part of this thesis was on the non-selective evolution of growing *Pseudomonas putida* populations consisting of cooperators and defectors. Non-selective evolution was previously mainly researched in populations with constant size. There, the populations fixate to either cooperators or defectors due to effects like genetic drift. To examine non-selective evolution of microbial populations with increasing population size, co-cultures with random initial cell numbers and cooperator fractions were generated via Poisson dilution. To obtain conditions for non-selective evolution, a medium was used with high iron concentrations. This leads to a downregulation of pyoverdine production of the wildtype *P. putida* KT2440 cooperator and to equal growth rates of cooperators and defectors. This experimental procedure resulted in a conservation of initial cooperator fraction during exponential growth phase. These results are in agreement with theoretical predictions based on the Pólya urn model. This shows, that non-selective evolution of exponentially growing populations prevents fixation caused from genetic drift and plays an important role in maintaining coexistence of cooperators and defectors.

In the second part, the cooperative interactions of co-cultures of *P. putida* cooperators and defectors were analyzed under selective conditions, strict iron limitation, as well as the central role of pyoverdine in mediating them. Hereby, the constitutive cooperator KP1 was used in order to avoid adaption of pyoverdine production to iron availability. Pyoverdine as common good was often used for theoretical models dealing with the dilemma of cooperators. However, previous models underestimated the impact of specific biochemical dynamics of pyoverdine on the social interactions. To identify these specific dynamics, the pyoverdine concentration dependent growth stimulation of defectors was examined under strict iron limitation and both a threshold and saturation concentration was identified. Furthermore, the cost and benefit of cooperative behavior was experimentally distinguished and all these results were implemented into a theoretical model. A systems biology metapopulation approach was developed with stochastic distribution of initial cooperator fraction and with higher initial cell densities compared to previous studies with Poisson dilution. Here, a transient increase of cooperativity was observed in the first hours of exponential growth under strict iron limitation. This result was supported by the model based on the basics of the system and biochemical properties of pyoverdine. In contrast to previous studies it could be shown that specific biochemical dynamics of common goods play a key role in mediating cooperative interactions.

To sum up, this thesis outlines that exponential growth under non-selective conditions lead to a stable coexistence of *P. putida* co-cultures consisting of cooperators and defectors. Moreover, under selective conditions, in the metapopulation a transient increase of cooperativity mediated by the common good pyoverdine was observed. Here, the impact of specific biochemical dynamics of pyoverdine was highlighted in mediating cooperative interactions.

## Zusammenfassung

In der Natur leben Bakterien in komplexen Gesellschaften zusammen. Dort können entweder neutrale Effekte wie Gendrift unter nichtselektiven Bedingungen oder soziale Interaktionen, z. B. Kooperativität, unter selektiven Bedingungen vorliegen. Unter selektiven Bedingungen investieren einige Bakterien in eine kooperative Eigenschaft. Dieses Investment ist kostspielig, aber von diesem profitiert die ganze Population inklusive Defektoren, die die kooperative Eigenschaft nicht besitzen. Die Kooperatoren befinden sich in einem Dilemma, weil Defektoren einen Selektionsvorteil haben, aber die kooperative Eigenschaft überlebenswichtig für die komplette Population ist. Um ein Aussterben dieser essentiellen Bakterien und folgenden Zusammenbruch der gesamten Population zu verhindern, sind kooperative Interaktionen unerlässlich. Die Produktion eines Allgemeingutes ist ein Beispiel eines mikrobiellen Systems mit dem man die Entwicklung von Kooperativität untersuchen kann. Hier produzieren kooperative Bakterien extrazelluläre Verbindungen und ein Beispiel sind die Siderophore, eine Gruppe von Eisenchelatoren zu welcher Pyoverdin, das primäre Siderophor fluoreszierender Pseudomonaden, gehört. Diese werden für das Wachstum unter eisenlimitierenden Bedingungen benötigt und sind über lange Zeiträume stabil. Die Pyoverdinproduktion kann in Abhängigkeit zur Pyoverdin- oder Eisenkonzentration in der Umgebung reguliert werden. Die Kooperativität kann in einem Metapopulationsansatz bestehend aus vielen Subpopulationen untersucht werden. Hier gibt es Selektion auf mehreren Ebenen, wobei in Subpopulationen Defektoren einen Selektionsvorteil haben und somit ihr Anteil über die Zeit zunimmt. Aber es gibt auch eine Selektion zwischen Subpopulationen, bei welcher Subpopulationen mit höherem Startkooperatorenanteil zu höheren Zelldichten in der gleichen Zeitperiode wachsen. Das Zusammenspiel beider Selektionen könnte in einer Zunahme des Kooperatorenanteils der Metapopulation resultieren. Diese Zunahme wäre in Übereinstimmung mit dem statistischen Phänomen Simpsons Paradoxon, bei welchem ein umgekehrter Trend zwischen Subpopulationen und der Metapopulationen bestehend aus allen Subpopulationen beobachtet wird. Um solch ein Szenario zu erreichen, braucht es eine stochastische Verteilung des Startkooperationenanteils zwischen den Subpopulationen.

Im ersten Teil der Dissertation war der Fokus auf der nichtselektiven Evolution von wachsenden aus Kooperatoren und Defektoren bestehenden *Pseudomonas putida* Ko-Kulturen. Nichtselektive Evolution wurde bisher vor allem nur bei Populationen mit konstanter Größe erforscht. Dabei übernehmen entweder Kooperatoren oder Defektoren aufgrund von Effekten wie Gen-Drift die komplette Population. Um die nichtselektive Evolution von mikrobiellen Populationen mit zunehmender Gruppengröße zu untersuchen, wurden Ko-Kulturen mit zufälliger Startzellzahl und zufälligem Startkooperatorenanteil mittels Poisson-Verdünnung generiert. Für passende Bedingungen hinsichtlich nichtselektiver Evolution wurde ein Medium mit hoher Eisenkonzentration benutzt. Dies führt zur Herunterregulierung der Pyoverdinproduktion unseres Wildtypkooperators *P. putida* KT2440

und zu gleichen Wachstumsraten von Kooperatoren und Defektoren. Diese experimentelle Vorgehensweise führte zu einer Konservierung des Startkooperatorenanteils während der exponentiellen Wachstumsphase. Diese Resultate passen zu theoretischen Vorhersagen basierend auf dem Pólya-Urnenmodell. Dies zeigt, dass nichtselektive Evolution von exponentiell wachsenden Populationen die Fixierung hinzu einer Spezies, welche durch Gen-Drift verursacht wird, verhindert und eine wichtige Rolle bei der Aufrechterhaltung der Koexistenz von Kooperatoren und Defektoren spielt.

Im zweiten Teil wurden kooperative Interaktionen unter selektiven Bedingungen, d. h. starke Eisenlimitierung, zwischen Ko-Kulturen von *P. putida* Kooperatoren und Defektoren sowie die zentrale Rolle von Pyoverdin in der Mediation dieser analysiert. Hierbei wurde der konstitutive Kooperator KPI benutzt, um eine Anpassung der Pyoverdinproduktion an die Eisenverfügbarkeit zu verhindern. Pyoverdin als Allgemeingut wurde oft für theoretische Modelle verwendet, die sich um das Dilemma von Kooperatoren kümmern. Jedoch unterschätzten vorherige Modelle den Einfluss spezieller biochemischer Dynamiken von Pyoverdin auf die sozialen Interaktionen. Um die speziellen Dynamiken zu identifizieren, wurden die pyoverdinkonzentrationsabhängige Wachstumssimulation von Defektoren unter starker Eisenlimitierung untersucht und es wurde sowohl eine benötigte Minimalkonzentration für eine Stimulation als auch eine Konzentration, ab welcher eine Sättigung der Wachstumsstimulation vorliegt, identifiziert. Zudem wurden experimentell die Kosten und der Nutzen der kooperativen Eigenschaft bestimmt und alle Resultate in ein theoretisches Modell implementiert. Ein systembiologischer Metapopulationsansatzes mit stochastisch verteilten Startkooperatorenanteilen wurde entwickelt, welcher höhere Startzellkonzentrationen verglichen zu vorherigen Studien mit der Poisson-Verdünnung besaß. Hier wurde ein transienter Anstieg der Kooperativität in den ersten Stunden der exponentiellen Wachstumsphase bei strenger Eisenlimitierung beobachtet. Dieses Ergebnis wurde durch das Modell unterstützt, welches auf den Grundlagen des Systems und dem biochemischen Eigenschaften von Pyoverdin basierte. Im Unterschied zu vorherigen Studien konnte gezeigt werden, dass die speziellen biochemischen Dynamiken von Allgemeingütern eine Schlüsselrolle bei der Mediation von kooperativen Interaktionen spielen.

Zusammenfassend stellt diese Dissertation heraus, wie exponentielles Wachstum unter nichtselektiven Bedingungen zu einer stabilen Koexistenz von *P.putida* Ko-Kulturen bestehend aus Kooperatoren und Defektoren führt. Darüber hinaus wurde ein transienter Anstieg der Kooperativität in unserer Metapopulation unter selektiven Bedingungen mit Pyoverdin als Allgemeingut beobachtet. Hier wurde dargestellt, welche wichtigen Einfluss die speziellen biochemischen Dynamiken des Pyoverdins bei der Mediation kooperativer Interaktionen besitzen.

## **Chapter I**

### **Introduction**

# CHAPTER I

## 1. Introduction

Cooperativity plays an important role in the social behavior of bacteria in complex ecosystems (Crespi, 2001, Velicer, 2003, West & Cooper, 2016, West et al., 2006). One example is multi-species biofilms in nature, which are generally seen as the common ecosystem of cooperating bacteria under natural conditions (Nadell et al., 2016, Flemming et al., 2016). The cooperative interaction examined in this thesis is the production of a public good, specifically the siderophore pyoverdine produced by *Pseudomonas putida*, which is of benefit for the whole population. A central question in these public good systems is how the producers can withstand invasion by defectors that do not need to pay the production costs and therefore have a growth advantage. If natural selection were the only process at work, this advantage would cause the producers to go extinct, which could lead to a collapse of the entire population. Properties or behaviors supporting cooperativity are indispensable for preventing such a scenario, especially in environments with high selective pressure, for example under harsh or changing environmental conditions.

### 1.1. Theoretical aspects about cooperation and its dilemma

The understanding of cooperative behavior, both in bacteria and higher organisms, has been a challenge in evolutionary theory since Darwin (Axelrod & Hamilton, 1981). Humans are seen as the “champions of cooperation”, because in all societies in human evolution, cooperation was the decisive organizational principle (Nowak, 2006). Further examples include symbioses between rhizobia and legumes, the light organs of squids and the interplay of animal pollinators with nectar-producing flowers (Sachs et al., 2004). The dilemma of cooperation or cooperators is, that some individuals (the producers or cooperators, C) carry out a cooperative behavior by paying a cost, while others (the so called free riders or defectors, D) are receiving a benefit without investing anything (Hamilton, 1963, Hamilton, 1964b, Hamilton, 1964a, Nowak, 2006). Populations of cooperators can easily be exploited by the occurrence of defectors (for example via mutation), which have a higher average fitness in mixed populations. In order to prevent the extinction of cooperators and the collapse of the whole population, the system needs properties or behaviors supporting cooperation (**Fig. I.1**).

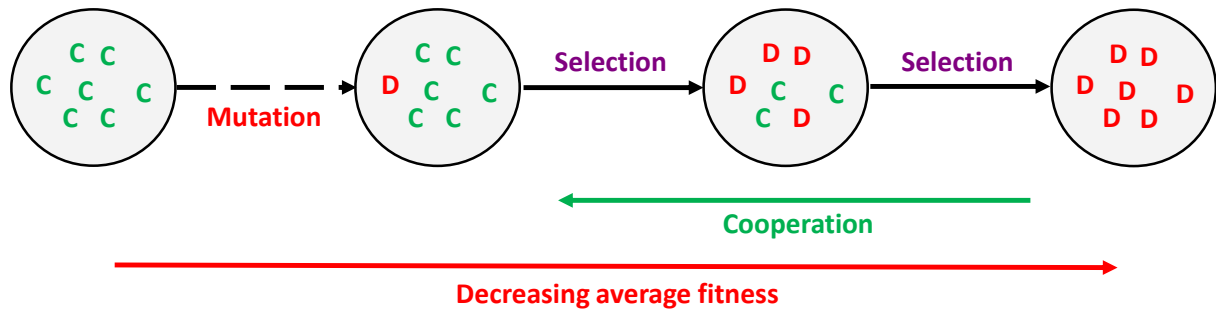


**Figure I.1: The dilemma of cooperators.** In a population consisting of cooperators (C), who all produce a cooperative trait, random mutagenesis for example could lead to the evolution of a defector (D). If there is no cooperative behavior between the partners and natural selection is the only process at work, the defectors will spread and overtake the whole population and this leads to the extinction of cooperators. The average fitness of the population during this process would decline until the whole population collapses (modified with author's permission from (Nowak, 2006)).

One solution for overcoming this dilemma is kin selection, meaning that there is a genetic relatedness between a donor and the recipient of its altruistic act, which must be higher than the ratio of cost to benefit of this act to develop stable cooperativity (Foster & Wenseleers, 2006, Frank, 1998, Hamilton, 1964b, Hamilton, 1964a, Nowak, 2006).

Another solution as an explanation for cooperation between unrelated individuals, is direct reciprocity, in which the recipient responds appropriately to the action from the donor (Trivers, 1971). This has similarities to the theory of a repetitive Prisoner's Dilemma game (Luce & Raiffa, 1957, Trivers, 1971). The cooperators react cooperatively to other cooperators but won't help defectors after the first encounter. The probability of another encounter is a key variable for the successful development of cooperativity in this scenario (Nowak, 2006).

In contrast to direct reciprocity, indirect reciprocity relies on the reputation of an individual. Cooperators identify defectors by the defectors' reputation from earlier encounters with other population members where they behaved defectively. Here the probability of knowing someone's reputation is essential for promoting cooperativity and overcoming the dilemma (Nowak, 2006). Furthermore, in spatial structured populations interactions according to network reciprocity can occur, where cooperators can overcome the dilemma by forming cooperative network clusters, mainly by interacting with each other and trying to exclude interactions with defective members (Nowak & May, 1992). Additionally, selection can also take place between populations instead of individuals, in the form of population or multilevel selection (Keller, 1999, Rainey & Rainey, 2003, Smith, 1964, Wilson, 1975). At the lower

level (intra-population, between individuals inside a population) defectors have a selection advantage by saving the cost of the altruistic act, at the higher level (inter-population, between different subpopulations inside a global population), cooperation is favored by populations with more cooperators having higher fitness than those with fewer (*Nowak, 2006*). In this case, cooperators can overcome the dilemma by outcompeting populations with a higher defector ratio based on stronger inter-population selection advantages.

## 1.2. Cooperative interactions in microbial systems

In the last few decades microorganisms have been seen not so much as single organisms; rather the idea of multicellular behavior has become more and more convincing, for example in the case of biofilm formation, quorum sensing, dispersal, foraging and “chemical warfare” (*Crespi, 2001, Keller & Surette, 2006, Kreft, 2004, Lazdunski et al., 2004, Parsek & Greenberg, 2005, Webb et al., 2003, West et al., 2006*). Many multicellular behaviors are also linked to bacterial virulence, where great numbers of new insights into molecular mechanisms and their genetic regulation have been realized in the last several decades (*Crespi, 2001, Keller & Surette, 2006, Lazdunski et al., 2004, Parsek & Greenberg, 2005, Velicer, 2003, Webb et al., 2003, West et al., 2006*). For all of these multicellular behaviors, the question arose as to which extend cooperative interactions are developed and maintained. Generally, microorganisms respond well to experimental evolution and genetic manipulation, making them good subjects for dealing with the dilemma of cooperators (*Elena & Lenski, 2003*).

A good demonstration of cooperativity in microbial systems is public good production, where cooperators synthesize products costly to themselves but beneficial for the whole population or a local population; these cooperators might face then the dilemma of cooperators (*Frank, 1998*) (shown in **Fig. I.1**). Systems with public goods that have been examined for cooperative interactions include iron-scavenging molecules, so called siderophores (*Griffin et al., 2004, West & Buckling, 2003*), quorum-sensing (QS) molecules (*Diggle et al., 2007, Keller & Surette, 2006, Lazdunski et al., 2004*), biofilm components (*Davies & Geesey, 1995, Rainey & Rainey, 2003*), toxic or antibiotic compounds (*Riley & Wertz, 2002*) as well as resistance mechanisms (*Dugatkin et al., 2005*), immune-modulation molecules (*Hooi et al., 2004, Tateda et al., 2003*), biosurfactants (*Daniels et al., 2004*) and extracellular products for nutrition (*Greig & Travisano, 2004, Lai et al., 2018*).

Of these, a good example for public goods is quorum-sensing (QS) molecules (*Diggle et al., 2007, Keller & Surette, 2006, Lazdunski et al., 2004*). Here, host-pathogen interactions offer potential roles for quorum signaling to coordinate a rapid and overwhelming attack, so it's a nice example to investigate both cooperation and communication in bacteria (*Brown & Johnstone, 2001*).

Additionally, antibiotic or toxin resistance traits, such as  $\beta$ -lactamsases, as a public good can preserve or even increase microbial genetic diversity of the system under strong selective pressures. Resistant strains can overcome the dilemma of being completely outcompeted due to the addition of selective pressure, and sensitive strains do not go extinct if the resistance trait is shared between community members (*Dugatkin et al., 2005*). Over long-term evolution, new fitter strains may evolve, perhaps with multiple resistances (*Dugatkin et al., 2005*). Furthermore, cooperative behavior can also be stabilized by pleiotrophy in this system, by carrying both resistance and production genes on one plasmid, making loss of cooperative behavior costly; this is one possible mechanism to overcome the dilemma (*Foster et al., 2004, Riley & Wertz, 2002, Travisano & Velicer, 2004*).

Another example of public goods is biosurfactants, which promote swarming motility in order to find new niches with better nutrient supply when local nutrient concentrations get low, thereby helping the population to survive via spreading (*Daniels et al., 2004, Deziel et al., 2003*). Cooperators can overcome the dilemma by spatial clustering, resulting in a greater benefit for neighboring cooperators compared to defectors (a common solution in many cooperative studies), in this special case facilitating faster and wider spreading.

Yet another example is the enzyme invertase, which enables cells to utilize sucrose as carbon source, and so is a public good used for nutrition. Therefore, the population has a benefit only when sucrose instead of glucose is the sole carbon source (*Greig & Travisano, 2004*). Here, cooperators may prevent extinction by privatizing a portion of the invertase by adsorption at the membrane or by having it prevalent in cytoplasm. But defectors may also hedge their bets by harboring a possible "silenced" unused invertase biosynthesis gene copy for environmental changes, which make it even harder for cooperators to overcome the dilemma (*Greig & Travisano, 2004*).

To examine these public good interactions, it is a good strategy to clarify the production cost and population based benefit from it, leading to direct and indirect fitness benefits (*Griffin et*

*al.*, 2004). First investigations for this could be measurements of relative fitness of the cooperator, harboring social trait, and non-cooperative mutant, both alone and in mixed cultures, optimally under conditions of favoring and non-favoring of cooperative behavior (*West et al.*, 2006). Therefore, artificial knock-out strains of cooperative behavior have the advantage of producing well-defined, clear and large effects, whereas in natural conditions point or transposon mutations of genes may be more prevalent (*Velicer et al.*, 2000, *Griffin et al.*, 2004, *Foster et al.*, 2004). A good combination for the examination of cooperative behavior is to use a mixture of results obtained by both artificial and natural environmental conditions; using only artificial lab experiments might lead to incorrect conclusions (*West et al.*, 2006). Furthermore, previously established cooperative behaviors from vertebrates and invertebrates are useful for developing hypotheses of microbial cooperative interactions; for example, the division of labor known from insect colonies is also prevalent in bacterial populations (*Crespi*, 2001, *West et al.*, 2006).

### **1.3. Uptake of the essential element iron by public good-siderophores**

Iron is essential for all cells, but occurs mainly in insoluble forms in nature. Therefore, all living organisms have developed ways of scavenging iron depending on the environment. Bacterial cells therefore have developed sophisticated but costly uptake mechanisms via soluble iron chelation molecules.

#### **1.3.1. Iron acquisition strategies**

Iron is an essential element, important in enzymatic processes as biocatalyst or electron carrier and essential for all cellular organisms; cells need intracellular concentrations of  $10^{-8}$  to  $10^{-6}$  M for optimal growths (*Andrews et al.*, 2003, *Guerinot*, 1994, *Guerinot & Yi*, 1994, *Litwin & Calderwood*, 1993). There are only a few organisms that do not use iron: one of these exceptions is *Lactobacillus plantarum*, utilizing manganese and cobalt as biocatalysts (*Archibald*, 1983, *Guerinot*, 1994); another is *Borrelia burgdorferi*, which has no iron-protein encoding genes; and *Treponema pallidum* appears to lack the requirement for iron (*Andrews et al.*, 2003, *Posey & Gherardini*, 2000).

Although iron is the fourth most common element in the earth's crust, it is found mostly in the almost insoluble ferric form  $\text{Fe}^{3+}$  rather than in the soluble ferrous form  $\text{Fe}^{2+}$ , due to the oxidation of ferrous ions under aerobic conditions. Nevertheless, some aerobic and microaerophilic bacteria have sophisticated uptake systems for  $\text{Fe}^{2+}$ ; for example

*Pseudomonas roseus fluorescens* produces Proferrosamine A, a chelator of ferrous iron ions, which is also essential for the synthesis of ferric iron chelators (Vande Woestyne *et al.*, 1991). Under anaerobic conditions, in the guts of host organisms for example, the uptake of  $\text{Fe}^{2+}$  via membrane transporters is more prevalent due to high concentrations of dissolved ferrous iron ions (Cao *et al.*, 2007, Kammler *et al.*, 1993, Marshall *et al.*, 2009, Stojilkovic *et al.*, 1993).

However, the major form is  $\text{Fe}^{3+}$  ions, which can reach concentrations only up to  $10^{-17}$  M in aerobic and aquatic environments (Guerinot & Yi, 1994). Cells must overcome  $\text{Fe}^{3+}$  insolubility for sufficient iron uptake, but also regulate the uptake to prevent too high iron concentrations, which lead to the catalysation of toxic hydroxyl radicals (Guerinot, 1994, Guerinot & Yi, 1994, Litwin & Calderwood, 1993, Neilands, 1991). In the human body, intracellularly heme, ferritin and iron-sulfur proteins contain the most iron, extracellularly carrier glycoproteins like transferrin or lactoferrin complexing iron (Griffiths, 1991, Guerinot, 1994, Payne, 1993, Payne, 1988). Major strategies of bacteria and fungi for  $\text{Fe}^{3+}$  acquisition are the production and utilization of siderophores (ferric specific chelators; the term is Greek for iron bearers), the reduction of  $\text{Fe}^{3+}$  to  $\text{Fe}^{2+}$  coupled with the transport of  $\text{Fe}^{2+}$  and/or the usage of host iron compounds like heme, lactoferrin and transferrin (Guerinot, 1994). Generally, most siderophores from microorganisms have higher affinities for  $\text{Fe}^{3+}$  than the iron carriers in the human body, which are transferrin or lactoferrin; this plays an important role in virulence for competing efficiently for iron (Griffiths, 1991, Guerinot, 1994, Husson *et al.*, 1993). Some pathogens like *Neisseria gonorrhoeae*, *Neisseria meningitidis*, and *Hemophilus influenzae* do not rely on siderophores, but directly utilize iron bound to transferrin and lactoferrin; these are often found in locations serving as primary bacterial infection sites (Guerinot, 1994, Otto *et al.*, 1992).

### 1.3.2. The iron scavenging group of siderophores

Siderophores are low molecular weight iron chelators, being generally less than 100 Daltons, which facilitate the chelation and transport of  $\text{Fe}^{3+}$  (Guerinot, 1994). Many siderophores are often composed of cyclic peptides, assembled via non-ribosomal peptide synthetases similar to those used for non-ribosomal peptide antibiotics biosynthesis (Andrews *et al.*, 2003). Despite structural variations, the chrome azurol S assay is an easy structurally independent method of detecting siderophores, as they all form six-coordinate octahedral complexes with  $\text{Fe}^{3+}$  (Guerinot, 1994, Schwyn & Neilands, 1987). Siderophore transport in Gram-negative bacteria is mediated by specific binding proteins and associated transporters (Andrews *et al.*,

2003, Koster, 2001). Ferric siderophore complexes transported into periplasm need to release iron for cellular metabolism, which involves the reduction of  $\text{Fe}^{3+}$  to  $\text{Fe}^{2+}$ , resulting in dissociation caused by the low affinity of siderophores to  $\text{Fe}^{2+}$  (Andrews *et al.*, 2003). Gram-positive bacteria lack periplasm, so they differ in  $\text{Fe}^{3+}$ -siderophore transport, but nevertheless produce both lipoprotein receptors and ABC transporters similar to those of Gram-negative bacteria (Hider & Kong, 2010).

Model gram-negative bacterium *Escherichia coli* produces two siderophores, aerobactin and enterobactin/enterochelin, which can be sensed and uptaken via six receptors (induced by iron starvation to avoid targeting of receptors, e.g. by antibiotics) and three associated ABC systems (Andrews *et al.*, 2003, Guerinot, 1994). Furthermore, these receptors and ABC systems can sense and uptake not only their native siderophores but also fungal hydroxamates, ferrioxamine, catechols and ferric citrate (Andrews *et al.*, 2003, Braun & Hantke, 1991, Frost & Rosenberg, 1973, Guerinot, 1994). Under iron limiting conditions, *Vibrio cholera* can produce the siderophore vibriobactin, marine bacteria can produce alterobactin and aerobactin and cyanobacteria can produce ferrioxamine (Guerinot, 1994, Reid *et al.*, 1993, Sigel & Payne, 1982). Many mycobacteria produce three types of siderophores, mycobactin, carboxymycobactin and exochelins (Hider & Kong, 2010). Fluorescent pseudomonads produce one primary siderophore, pyoverdine, and one secondary lower affinity siderophore, pyochelin (Cezard *et al.*, 2015).

Furthermore, genes of outer membrane receptor proteins for not only ferric pyoverdine and ferric pyocheline but also ferric enterobactin were all found in *Pseudomonas aeruginosa*, which means it is able to utilize siderophores of other genera (Ankenbauer, 1992, Dean & Poole, 1993, Guerinot, 1994, Poole *et al.*, 1993). However, pyoverdines of fluorescent pseudomonads can be used only by bacteria of this group (Matthijs *et al.*, 2009). Enterobactin has the highest ferric iron ion affinity, followed by pyoverdine and pyochelin (Guerinot, 1994). When enterobactin is prevalent, expression levels of the corresponding receptor is upregulated, whereas the other two receptors are downregulated, indicating that the affinity of siderophores for ferric iron ions leads to a hierarchy of iron transport systems in *P. aeruginosa* as it adjusts to different environmental conditions (Dean & Poole, 1993, Guerinot, 1994).

### 1.3.3. Siderophores of the genus *Pseudomonas*

Pyoverdines (sometimes called pseudobactins), the main siderophores of *Pseudomonas*, are responsible for the characteristic fluorescent pigments of fluorescent pseudomonads and can be typed in three different pyoverdine systems via the structural differences of their peptidic residues: succinyl, succinamide or  $\alpha$ -ketoglutaryl (Elliott, 1958, Meyer et al., 1987, Meyer et al., 1997). All pyoverdines of these three systems consist of three parts: a chromophore (identical in all pyoverdines), a peptidic moiety of 6 to 14 amino acids and an acyl side-chain deriving a dicarboxylic acid (Cezard et al., 2015, Cornelis et al., 1989). The combination of D- and L-amino acids in the peptidic chain allows pyoverdine to bind iron with a 1:1 stoichiometry (Cezard et al., 2015). After iron binding, the fluorescence of pyoverdine is quenched and shows a dark brown color, while apo-pyoverdine is yellow-green fluorescent (Albrecht-Gary et al., 1994, Cezard et al., 2015, Schalk et al., 1999). Like all other siderophores, pyoverdine has a higher affinity for  $\text{Fe}^{3+}$  ( $K_a$  of  $10^{31} \text{ M}^{-1}$ ) than for  $\text{Fe}^{2+}$  ( $10^9 \text{ M}^{-1}$ ) (Albrecht-Gary et al., 1994). The peptidic moiety incorporates unusual amino acids, responsible for the recognition process whose composition is unique in each strain (Cezard et al., 2015). A modern powerful method of distinguishing the pyoverdine type of various strains is mass spectrometry, which provides information regarding both mass and structure, aiding the examination of the taxonomy of different strains (Meyer et al., 2008, Ye et al., 2013).

Two well-studied pyoverdine producers are the opportunistic human pathogen *P. aeruginosa* and the plant growth-promoting *P. putida* WCS358, whose siderophores are structurally related but differing in the shape of the peptide moiety (Abdallah, 1991, Guerinot, 1994, Venturi et al., 1995b, Venturi et al., 1993). The strain of the studies in this thesis is *P. putida* KT2440, which is an exception to pseudomonads, as it produces only the siderophore pyoverdine (whose molecular mass is 1,073; the predicted peptide sequence is: succinamide – chromophore – aspartic acid – cyclic structured hydroxyaspartic acid and diaminobutanoic acid – glycine – serine – cyclo – hydroxyornithine), so pyoverdine-negative mutants do not show any siderophore activity (Cornelis, 2010, Matthijs et al., 2009, Ravel & Cornelis, 2003). But it has been recently shown, that *P. putida* KT2440 produces three different pyoverdines with differences in the side chain and conformation (Wei & Aristilde, 2015).

Pyochelin is the most important secondary siderophore of pseudomonads (produced in lower amounts than pyoverdine), having a lower iron affinity than pyoverdine, and also being

associated with virulence in *P. aeruginosa* (Cox, 1982, Guerinot, 1994, Visca et al., 1992). The intermediate product of pyocheline synthesis, salicylic acid, might also act as a siderophore, because of its similarity to azurechelin of *Burkholderia cepacia* (Meyer, 1992, Guerinot, 1994). Generally, secondary siderophores are produced either when iron limitation is not that strict or they have additional functions like elicitors of plant defense, inflammation or degradation as well as induction of secondary metabolites (Audenaert et al., 2002, Britigan et al., 1997, Cornelis, 2010, Matthijs et al., 2007, Moon et al., 2008, Ravel & Cornelis, 2003, Sun et al., 2006, Vinayavekhin & Saghatelian, 2009).

#### 1.3.4. Pyoverdine biosynthesis, regulation and iron selectivity in Pseudomonads

In *E. coli* or pseudomonads, like in other siderophore producing Gram-negative bacteria, all genes regarding iron uptake are negatively regulated by Fur. Thereby, Fur-Fe<sup>2+</sup>-complexes bind to the operator DNA at the so called “iron box” or “Fur box” (thought to be an overlapping 13 base pair “6-1-6” motif on the promoter allowing two Fur dimers to bind) (Andrews et al., 2003, Escolar et al., 1999, Guerinot, 1994, Hantke, 1981, Lavrrar et al., 2002, Stojiljkovic et al., 1994). One of the Fur-repressed genes is the master activator of pyoverdine synthesis (called PvdS in *P. aeruginosa* and PfrI in *P. putida* KT2440), an extracytoplasmic function (ECF)  $\sigma$  factor (see **Fig. I.2**) (Andrews et al., 2003, Dos Santos et al., 2004, Poole et al., 1993, Tiburzi et al., 2008, van Oeffelen et al., 2008, Venturi et al., 1995a, Visca et al., 2002). In pseudomonads, the activities of PfrI/PvdS and FpvI (another ECF  $\sigma$  factor important for regulation of pyoverdine transporters) are inhibited in the absence of pyoverdine via the anti- $\sigma$  factor FpvR (Beare et al., 2003, Edgar et al., 2014, Lamont et al., 2002, Llamas et al., 2014). This is the only cell-surface signaling pathway known, where a single anti- $\sigma$ -factor inhibits two different  $\sigma$ -factors (Beare et al., 2003, Edgar et al., 2014, Lamont et al., 2002, Llamas et al., 2014). Over a positive feedback loop, ferric pyoverdine interacts with FpvA and thereby leads to proteolysis of FpvR releasing PfrI, which upregulates pyoverdine biosynthesis (Draper et al., 2011, Edgar et al., 2014, James et al., 2005, Shen et al., 2002, Shirley & Lamont, 2009). Recent research also indicates the importance of small regulatory RNA in pyoverdine regulation (Little et al., 2018).

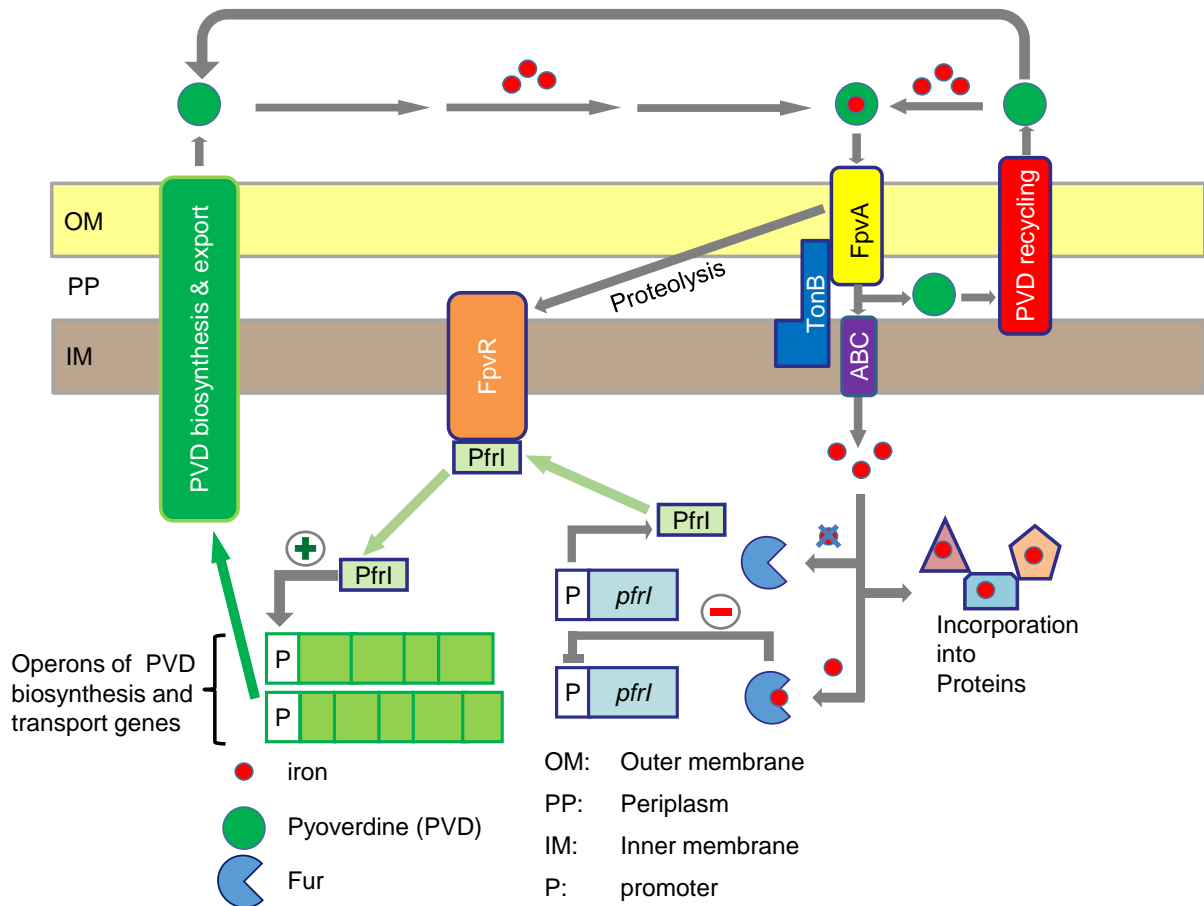


**Figure I.2: Regulation of synthesis and recycling of pyoverdine.** Under high cytoplasmic iron conditions, Fur represses *pfrI* expression. If iron is limited, *pfrI* expression is induced. PfrI binds to the transmembrane anti- $\sigma$ -factor FpvR. If ferric pyoverdine binds to the pyoverdine outer membrane receptor FpvA, FpvR is proteolyzed and PfrI can induce the expression of pyoverdine synthesis and transport related genes (chromophore, peptide NRPS and transporters). Then, a pyoverdine precursor is produced in the cytoplasm, transported to the periplasm for maturation and the mature pyoverdine is transported into the environment. This apo-pyoverdine binds Fe<sup>3+</sup> and the ferric pyoverdine is transported after recognition via FpvA (with the help of TonB) into the periplasm. Here, Fe<sup>3+</sup> is reduced to Fe<sup>2+</sup> and dissociates with pyoverdine. Afterwards, Fe<sup>2+</sup> is transported via an ABC transporter into the cytoplasm, while apo-pyoverdine is recycled by pumping it via the PvdRT-OmpQ efflux pump back into the environment (figure based on results of (Ringel et al., 2018, Gao et al., 2018, Edgar et al., 2017, Ringel et al., 2016, Cezard et al., 2015, Hannauer et al., 2012a, Matthijs et al., 2009)).

During pyoverdine biosynthesis in *P. putida* KT2440, the precursor is assembled in the cytoplasm by four nonribosomal peptide-synthetases (NRPS) (PvdL, PvdI, PvdJ and PvdD), while three additional enzymes are also involved in this process (PvdA, PvdF and PvdH) by producing two non-proteogenic amino acids for the precursor (Ackerley et al., 2003, Gasser et al., 2015, Mossialos et al., 2002, Ravel & Cornelis, 2003, Visca et al., 2007). Thus, only PvdL (responsible for the synthesis of the chromophore precursor) is highly conserved in all pseudomonads; the other NRPS differ in structure, because they are needed for the

incorporation of strain-specific non-proteinogenic amino acids (Cezard *et al.*, 2015, Mossialos *et al.*, 2002, Ravel & Cornelis, 2003, Schalk & Guillon, 2013, Visca *et al.*, 2007).

Afterwards, the cytoplasmic precursor is transported by the ABC transporter PvdE into the periplasm, where it is matured by the enzymes PvdN, PvdO, PvdP and PvdQ (Gasser *et al.*, 2015, Yeterian *et al.*, 2010). Here, the precursor is converted into ferribactin by excision of the fatty acid chain and afterwards this is converted into the fluorescent mature pyoverdine by cyclizing the chromophore (Drake & Gulick, 2011, Gasser *et al.*, 2015, Hannauer *et al.*, 2012b, Nadal-Jimenez *et al.*, 2014, Yeterian *et al.*, 2010). After biosynthesis, pyoverdine is stored throughout the periplasm and is exported by the ATP-dependent efflux pump PvdRT-OpmQ (Gasser *et al.*, 2015, Hannauer *et al.*, 2010, Yeterian *et al.*, 2010). In other pseudomonads there are recently-found indications that type VI secretion affects the secretion of pyoverdine or operates as an independent iron uptake system (Chen *et al.*, 2016, Lin *et al.*, 2017).

After chelating ferric iron ions, FpvA (a specific TonB dependent membrane transporter for pyoverdines of all three classes) recognizes ferric pyoverdines and transports them into the periplasm (Bouvier & Cezard, 2017, Brillet *et al.*, 2007, Cezard *et al.*, 2015, Cobessi *et al.*, 2005, Greenwald *et al.*, 2009, Schalk *et al.*, 1999, Wirth *et al.*, 2007). The ABC transporter encoded by the *fpvCDEF* operon, along with the genes *fpvWXYZ* of the same operon seems to be involved in the transport of iron across the inner membrane and is necessary for an efficient dissociation of ferric pyoverdine complex along with FpvG and FpvH (Baune *et al.*, 2017, Brillet *et al.*, 2012, Lin *et al.*, 2017). The dissociation seems to occur without the chemical modification of pyoverdine, but rather by the reduction of Fe<sup>3+</sup> followed by ligand exchange (Greenwald *et al.*, 2007). Then the PvdRT-OmpQ efflux pumps the *apo*-pyoverdine from the periplasm into the environment in order to recycle pyoverdine (Hannauer *et al.*, 2012a).

#### **1.4. Social interactions mediated via siderophores might overcome the dilemma of cooperators**

Producers (cooperators) of siderophores can be exploited by non-producers (defectors) and face the dilemma of cooperators (**Fig. I.1**), and must develop cooperative mechanisms to avoid extinction. This system provides an opportunity to examine conditions where cooperators can overcome this dilemma and the mechanisms they use to maintain coexistence.

Siderophore production is beneficial under iron limiting conditions, but costly for the cooperators, as demonstrated by experiments with the pseudomonad model organism *P. aeruginosa* using a co-culture of cooperators and defectors (Griffin *et al.*, 2004, West *et al.*, 2006) (**Fig. I.3**). In a monoculture and under iron limiting conditions, cooperator populations grow faster, whereas in co-cultures defectors benefit from the production of siderophores without paying the cost, and therefore increase in frequency and outcompete cooperators (Griffin *et al.*, 2004, West *et al.*, 2006).

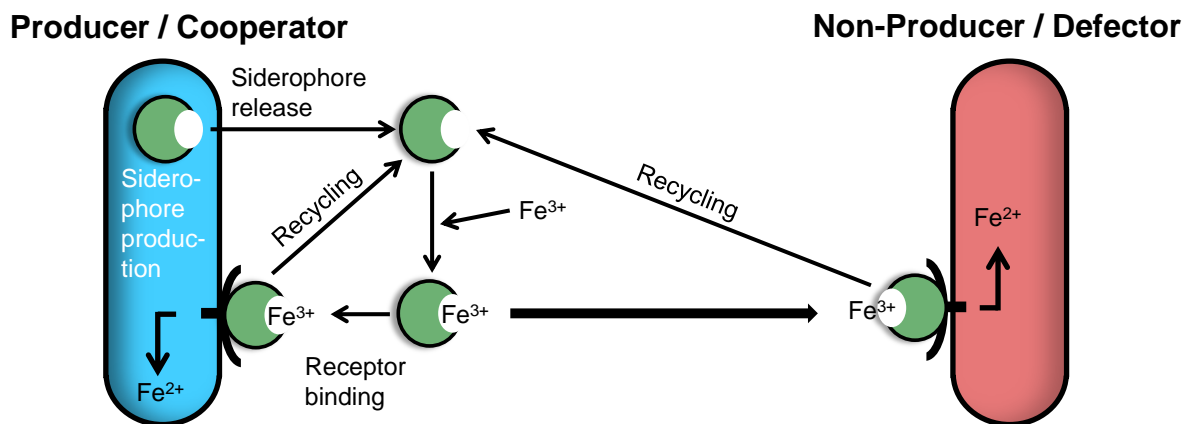


**Figure I.3: Siderophores as public good.** A cooperator (blue) synthesizes the iron-scavenging molecule siderophore (green) and excretes it into the medium, where it binds  $Fe^{3+}$  ions. The ferric iron-siderophore complex is recognized via receptors by both producer and defector (red), and in the periplasm the iron is reduced and released, supplying the cell with essential iron. The unloaded siderophore is recycled for further iron scavenging. In mixed populations of cooperators and defectors, the defectors have a selection advantage by benefitting from siderophores without producing them.

Generally, for public goods production the presumed dominating cooperative mechanism for overcoming the dilemma is kin selection, where cooperators outcompete defectors under conditions with high relatedness (Griffin *et al.*, 2004, Hamilton, 1963, Rousset, 2004, West *et al.*, 2006). Here it has also been demonstrated that higher investment in siderophore production within populations keeps the populations under high relatedness over multiple generations (Griffin *et al.*, 2004, Keller & Surette, 2006). Relatedness here is measured with respect to the “altruist allele”, in this case siderophore production (which increases with the concentration of cooperators and varies across species) (Frank, 1998, Griffin *et al.*, 2004). Additionally, cooperation is favored when relatively high relatedness is combined with relatively low local competition obtained by dispersal in populations instead of individuals (Gardner & West, 2006, Kummerli *et al.*, 2009a). Furthermore, ecological factors which reduce pyoverdine production effort, by decreasing iron limitation and/or increasing

opportunity for pyoverdine recycling, contribute to the evolutionary maintenance of cooperativity, thereby reducing or even negating the exploitation of defectors (*Dumas & Kummerli, 2012*). Finally, according to kin selection theory, relative defector fitness decreases with increasing defector abundance relative to cooperators (*Buckling et al., 2007, Frank, 1998, Ross-Gillespie et al., 2007*). This negative dependency of abundance is also valid for cooperators, whose relative fitness is higher when their abundance is lower (*Ross-Gillespie et al., 2007*).

Many cooperation experiments are based on simplifications, however, siderophore production can variate facultatively in response to environmental conditions (e.g. iron availability, cell density, frequency of strains), which creates an additional opportunity to address cooperation under environment dependency (*Buckling et al., 2007, Joyner & Lindow, 2000, Kummerli et al., 2009c, Ratledge & Dover, 2000*). Additionally, because siderophore is a durable public good, its facultative production represents a powerful mechanism for reducing selection by downregulating its production by cooperators (*Brockhurst et al., 2008, Hamilton, 1964a, Kummerli & Brown, 2010*). This makes durability a specific parameter (influenced by structure and environmental conditions like iron availability) affecting social interactions between cooperators and defectors (*Kummerli & Brown, 2010*). The degradation of siderophores in iron-rich conditions indicates consumption in non-selecting conditions and makes cooperators inevitable when the environment changes into iron limitation (*Kummerli & Brown, 2010*). Over long term evolution, siderophore cooperators and defectors can coexist, adapting to one another and the abiotic environment, with both increasing fitness over time (*Kummerli et al., 2015*). Additionally, other ecological conditions like disturbances, resource partitioning or competition between species, parasitism and predation have an effect on the evolution of cooperation, and may provide unique insights into how cooperation directed via kin selection can overcome the dilemma of cooperators (*Brockhurst, 2007, Brockhurst et al., 2006, Buckling et al., 2007*).

Spatial clustering is another mechanism of overcoming the dilemma, because siderophores tend to stay in the vicinity of cooperator subpopulations, which benefit preferentially from their own production and balance the advantage of defectors (*Julou et al., 2013*). Here, cooperation is maintained when the siderophore exchange rate is slower than their growth rate, because then siderophore exchange mainly benefits clonal patches of cooperators (*Julou et al., 2013*). Furthermore, high diffusion rates reduce reusability of siderophores by cooperators and

weakens cooperative behavior, whereas high viscosity reduces siderophore diffusion, thereby increasing selection for cooperation (*Kummerli et al., 2009b, Le Gac & Doebeli, 2010, Kummerli & Brown, 2010*).

Diversity in pyoverdine (the most common and important siderophore) structures and recognition mechanisms have been found (*Meyer et al., 2008, Meyer et al., 1997, Smith et al., 2005, Ye et al., 2013*). In iron limiting conditions it is beneficial for siderophore cooperators to make unique siderophores (distinct in structure from major varieties present in the environment). But this advantage can be continually compromised as defectors acquire compatible receptors, resulting in a kind of “arms race” (*Smith et al., 2005*). Cooperative behavior with an additional loner strain (a producer of an independent but rather inefficient good) results in “rock-paper-scissors” dynamics, where cooperators outcompete loners, defectors outcompete cooperators and loners outcompete defectors (*Inglis et al., 2016*). Therefore, under well mixed conditions favoring defectors over cooperators, the loners can stabilize the coexistence of defectors and cooperators (*Knebel et al., 2013, Inglis et al., 2016*).

### **1.5. Simpson’s paradox and theoretical cooperation models of growing populations**

Simpson’s paradox is a statistical phenomenon, observing a reversal of a trend in different populations when those populations are combined (*Blyth, 1972, Simpson, 1951, Xavier, 2011*). For a real life example, consider the case of personal income tax rates in the USA. From 1974 to 1978 the tax rate decreased in every tax bracket, meaning people with comparable salaries paid less tax in 1978 than in 1974 (*Wagner, 1982*). Yet, the average tax paid for all citizens increased over the same time period (*Wagner, 1982*). This paradoxical phenomenon was caused by a large increase in salaries due to inflation, such that many people moved to higher salary brackets and therefore paid higher tax rates, which reversed the trend of decreasing tax rates in all brackets (*Wagner, 1982*).

Similarly, **Fig. I.4** illustrates how Simpson’s paradox can occur in a growing microbial population divided into subpopulations (*Chuang et al., 2009*). The growth under selective conditions and the interactions between cooperators and defectors mediated by a public good in the mixed subpopulations are as described above. Another demonstration of Simpson’s paradox in a microbial cooperation system was done via a synthetic public good cooperation system in *E. coli*, which is the production of AHL autoinducers via a plasmid as a public good

regulating the autoinducer dependent chloramphenicol resistance (Chuang *et al.*, 2009, Xavier, 2011). In the experiments, subpopulations with low initial cell numbers were generated via Poisson dilution resulting in sufficiently large variances in initial cell number and initial cooperator fraction. These conditions allow multi-level selection, where single cells compete with each other inside a subpopulation and subpopulations compete with other subpopulations within a global gene pool (Xavier, 2011). These subpopulations grown under antibiotic stress, so that defectors are selected within the subpopulations, yet subpopulations with higher initial cooperator fractions grow to higher cell densities in the same time (Chuang *et al.*, 2009). So it could be that the global cooperator fraction (sum of all subpopulations) increases, thereby overcoming the dilemma of cooperators (Chuang *et al.*, 2009).

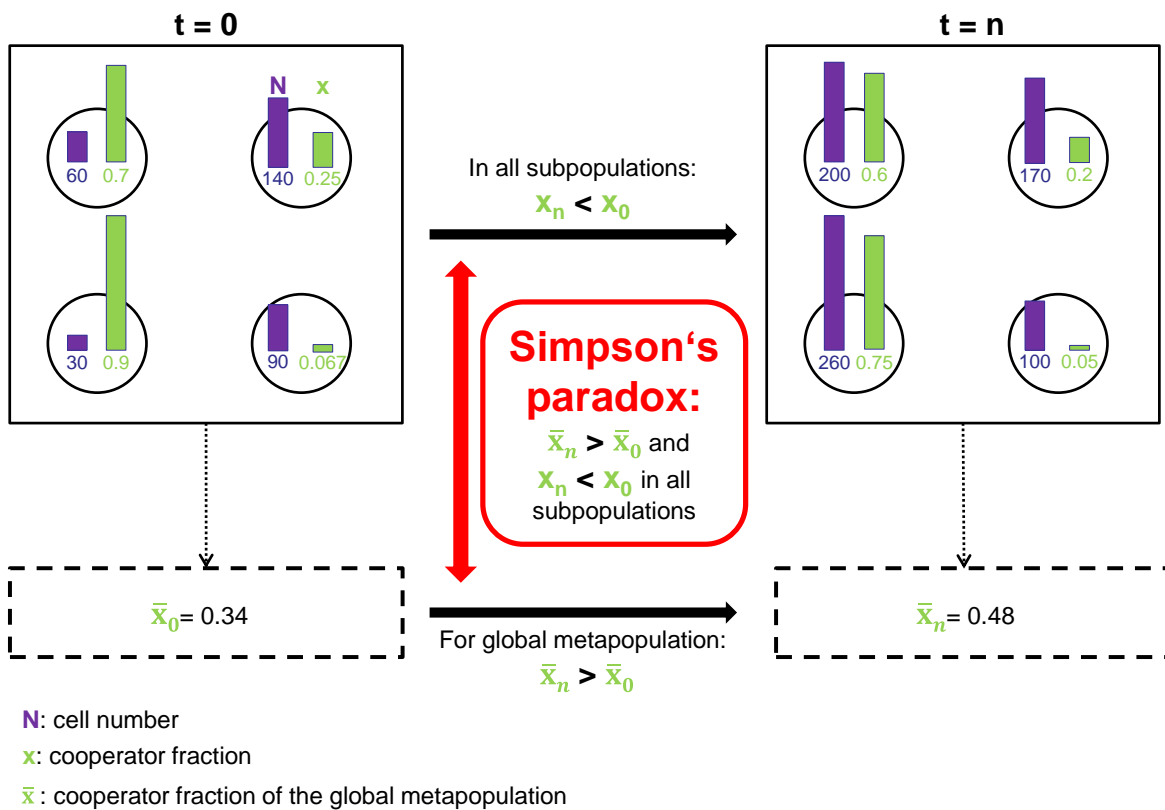


**Figure I.4: Theoretical principle of Simpson's paradox.** Mixed subpopulations of cooperators and defectors are illustrated differing in initial cell number  $N$  (purple at  $t_0$ ) and initial cooperator fraction  $x$  (green at  $t_0$ ). Due to the selection advantage of defectors, the frequency of cooperators decreases in subpopulations over time  $n$  ( $x_n < x_0$ ). But, subpopulations with a higher initial cooperator fraction grow faster and therefore lead to an increase of the cooperator fraction on the global metapopulation level ( $\bar{x}_n > \bar{x}_0$ ). Under these circumstances cooperative interactions can be observed according to Simpson's paradox overcoming the dilemma of cooperators (modified with author's permission after (Chuang *et al.*, 2009)).

Further studies with the abovementioned synthetic microbial system indicate a central problem in explaining the development of cooperativity with molecular mechanisms (*Chuang et al., 2010, Xavier & Foster, 2007*). Although this is a well-controllable system, social interactions are nevertheless complex and environmentally dependent, because for example parameters like costs and benefits are not constant, and rely on many factors like cooperator fraction, relatedness, etc. (*Chuang et al., 2010, Xavier & Foster, 2007*).

Extreme bottlenecks, for example in this study generated via Poisson dilution or ecologically generated population bottlenecks in nature support the evolution of cooperation (*Brockhurst, 2007, Griffin et al., 2004*). They indirectly favor cooperators through their effect on increasing variance of population distributions (*Chuang et al., 2009, Killingback et al., 2006, Xavier, 2011*). Similar social interactions may evolve in natural microbial systems, however, evolution may also have selected genetic backgrounds, ensuring that cooperators have a growth advantage under these natural conditions, negating the dilemma (*Chuang et al., 2009, Crespi, 2001, Dunny et al., 2008, Foster & Wenseleers, 2006, Kerr et al., 2006, Rainey et al., 2000*).

Theoretical models of the system in **Fig I.3** deal on the one hand with neutral evolution, where cooperators and defectors coexist much longer than under selective conditions (*Cremer et al., 2009, Reichenbach & Frey, 2008, Reichenbach et al., 2007a, Reichenbach et al., 2007b*). On the other hand, studies of the system in **Fig I.4** examining the impact of environmental factors like population growth regime or population bottlenecks on siderophore cooperators and defectors show, that these factors could explain the establishment of cooperative interactions (*Melbinger et al., 2015*). Besides, consequences of an interdependency between evolutionary and population dynamics have been investigated over a theoretical approach (*Cremer et al., 2011, Melbinger et al., 2010*). Here, a transient increase of cooperators can emerge by a fluctuation-induced effect during one growth life cycle (*Melbinger et al., 2010*). Additional specific simulations of the public good siderophore have provided insights into the evolution of the transient increase and its dependence on system parameters, including selection pressure, initial cooperator fraction, cell number and growth advantage of more cooperative subpopulations (*Cremer et al., 2011*). Furthermore, in simulations with repetitive microbial life cycles like at *Chuang et al.* (*Chuang et al., 2009*) the cooperator fraction can either decrease, increase transiently or increase permanently during one life cycle (*Cremer et al., 2012*). But a stable increase of the cooperator fraction is possible

over repetitive regrouping, until cooperators even overtake the whole population, which means these regular life cycles are favoring cooperation (*Cremer et al., 2012*).

## **1.6. Thesis objective**

The objective of this thesis is to examine conditions for the development of cooperativity in synthetic ecosystems. To this end, phenotypic heterogeneity, ecological factors, environmental conditions and the properties of the underlying gene regulatory network were considered, all of which affect population dynamics. In particular, the focus was on social and ecological factors like selection pressure, growth advantage of more cooperative populations, and initial composition of initial subpopulations. This thesis is part of a cooperative project with theoretical physicists, linking theoretical approaches and models with experimental results. Accordingly, I have focused on the experimental side by proving their simulations of theoretical models. For the experiments, a natural bacterial model system was used, specifically the production of the siderophore pyoverdine as a public good. Pyoverdine is used to scavenge iron ions from the medium, so that cells can also grow in iron-limiting conditions. *Pseudomonas putida* KT2440, a fluorescent soil bacterium, was selected, which produces only the siderophore pyoverdine (the production of which is not regulated via cell density-dependent mechanisms like quorum sensing). This makes the system easier to examine than the siderophore biosynthesis system of *Pseudomonas aeruginosa*. For the experiments, mutants were constructed lacking the pyoverdine production mechanism. As experimental set-up, well-mixed liquid co-cultures of pyoverdine cooperators and defectors were used. Conditions for the development of cooperativity and for neutral evolution were analyzed via a metapopulation approach, meaning the global metapopulation consists of many subpopulations. With this setup, competition can be achieved between intra-population selection (defectors grow faster than cooperators in mixed populations) and inter-population selection (populations with more cooperators grow faster) under selective iron-limiting growth conditions. To monitor cell growth and the fraction of pyoverdine cooperators over time, cell numbers were assessed via colony forming units and cooperators were identified via fluorescence of colonies resulting from pyoverdine.

## **Chapter II**

Here, the neutral evolution of co-cultures of pyoverdine producers (cooperators) and pyoverdine non-producers (defectors) under iron rich conditions is examined.

Metapopulations consisting of subpopulations with a random distribution of initial cell numbers and initial cooperator fractions were generated via Poisson dilution to very low cell numbers. Both theoretical models and experimental results support the conservation of the cooperator fraction until the end of the exponential growth phase.

### **Chapter III**

In this chapter the system is investigated under selective conditions. Metapopulations consisting of subpopulations with random initial cooperator fractions were grown under iron limitation and the time course of global cooperator fraction was monitored. A transient increase in the global cooperator fraction was observed and the role of pyoverdine as a central element in social interactions was indicated both by theoretical and experimental outcomes.

**Non-Selective Evolution of Growing Populations**

Karl Wienand, Matthias Lechner, Felix Becker, Heinrich Jung, Erwin Frey

PLOS ONE, August 2015, Volume 10, Issue 8, e0134300

## RESEARCH ARTICLE

# Non-Selective Evolution of Growing Populations

Karl Wienand<sup>1</sup>✉, Matthias Lechner<sup>1</sup>✉, Felix Becker<sup>2</sup>✉, Heinrich Jung<sup>2</sup>, Erwin Frey<sup>1</sup>\*

**1** Arnold-Sommerfeld-Center for Theoretical Physics and Center for NanoScience, Physics Department, Ludwig-Maximilians-Universität, Munich, Germany, **2** Department of Biology 1, Microbiology, Ludwig-Maximilians-Universität, Martinsried, Germany

✉ These authors contributed equally to this work.

\* [frey@lmu.de](mailto:frey@lmu.de)



CrossMark  
click for updates

## OPEN ACCESS

**Citation:** Wienand K, Lechner M, Becker F, Jung H, Frey E (2015) Non-Selective Evolution of Growing Populations. PLoS ONE 10(8): e0134300. doi:10.1371/journal.pone.0134300

**Editor:** Matjaz Perc, University of Maribor, SLOVENIA

**Received:** May 8, 2015

**Accepted:** July 7, 2015

**Published:** August 14, 2015

**Copyright:** © 2015 Wienand et al. This is an open access article distributed under the terms of the [Creative Commons Attribution License](https://creativecommons.org/licenses/by/4.0/), which permits unrestricted use, distribution, and reproduction in any medium, provided the original author and source are credited.

**Data Availability Statement:** All relevant data are within the paper and its Supporting Information files.

**Funding:** EF was funded by the Deutsche Forschungsgemeinschaft, Priority Programme 1617 "Phenotypic heterogeneity and sociobiology of bacterial populations", grant FR 850/11-1 and the German Excellence Initiative via the programme "Nanosystems Initiative Munich" (NIM). HJ was funded by the Deutsche Forschungsgemeinschaft, Priority Programme 1617 "Phenotypic heterogeneity and sociobiology of bacterial populations", grant JU 333/5-1 (<http://www.spp1617.org/>). KW was supported by the Elitenetzwerk Bayern. The funders had no role in study design, data collection and

## Abstract

Non-selective effects, like genetic drift, are an important factor in modern conceptions of evolution, and have been extensively studied for constant population sizes (Kimura, 1955; Otto and Whitlock, 1997). Here, we consider non-selective evolution in the case of growing populations that are of small size and have varying trait compositions (e.g. after a population bottleneck). We find that, in these conditions, populations never fixate to a trait, but tend to a random limit composition, and that the distribution of compositions "freezes" to a steady state. This final state is crucially influenced by the initial conditions. We obtain these findings from a combined theoretical and experimental approach, using multiple mixed subpopulations of two *Pseudomonas putida* strains in non-selective growth conditions (Matthijs et al, 2009) as model system. The experimental results for the population dynamics match the theoretical predictions based on the Pólya urn model (Eggenberger and Pólya, 1923) for all analyzed parameter regimes. In summary, we show that exponential growth stops genetic drift. This result contrasts with previous theoretical analyses of non-selective evolution (e.g. genetic drift), which investigated how traits spread and eventually take over populations (fixate) (Kimura, 1955; Otto and Whitlock, 1997). Moreover, our work highlights how deeply growth influences non-selective evolution, and how it plays a key role in maintaining genetic variability. Consequently, it is of particular importance in life-cycles models (Melbinger et al, 2010; Cremer et al, 2011; Cremer et al, 2012) of periodically shrinking and expanding populations.

## Introduction

Stochastic effects play an important role in population dynamics [8–11], particularly when competition between individuals is non-selective. Most previous theoretical analyses have studied how a non-selectively evolving trait can spread and eventually replace all other variants (fixate) under conditions in which the population size remains constant [2, 12, 13]. However, both natural and laboratory populations frequently experience exponential growth. Here we show that genetic diversity in growing populations is maintained despite demographic noise,

analysis, decision to publish, or preparation of the manuscript.

**Competing Interests:** The authors have declared that no competing interests exist.

and reaches a stationary but random limit. We used a well-controlled model system in which well-mixed co-cultures of a wild-type *Pseudomonas putida* strain and an isogenic mutant were grown under non-selective conditions. Multiple subpopulations were generated, each containing a random number of individuals of each strain. Depending on the average initial population size and the strain ratio, we observed distinct stationary probability distributions for their genetic composition. Moreover, we showed that the dynamics of growing populations can be mapped to Pólya urn models [4], permitting the observed maintenance of genetic diversity to be understood as the random limit property of a fair game between individual strains. Generalizing the Pólya urn model to include the effects of random initial sampling and exponential growth allowed us to predict the evolution of the composition distribution. Using numerical and analytical methods we found that the distribution broadens at first but quickly “freezes” to a stationary distribution, which agrees with the experimental findings. Our results provide new insights into the role of demographic noise in growing populations.

## Results and Discussion

Evolutionary dynamics is driven by the complex interplay between selective and non-selective (or neutral) effects. The paradigm of non-selective evolution originates from the seminal work of Kimura [1], in which he solved the Wright-Fisher model, thus showing that non-selective effects—and specifically genetic drift—can have a determinant role in evolution. His results sparked an ongoing debate about the nature and potency of randomness as a fundamental evolutionary force [13–15]. For very small populations genetic drift is generally considered an important factor [13], as the theory successfully predicts the outcomes of neutral evolution experiments [9, 16].

In most theoretical analyses, constant (or effectively constant) population sizes are assumed, and the role of population growth is neglected. Bacterial populations, however, often undergo rapid growth—especially when they are small. For example, as few as 10 individuals of some highly virulent pathogens (e.g. enterohemorrhagic *Escherichia coli* or *Shigella dysenteriae*) suffice to initiate a deadly infection in a human host [17, 18]. Another case of small, growing populations are water-borne bacteria that feed on phytoplankton products. Due to nutrient limitation in open water, these bacteria typically live in small populations in close proximity to the planktonic organism [19]. During spring blooms, the phytoplankton releases more organic material, boosting the bacterial growth rate [19–21]. In nature, such small populations often form by adventitious dispersal from a larger reservoir population [22]. A typical example is the spreading of pathogens from host to host. This random “sampling” from a reservoir yields small populations whose genetic compositions differ from that of the reservoir (a phenomenon known as the *founder effect* [23]). Recent studies also showed that the combination of population growth and stochastic fluctuations can have a major impact on the evolution [5–7, 24] and genetics [25] of small populations.

To probe how population growth shapes genetic diversity, we used a well-characterized microbial model system, namely the soil bacterium *Pseudomonas putida* KT2440 [3, 29, 27]. The wild-type strain KT2440 produces pyoverdine, an iron-scavenging molecule that supports growth when iron becomes scarce in the environment. Here we consider co-cultures of two genetically distinct strains: the wild-type, pyoverdine-producing strain KT2440 (strain A) and the mutant non-producer strain 3E2 (strain B). We set up conditions of non-selective competition between these strains by using an iron-replete medium (casamino acids, supplemented with 200  $\mu\text{M}$   $\text{FeCl}_3$ ). In this medium, production of pyoverdine is effectively repressed [27], such that both strains have the same growth rate and neither has an advantage (see S2 Table). Producer (KT2440 wild type) and non-producer (3E2) strains were first mixed and diluted to

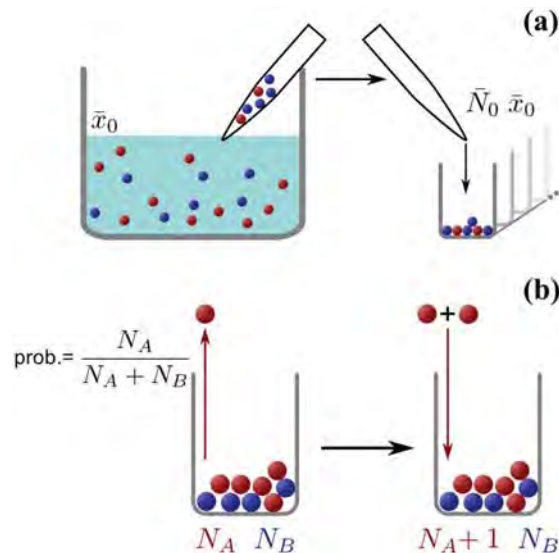


**Fig 1. Schematic depiction of urn sampling and growth.** (a) Schematic illustration of the random initial conditions. An infinite reservoir contains a diluted mixture of bacteria, a fraction  $\bar{x}_0$  of which are of strain A. We draw small volumes of liquid from the reservoir containing small, random numbers of individuals, which conform to a Poisson distribution with mean (determined by the dilution of the reservoir population). A certain fraction of this initial population is of strain A. The mean value of this fraction is equal to  $\bar{x}_0$ . We use these individuals to initiate populations in the wells of a microtiter plate, so that each population starts with a random size  $N_0$  and a random fraction of A-individuals  $x_0$ . (b) Illustration of the Pólya urn model. If a bacterial population is represented as an urn, each individual as a marble and each bacterial strain as a color, this urn model captures the essentials of bacterial reproduction in our populations. At each iteration, a marble is drawn at random and returned to the urn, together with another one of the same color. The probability of extracting a marble of either color is determined solely by its relative abundance, making the process non-selective (since no strain has inherent advantages, see S2 Table). The rate of growth in population size can be rendered exponential (see S2 Fig) by letting the waiting time between successive iterations be exponentially distributed (also known as Poissonization).

doi:10.1371/journal.pone.0134300.g001

yield Poisson dilution conditions. Then we initiated a large number of subpopulations from this reservoir by pipetting aliquots of the cell suspension into the wells of a 96-well plate, thereby generating a large ensemble of subpopulations with a random distribution of initial cell number  $N_0$  and producer fraction  $x_0$  (Fig 1). Use of shaken liquid cultures ensured homogeneous well-mixed conditions for all cells in the same well (access to nutrients, oxygen, etc.), and exponential growth was observed in all cases (see S2 Fig).

This experimental setting is well described within the mathematical framework of a *Pólya urn model*. Consider each bacterium in the population as a marble in an urn, and its genotype as the color of the marble (e.g. red for strain A, and blue for strain B). Population growth results from single reproduction events in which an individual randomly divides. This is mathematically equivalent to a stochastic event in which a marble is chosen at random from the urn and put back, together with another one of the same color. This random process, introduced by Eggenberger and Pólya [4], exhibits several important properties [28–31]. It is *self-reinforcing*: each time a marble is extracted, another one of the same color is added, increasing the likelihood of extracting a marble of that color again. In the context of bacterial populations, this means that every birth event for one strain makes it more likely that further birth events of that same strain will occur in the future. Note, however, that *fixation*, i.e., complete loss of one type

of marble from the population, cannot occur, simply because in the Pólya urn model marbles are neither removed nor do they change their color. This fully reflects the experimental conditions: During exponential growth, rates of cell death are negligible, and within the observation time mutations will be extremely rare, given the population sizes considered. The bacteria in each well reproduce randomly at a per-capita (average) rate  $\mu$ . To translate this to the urn model, drawing of a marble is assumed to be a stochastic Poisson process, with a “per-marble” rate  $\mu$  (a procedure known as *Poissonization* or *embedding* [32, 33]). Mathematically, the growth process is then described by a Master Equation: The time evolution for the probability  $P(N_A, t)$  of finding  $N_A$  individuals of strain  $A$  at time  $t$  reads

$$\frac{d}{dt}P(N_A; t) = (N_A - 1)P(N_A - 1; t) - N_A P(N_A; t), \quad (1)$$

where we have set the growth rate to  $\mu = 1$  in order to fix the time scale (for an introduction to the mathematical concepts see, e.g., [34]); the corresponding Master equation for individuals of strain  $B$  is of identical form. To study the composition of the populations, we use the more convenient quantities  $N = N_A + N_B$  (total size) and  $x = N_A/N$  (fraction of individuals of strain  $A$ ).

To start the experiment, we inoculated the wells of 96-well-plates by drawing small volumes of diluted liquid bacterial culture from a large reservoir (Fig 1(a)). Each volume contains a random number of bacteria whose mean value is controlled by the dilution of the reservoir. The fraction of bacteria of strain  $A$  (wild type) in that volume is also random, with its mean value  $\bar{x}_0$  given by the fraction of strain  $A$  in the reservoir. In the mathematical formulation, this setup corresponds to stochastic initial conditions for the Pólya urn model: the initial population size  $N_0$  for each well is given by a Poisson distribution with mean  $\bar{N}_0$ , and each individual is assigned to strain  $A$  or  $B$  with probability  $\bar{x}_0$  and  $1 - \bar{x}_0$ , respectively. This procedure is also equivalent to treating the initial numbers of  $A$ - and  $B$ -individuals as independent, Poisson-distributed random variables with mean values  $\bar{N}_0 \bar{x}_0$  and  $\bar{N}_0 (1 - \bar{x}_0)$ , respectively [6].

Fig 2 shows a time series of the histogram for the composition  $x$  of all subpopulations considered, as obtained from a stochastic simulation of the Master Eq (1) for a given random initial condition (with  $\bar{N}_0 = 10$  and  $\bar{x}_0 = 0.33$ ). Surprisingly, the distribution first broadens, but then quickly “freezes” to a steady state (see S1 Video). This is genuinely different from Kimura’s result for populations with constant size [1] (or similar results with effectively constant size [2]) where the balance between stochastic birth and death events leads to genetic drift, and thereby eventually to the extinction of one of the two strains. In contrast, for a growing population, death events are negligible, and therefore there is no fixation of the population during growth. Instead, fixation arises as a direct consequence of the initial sampling process, as can be seen from the heights of the black bins in the histogram (at  $x = 0$  and  $x = 1$ ), which remain constant over time (Fig 2). During growth, the composition of each subpopulation, instead of drifting to fixation at either  $x = 0$  or  $x = 1$ , reaches a stationary limit value  $x^*$ , where it remains thereafter [35]. This limit value is random: starting several subpopulations (urns) from the exact same initial composition of strain  $A$  and  $B$  (blue and red marbles), each reaches a limit, but in general these limits differ from one another. Once all of the subpopulations in an ensemble reach their limit, the distribution of the population composition freezes to a steady state, which is equal to the probability distribution of  $x^*$ . Similar random limit properties appear in other fields, with *lock-in* in economics as the best-known example [30].

The inset in Fig 2 shows approximate solutions for the time evolution of mean, standard deviation, and skewness of the composition  $x$ , which we obtained by analytically solving the Master Eq (1) (see S2 Text). The analytical results agree well with their numerical counterparts. In particular, the mean value remains constant over time, as it must for a non-selective process.

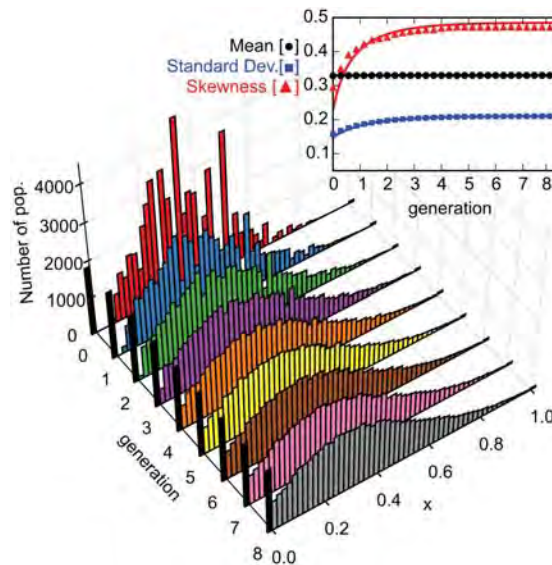


**Fig 2. Time series for the simulated distribution of the population composition  $x$ .** The distribution initially broadens, then freezes to a steady state (see [S1 Video](#)). The fraction of populations that have  $x = 0$  or  $x = 1$  (indicated by the black bins) remains constant during the time evolution, as expected for a Pólya urn process, and in contrast to expectations from genetic drift (see [S1 Table](#)). In each well the population follows a stochastic path and reaches a (random) limit composition, and the distribution freezes only when all populations reached their limit. The parameter values used in the simulation are  $\bar{N}_0 = 10$  and  $\bar{x}_0 = 0.33$ . The inset shows the mean, standard deviation and skewness as a function of the number of generations, with symbols denoting numerical simulations, and the solid lines corresponding to the theoretical prediction of [Eq \(2\)](#) (and also those in [S2 Text](#)). Analytical and numerical values agree. The mean ( $\langle x \rangle$ ) remains constant throughout the evolution, as expected for a non-selective process; standard deviation and skewness saturate to limit values, confirming the freezing of the distribution.

doi:10.1371/journal.pone.0134300.g002

For the time evolution of the variance, which is a measure for the spread of a distribution, we obtain to leading order in population size

$$\text{Var}_{\text{poi}}[x](t) = \frac{2 - e^{-t}}{\bar{N}_0} \bar{x}_0 (1 - \bar{x}_0). \quad (2)$$

The broadening and freezing of the distribution is reflected in the exponential decay term of the variance. Note that the skewness increases as well, because growth is self-reinforcing (see inset in [Fig 2](#)). To further test the validity of the stochastic simulations, we also calculated the limit values of the average and variance after extended periods of evolution exactly, and found that they match the numerical solutions of the Master Equation perfectly (see [S1 Text](#)).

We tested these theoretical predictions using *P. putida* as a bacterial model system. We mixed the wild-type and mutant strains in order to obtain different initial fractions  $\bar{x}_0$ . The degree of dilution of the mixture determines the average initial cell number  $\bar{N}_0$ , with which we inoculated 120 wells per experiment (96-well plate format). In order to compare the experimental data with our model, we set up simulations that matched the experimental configuration by initializing  $\bar{N}_0$  and  $\bar{x}_0$  with the same values as measured in the experiments. We simulated the time evolution of about  $10^4$  populations, grouped in “virtual plates” of 120 wells each. Every virtual plate produced a histogram like the one we obtained from experiments. We then generated an average histogram of the virtual plates and used its values to compute the

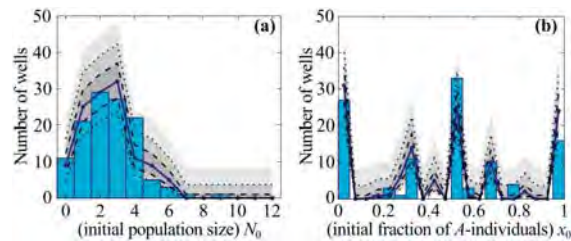


**Fig 3. Initial distributions for population size  $N_0$  and composition  $x_0$  (parameter values  $\bar{N}_0 = 2.55$ ,  $\bar{x}_0 = 0.45$ ).** The experimental distributions (bars) for  $N_0$  (panel (a)) and  $x_0$  (panel (b)) are measured from 120-well ensembles. The average  $\bar{N}_0$  and  $\bar{x}_0$  calculated from the measured values determine the parameters for the simulated distributions. The theoretical average distribution (solid blue line) is the average of the same distributions generated for 84 sets of 120 wells. Using that average we calculate the Wilson binomial confidence intervals (gray areas) for 68% (between dashed lines), 95% (between dotted lines) and 99.73% confidence. The measured and simulated distributions agree well within statistical error, confirming our assumption that individuals of strain A and B in the experiments start Poisson-distributed with mean  $\bar{N}_0\bar{x}_0$  and  $\bar{N}_0(1 - \bar{x}_0)$ , respectively. The ragged distribution of  $x_0$  derives from a small-number effect, and disappears at larger values of  $N_0$  (see main text, and also S3 Fig).

doi:10.1371/journal.pone.0134300.g003

binomial confidence intervals [36] for the count in each bin, and compared those with the experimental distribution.

Fig 3(a) shows a representative experimental histogram of the initial population sizes  $N_0$  for strong dilution with  $\bar{N}_0 = 2.55$ . It is well approximated by a Poisson distribution, and agrees with the simulation results within statistical errors (blue line and shaded gray areas in Fig 3(a)). Fig 3(b) shows the probability distribution of the corresponding initial compositions  $x_0$  of the populations, where again theoretical and experimental values agree well within statistical error. Note also that in every well the composition  $x_0$  must be a simple fraction; this means that only a few numerical values are possible for small initial population sizes  $N_0$ . This small-number effect explains why the distribution of  $x_0$  in Fig 3(b) is so ragged. The distribution becomes much smoother for larger initial population sizes (see S3 Fig). Taken together, these results for the distribution of initial population size and composition confirm that the inoculation of the individual wells is a stochastic sampling process with Poissonian statistics.

Next, we were interested in how the composition of the bacterial population would evolve under non-selective (neutral) growth conditions. To this end we let the 120 populations grow for an 11-hour period, during which they remained in exponential growth phase (see S2 Fig). Then we measured the population size  $N(t)$  in each well by counting colony-forming units, and  $x(t)$  by counting the pyoverdine-producing colonies (see Materials and Methods). Fig 4 shows the final outcome for four different initial conditions, i.e. combinations of the initial average population size  $\bar{N}_0$  and composition  $\bar{x}_0$ . We first wanted to know what determines the number of wells that contain only individuals of either strain A or strain B, i.e. that are fixated. To this end we compared the experimentally observed values with the corresponding predictions from the numerical simulations of the Pólya urn model (Fig 4). Since both results agree within statistical error, we conclude that fixation of a population is a consequence of the initial sampling process and is not due to fixation during population growth (see also S1 Table). This is especially obvious for small average initial population size or compositions close to  $x = 0$  or  $x = 1$ , where a large fraction of the wells contains cells of strain A or B only (Fig 4(a) and 4(d)). Next we wished to learn how the final distribution of the population composition (i.e. the random limits,  $x^*$ ) depends on the initial average composition  $\bar{x}_0$ . For  $\bar{x}_0 = 0.5$ , we observed both by experiment and theoretically that the initial distribution significantly broadened (by a factor

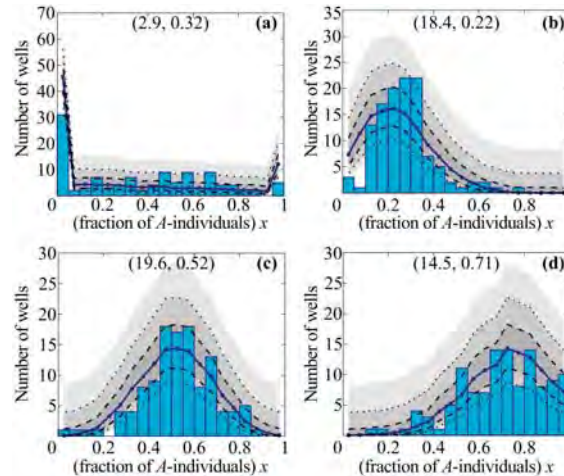


**Fig 4. Steady-state distributions of population composition  $x$  for different initial conditions.** The experimental distribution (bars) is the result of growth on 120 independent wells. We use the measured average  $\bar{x}_0$  and  $\bar{N}_0$  from the experiments to initialize the simulations of several 120-well ensembles. After growth, we compute the histogram for each of these ensembles and obtain the average theoretical distribution (blue line). Using the values from this distribution, we compute the three confidence intervals (shaded gray areas) for each bin for 68% (between dashed lines), 95% (between dotted lines) and 99.73% confidence. The two sets of data match: most experimental data agree with the first prediction confidence region, practically all with the second one. The limit distributions are clearly different from the initial ones (see S1 Fig). The importance of growth in changing the distributions depends on the initial size  $N_0$  (see main text, and S1 Fig). Parameter values:  $\bar{N}_0 = 2.9$ ,  $\bar{x}_0 = 0.32$  (panel (a));  $\bar{N}_0 = 18.4$ ,  $\bar{x}_0 = 0.22$  (panel (b));  $\bar{N}_0 = 19.6$ ,  $\bar{x}_0 = 0.52$  (panel (c));  $\bar{N}_0 = 14.5$ ,  $\bar{x}_0 = 0.71$  (panel (d)).

doi:10.1371/journal.pone.0134300.g004

of  $\sqrt{2}$ ) but remained symmetrical (Fig 4(c) and S1 Fig). In contrast, starting from distributions with average values below or above 0.5 caused the final distribution to broaden and also become skewed towards smaller or larger values of  $x$ , respectively (Fig 4(b) and 4(d)). Moreover, we found quantitative agreement between experiment and numerical simulations within statistical errors in all analyzed parameter regimes (see blue lines and shaded areas in Fig 4): most experimental histograms fall within the first confidence interval of the prediction (darkest gray areas, between dashed lines), and almost all fall within the 99.73% confidence interval.

Taken together, our combined theoretical and experimental analysis gives a coherent picture of evolution during non-selective (exponential) growth. We have shown, experimentally and by analogy with the Pólya urn model, that for each well-mixed population the composition of the population reaches a random stationary limit, and, unlike populations with constant size, generally does not fixate. For a large ensemble of populations, this implies that the probability distribution for the population composition converges to limit distributions (Figs 2 and 4), which are nothing like Kimura's result for constant-sized populations. Our result is also quite different from that obtained in range expansion experiments [37] or other settings featuring population growth without death on two-dimensional substrates. There, monoclonal sectoring patterns arise as a consequence of random genetic drift, which drives population differentiation along the expanding fronts of bacterial colonies, unlike our well-mixed populations that freeze to coexistence.

Our study also shows that, in a growing population with stochastic initial conditions, demographic noise has two possible sources: the initial sampling process by which subpopulations are formed, and the subsequent growth process. The initial average population size  $\bar{N}_0$  sets

their relative weight (see [S3 Text](#) and [S1 Fig](#)). For very small  $\bar{N}_0$ , of the order of one or two individuals, the formation process already determines the final composition distribution: most populations start off fixated, many with just a single founder individual, and the composition of each well remains the same during growth. For very large  $\bar{N}_0$ , of the order of a few hundreds, the sampling process is again central: the composition distribution changes very little before freezing, and growth generates only a very limited amount of variation. In these two limiting regimes, neglecting stochastic effects during growth leaves the evolutionary outcome practically unchanged. In contrast, for small founder colonies such as those typically found during population bottlenecks [[18](#), [19](#), [38](#)] ( $\bar{N}_0 \sim 10$ ), population growth is responsible for the major part of the variation observed in the final distribution.

Moreover, our results reveal that a growing population reaches a random limit composition much faster than genetic drift leads to fixation in populations of constant size. Typical fixation times for genetic drift increase logarithmically with the population size [[11](#)], while the time scale for freezing is independent of population size. This has important consequences for the role of stochastic effects when a population passes from exponential growth phase to stationary phase, in which growth rate and death rate are equal. Then, the composition of the population shows both freezing and fixation, albeit at quite distinct times because the relevant time scales differ markedly. During growth the composition distribution quickly freezes, as described above. Once the population reaches its stationary size, it slowly drifts to fixation, following Kimura-like dynamics.

We also believe that our results have a broad range of applications since growing populations are ubiquitous in nature. For example, experimental studies of *P. aeruginosa* [[22](#), [39](#)] have shown that typical life cycles pass through different steps with regularly occurring dispersal events being followed by the formation of new colonies. As initial colony sizes are typically small, such dispersal events coincide with *population bottlenecks* and subsequent exponential growth. During these phases of the life cycle, population dynamics is often selectively neutral and hence falls within the framework of the present work. The degree of diversity generated during these population bottlenecks has been shown to be crucial for some proposed mechanisms for the evolution of cooperation under selective pressure [[5–7](#), [40–42](#)]. Our analysis quantifies the ensuing degree of diversity and points to the relative importance of sampling versus growth for long-term behavior of the reservoirs. This may have important consequences for the degree of genetic diversity observed in natural populations with life-cycle structures [[38](#)].

## Materials and Methods

### Strains and cultivation conditions

The *P. putida* strains KT2440 (wild type) and 3E2 (mutant with defective pyoverdine synthesis) [[3](#)] were used as pyoverdine producers and non-producers, respectively. Cells were grown in casamino acid medium (CAA) containing per liter: 5 g casamino acids, 0.8445 g  $K_2HPO_4$ , 0.1404g  $MgSO_4 \cdot (H_2O)$  [[3](#)]. The CAA medium was supplemented with 200  $\mu M$   $FeCl_3$  (CAA-Fe) to suppress pyoverdine production (see [S2 Table](#)). Overnight cultures of the individual strains in CAA-Fe medium were adjusted to an  $OD_{600}$  of 1, diluted  $10^{-2}$  fold, mixed to yield the desired producer fraction, and further diluted to create Poisson distribution conditions. Producer/non-producer co-cultures were started by inoculating the central 60 wells of two 96-well plates thereby adjusting the average initial cell number  $\bar{N}_0$  to values between 2 and 25 cells/150  $\mu L$ . Wells at the border of the plates were filled with water to minimize evaporation from central wells. For non-selective growth, co-cultures were grown in CAA-Fe medium shaking at 30°C for given periods of time. Due to the random distribution of initial cell number  $N_0$  and producer fraction  $x_0$  in the 120 wells, each experiment was unique. An experiment was

limited to 120 wells to allow initiation of the analysis of the subpopulations in the individual wells without uncontrolled changes of growth parameters during analysis. The experiment duration was set to 11h to allow evolution to act for a significant number of generations (see [S1 Table](#)), while leaving bacteria in exponential growth phase (see [S2 Fig](#))

### Determination of growth parameters

Cell numbers  $N_0$  and  $N(t)$  were determined by counting the colony forming units (cfu) of individual wells. For this purpose 100 $\mu$ L aliquots of the individual wells were plated on cetrimide [\[43\]](#) or King's B agar (contains per liter: 20 g peptone, 10 g glycerol, 1.965 g  $K_2HPO_4(3H_2O)$ , 0.842 g  $MgSO_4(H_2O)$  [\[44\]](#)). Producer fractions  $x_0$  and  $x(t)$  were determined based on the capability of cells to produce the green fluorescent pyoverdine either by direct counting of fluorescent and non-fluorescent colonies on the plates or after growth in iron-limited CAA medium. The fraction of dead cells was determined by life/dead staining with propidium iodide [\[45\]](#), and was always  $<0.02$  of the total cell number under the experimental conditions.

### Simulation of growing populations

We performed simulations of 10080 wells using a Gillespie algorithm [\[46\]](#). The initial numbers of "cells" per well were drawn at random from a Poisson distribution with a mean value of  $\bar{N}_0$  measured in the corresponding experiment. The strain assigned to every individual in each well was determined by the outcome of a Bernoulli trial (i.e., coin-flip-like process) and the probability of assignment to strain A was set to the value of  $\bar{x}_0$  measured in the experiment. After initialization, wells were grouped into 84 virtual 120-well "plates", and a random waiting time was selected for each well, drawn from an exponential distribution with the population size as parameter. The Gillespie algorithm was run until the average size across all wells matched the average size measured at the end of the growth experiments, or until a specified time had elapsed (see [S2 Fig](#)).

### Supporting Information

**S1 Video. Time evolution of composition distribution.** The distribution of compositions  $x$  first broadens due to demographic noise, but soon "freezes" to a steady state. The steady state form is maintained as long as the populations grow. Parameter values are  $\bar{N}_0 = 10$ ,  $\bar{x}_0 = 0.33$  (as for [Fig 2](#)).  
(MP4)

**S1 Text. Exact calculations for steady-state composition distribution and moments.** Using the theory of Pólya urns, we calculate exactly the steady state values of: (i) the distribution of population compositions  $x$ , (ii) its mean value, and (iii) its variance.  
(PDF)

**S2 Text. Approximate calculations for the time evolution of the distribution moments.** We use the Master equation of the growth process ([Eq \(1\)](#)) to determine the time evolution of variance and skewness of the composition distribution. These values are used in [Eq \(2\)](#) and [Fig 2](#).  
(PDF)

**S1 Fig. Initial and steady state distributions, relative entropy.** Panels (a),(b),(c): Initial and final distributions of  $x$  for three regimes of  $\bar{N}_0$ . When  $\bar{N}_0$  is very small or very large (panels (a) and (b)), the evolutionary fate of the population is largely determined by the initial population sampling. Therefore, the initial distribution (red bars) and the steady-state one (green bars) look qualitatively very similar. For intermediate values of  $\bar{N}_0$ , however, population growth

becomes more important, and the distributions look very different. The amount of composition values the population can access through growth can be quantified looking at the “unpredictability” of the steady-state composition, once the initial one is known: the more unpredictable, the more are made accessible by growth. Mathematically, the measure for this is called *conditional entropy*: the higher the entropy, the more unpredictable the outcome. Panel (d) shows the conditional entropy as function of  $\bar{N}_0$ . Indeed, very small or very large initial populations experience little to no additional noise from growth, while in populations with intermediate values of  $\bar{N}_0$  ( $\bar{N}_0 \simeq 15$ ) growth is a major source of demographic noise. (Parameter values:  $\bar{N}_0 = 2$  (a),  $\bar{N}_0 = 2000$  (b),  $\bar{N}_0 = 20$  (c);  $\bar{x}_0 = 0.25$  in all panels) (TIF)

**S3 Text. Comparison of initial and steady-state distributions of  $x$ , and entropy of the steady state distribution conditioned on the initial one.** We use conditional entropy to analyze the impact of growth on the distribution of compositions  $x$ . The results are also depicted in [S1\(d\) Fig](#) (PDF)

**S2 Fig. Growth curve of a mixed population.** The population consists of pyoverdine producer (*P. putida* KT2440) and non-producer (*P. putida* 3E2) under non-selective (iron replete) conditions. Individual precultures of the strains were mixed and diluted in iron replete medium to yield  $\bar{N}_0 = 4$  (in 150  $\mu\text{L}$ ), and  $\bar{x}_0 = 0.5$ . Cells were grown aerobically at 30°C for 24 hours. The dots represent the mean  $N(t)$  of three independent replications, the bars the corresponding standard deviation. After a lag phase of about 2 hours, the cells start to grow exponentially and reach the stationary phase after about 14 h of growth. For the non-selective growth experiments used to test the predictions of the Pólya urn model, cells were grown for 11.5 h to ensure exponential growth conditions. (TIF)

**S3 Fig. Additional initial conditions measurements.** The experimental distributions (bars) are measured from 120-well ensembles, the average  $N_0$  and  $x_0$  from those sets the parameters for the simulated distributions. The theoretical average distribution (solid line) is the average of the same distributions generated for 84 sets of 120 wells. Using that average we calculate three Wilson binomial confidence intervals (gray areas). Experiments and theory agree within statistical error: the distribution of sizes (panels (a) and (c)) follows a Poisson distribution. The raggedness of the distribution of  $x$  for at small  $\bar{N}_0$  (see panel (b) and [Fig 3\(b\)](#) in main text) is due to a small size effect: since  $x$  must be a simple fraction, when  $N_0$  is small only a few values are available (see main text). This effect disappears for average initial sizes  $\bar{N}_0 \simeq 10$  (see panel (d)). Parameter values:  $\bar{N}_0 = 5.75$ ,  $\bar{x}_0 = 0.43$  (a) and (b);  $\bar{N}_0 = 26.49$ ,  $\bar{x}_0 = 0.45$  (c) and (d). (TIF)

**S1 Table. Comparison between results from our experiments and those in [9].** While experiments for constant-sized populations of *Drosophila* observe significant fixations within the first tens of generations, we instead observe freezing of the probability distribution for the population composition, without any fixation. (PDF)

**S2 Table. Comparison of growth and pyoverdine production per cell of *P. putida* KT2440 and 3E2.** Separate cultures of producer (*P. putida* KT2440) and non-producer (*P. putida* 3E2) were grown in iron-limiting (no addition of  $\text{FeCl}_3$ ) and iron-replete medium (addition of 200  $\mu\text{M}$   $\text{FeCl}_3$ ) at 30°C. The cell density was measured at 600 nm, and specific growth rates were calculated from density values of the exponential phase. The pyoverdine production was

determined by fluorescence emission measurements (excitation 400 nm, emission at 460 nm). The pyoverdine production per cell represents the ratio of pyoverdine fluorescence and optical density measured after 24 h of growth. The values in the table are averages over a minimum of five experiments, with the corresponding standard deviation. The fluorescence value for the non-producing mutant in iron-limiting medium is 0 because the culture failed to grow. (PDF)

## Acknowledgments

For fruitful discussions we thank Madeleine Opitz, Johannes Knebel, Markus Weber, Stefano Duca, Matthias Bauer, Kirsten Jung. We thank Michelle Eder (HJ lab) for excellent technical assistance. *P. putida* strain 3E2 was kindly provided by P. Cornelis (Vrije Universiteit Brussels, Belgium).

## Author Contributions

Conceived and designed the experiments: HJ FB. Performed the experiments: HJ FB. Analyzed the data: FB HJ ML KW EF. Contributed reagents/materials/analysis tools: EF ML KW. Wrote the paper: EF HJ ML KW. Designed theoretical analysis: EF ML KW. Performed theoretical analysis: ML KW.

## References

1. Kimura M (1955) Solution of a process of random genetic drift with a continuous model. PNAS. PMID: [16589632](#)
2. Otto SP, Whitlock MC (1997) The probability of fixation in populations of changing size. Genetics 146: 723–733. PMID: [9178020](#)
3. Matthijs S, Laus G, Meyer JM, Abbaspour-Tehrani K, Schäfer M, et al. (2009) Siderophore-mediated iron acquisition in the entomopathogenic bacterium *Pseudomonas entomophila* I48 and its close relative *Pseudomonas putida* KT2440. Biometals 22: 951–964. doi: [10.1007/s10534-009-9247-y](#) PMID: [19459056](#)
4. Eggenberger F, Pólya G (1923) Über die statistik verketteter vorgänge. ZAMM—Journal of Applied Mathematics and Mechanics / Zeitschrift für Angewandte Mathematik und Mechanik 3: 279–289.
5. Melbinger A, Cremer J, Frey E (2010) Evolutionary game theory in growing populations. Phys Rev Lett 105: 178101. doi: [10.1103/PhysRevLett.105.178101](#) PMID: [21231082](#)
6. Cremer J, Melbinger A, Frey E (2011) Evolutionary and population dynamics: a coupled approach. Phys Rev E 84: 051921. doi: [10.1103/PhysRevE.84.051921](#)
7. Cremer J, Melbinger A, Frey E (2012) Growth dynamics and the evolution of cooperation in microbial populations. Sci Rep 2: 281. doi: [10.1038/srep00281](#) PMID: [22355791](#)
8. Crow JF, Kimura M (1970) An Introduction to Population Genetics. Harper and Row.
9. Hartl DL, Clark AG (1989) Principles of population genetics. Sinauer, Sunderland, MD, USA, 2nd edition.
10. Frey E, Kroy K (2005) Brownian motion: a paradigm of soft matter and biological physics. Ann Phys 14: 20–50. doi: [10.1002/andp.200410132](#)
11. Blythe RA, McKane J (2007) Stochastic models of evolution in genetics, ecology and linguistics. J Stat Mech: 07018. doi: [10.1088/1742-5468/2007/07/P07018](#)
12. Caballero A (1994) Developments in the prediction of effective population size. Heredity 73: 657–679. doi: [10.1038/hdy.1994.174](#) PMID: [7814264](#)
13. Gillespie JH (2001) Is the population size of a species relevant to its evolution? Evolution 55: 2161–2169. doi: [10.1554/0014-3820\(2001\)055%5B2161:ITPSOA%5D2.0.CO;2](#) PMID: [11794777](#)
14. Hahn MW (2008) Toward a selection theory of molecular evolution. Evolution 62: 255–265. doi: [10.1111/j.1558-5646.2007.00308.x](#) PMID: [18302709](#)
15. Hurst LD (2009) Fundamental concepts in genetics: genetics and the understanding of selection. Nat Rev Genet 10: 83–93. doi: [10.1038/nrg2506](#) PMID: [19119264](#)

16. Buri P (1956) Gene frequency in small populations of mutant drosophila. *Evolution* 10: 367–402. doi: [10.2307/2406998](https://doi.org/10.2307/2406998)
17. Center for Food Safety and Applied Nutrition Causes of Foodborne Illness: Bad Bug Book—BBB—*Escherichia coli* O157:H7 (EHEC). Provides basic information about *Escherichia coli* O157:H7.
18. Kurjak A, Chervenak FA (2006) Textbook of Perinatal Medicine. Informa UK Ltd, 2nd edition.
19. Grossart HP, Levold F, Allgaier M, Simon M, Brinkhoff T (2005) Marine diatom species harbour distinct bacterial communities. *Environmental Microbiology* 7: 860–873. doi: [10.1111/j.1462-2920.2005.00759.x](https://doi.org/10.1111/j.1462-2920.2005.00759.x) PMID: [15892705](https://pubmed.ncbi.nlm.nih.gov/15892705/)
20. Bird DF, Kalf J (1984) Empirical relationships between bacterial abundance and chlorophyll concentration in fresh and marine waters. *Can J Fish Aquat Sci* 41: 1015–1023. doi: [10.1139/f84-118](https://doi.org/10.1139/f84-118)
21. Buchan A, LeCleir GR, Gulvik CA, González JM (2014) Master recyclers: features and functions of bacteria associated with phytoplankton blooms. *Nat Rev Micro* 12: 686–698. doi: [10.1038/nrmicro3326](https://doi.org/10.1038/nrmicro3326)
22. Stoodley P, Sauer K, Davies DG, Costerton JW (2002) Biofilms as complex differentiated communities. *Annual Review of Microbiology* 56: 187–209. doi: [10.1146/annurev.micro.56.012302.160705](https://doi.org/10.1146/annurev.micro.56.012302.160705) PMID: [12142477](https://pubmed.ncbi.nlm.nih.gov/12142477/)
23. Levin SA (1974) Dispersion and population interactions. *The American Naturalist* 108: 207–228. doi: [10.1086/282900](https://doi.org/10.1086/282900)
24. Sanchez A, Gore J (2013) Feedback between population and evolutionary dynamics determines the fate of social microbial populations. *PLoS biology* 11: e1001547. doi: [10.1371/journal.pbio.1001547](https://doi.org/10.1371/journal.pbio.1001547) PMID: [23637571](https://pubmed.ncbi.nlm.nih.gov/23637571/)
25. Parsons TL, Quince C, Plotkin JB (2010) Some consequences of demographic stochasticity in population genetics. *Genetics* 185: 1345–1354. doi: [10.1534/genetics.110.115030](https://doi.org/10.1534/genetics.110.115030) PMID: [20457879](https://pubmed.ncbi.nlm.nih.gov/20457879/)
26. Buckling A, Harrison F, Vos M, Brockhurst MA, Gardner A, et al. (2007) Siderophore-mediated cooperation and virulence in *Pseudomonas aeruginosa*. *FEMS Microbiol Ecol* 62: 135–41. doi: [10.1111/j.1574-6941.2007.00388.x](https://doi.org/10.1111/j.1574-6941.2007.00388.x) PMID: [17919300](https://pubmed.ncbi.nlm.nih.gov/17919300/)
27. Cornelis P, Matthijs S, Van Oeffelen L (2009) Iron uptake regulation in *Pseudomonas aeruginosa*. *Bio-metals* 22: 15–22. doi: [10.1007/s10534-008-9193-0](https://doi.org/10.1007/s10534-008-9193-0) PMID: [19130263](https://pubmed.ncbi.nlm.nih.gov/19130263/)
28. Cohen JE (1976) Irreproducible results and the breeding of pigs (or nondegenerate limit random variables in biology). *BioScience* 26: 391–394.
29. Schreiber SJ (2001) Urn models, replicator processes, and random genetic drift. *SIAM Journal on Applied Mathematics* 61: 2148–2167. doi: [10.1137/S0036139999352857](https://doi.org/10.1137/S0036139999352857)
30. Sornette D (2009) *Why Stock Markets Crash: Critical Events in Complex Financial Systems*. Princeton University Press.
31. Pemantle R (2007) A survey of random processes with reinforcement. *Probability Surveys* 4: 1–79. doi: [10.1214/07-PS094](https://doi.org/10.1214/07-PS094)
32. Athreya KB, Karlin S (1968) Embedding of urn schemes into continuous time markov branching processes and related limit theorems. *The Annals of Mathematical Statistics* 39: 1801–1817. doi: [10.1214/aoms/1177698013](https://doi.org/10.1214/aoms/1177698013)
33. Kotz S, Mahmoud H, Robert P (2000) On generalized pólya urn models. *Statistics & Probability Letters* 49: 163–173.
34. Allen L (2003) *An Introduction to Stochastic Processes with Biology Applications*. Prentice Hall.
35. Arthur WB, Ermoliev YM, Kaniovski YM (1987) Path-dependent processes and the emergence of macro-structure. *European Journal of Operational Research* 30: 294–303. doi: [10.1016/0377-2217\(87\)90074-9](https://doi.org/10.1016/0377-2217(87)90074-9)
36. Wilson EB (1927) Probable inference, the law of succession, and statistical inference. *Journal of the American Statistical Association* 22: 209–212. doi: [10.1080/01621459.1927.10502953](https://doi.org/10.1080/01621459.1927.10502953)
37. Hallatschek O, Hersen P, Ramanathan S, Nelson DR (2007) Genetic drift at expanding frontiers promotes gene segregation. *PNAS* 104: 19926–19930. doi: [10.1073/pnas.0710150104](https://doi.org/10.1073/pnas.0710150104) PMID: [18056799](https://pubmed.ncbi.nlm.nih.gov/18056799/)
38. Hammerschmidt K, Rose CJ, Kerr B, Rainey PB (2014) Life cycles, fitness decoupling and the evolution of multicellularity. *Nature* 515: 75–79. doi: [10.1038/nature13884](https://doi.org/10.1038/nature13884) PMID: [25373677](https://pubmed.ncbi.nlm.nih.gov/25373677/)
39. Hall-Stoodley L, Costerton JW, Stoodley P (2004) Bacterial biofilms: from the natural environment to infectious diseases. *Nat Rev Microbiol* 2: 95–108. doi: [10.1038/nrmicro821](https://doi.org/10.1038/nrmicro821) PMID: [15040259](https://pubmed.ncbi.nlm.nih.gov/15040259/)
40. Chuang JS, Rivoire O, Leibler S (2009) Simpson's paradox in a synthetic microbial system. *Science* 323: 272–5. doi: [10.1126/science.1166739](https://doi.org/10.1126/science.1166739) PMID: [19131632](https://pubmed.ncbi.nlm.nih.gov/19131632/)
41. Oliveira NM, Niehus R, Foster KR (2014) Evolutionary limits to cooperation in microbial communities. *PNAS* 111: 17941–17946. doi: [10.1073/pnas.1412673111](https://doi.org/10.1073/pnas.1412673111) PMID: [25453102](https://pubmed.ncbi.nlm.nih.gov/25453102/)
42. Melbinger A, Cremer J, Frey E The emergence of cooperation from a single cooperative mutant.

43. Brown VI, Lowbury E JL (1965) Use of an improved cetrinide agar medium and other culture methods for pseudomonas aeruginosa. *J Clin Pathol* 18: 752–756. doi: [10.1136/jcp.18.6.752](https://doi.org/10.1136/jcp.18.6.752) PMID: [4954265](https://pubmed.ncbi.nlm.nih.gov/4954265/)
44. King EO, Ward MK, Raney DE (1954) Two simple media for the demonstration of pyocyanin and fluorescin. *Journal of Laboratory and Clinical Medicine* 44: 301–307. PMID: [13184240](https://pubmed.ncbi.nlm.nih.gov/13184240/)
45. Suzuki T, Fujikura K, Higashiyama T, Takata K (1997) DNA staining for fluorescence and laser confocal microscopy. *J Histochem Cytochem* 45: 49–53. doi: [10.1177/002215549704500107](https://doi.org/10.1177/002215549704500107) PMID: [9010468](https://pubmed.ncbi.nlm.nih.gov/9010468/)
46. Gillespie D (1976) General method for numerically simulating stochastic time evolution of coupled chemical reactions. *J Comp Phys* 22: 403–434.

**Interactions mediated by a public good transiently increase cooperativity in growing *Pseudomonas putida* metapopulations**

Felix Becker, Karl Wienand, Matthias Lechner, Erwin Frey & Heinrich Jung  
Scientific Reports, March 2018, Volume 8, Issue 1, 4093

# SCIENTIFIC REPORTS

OPEN

## Interactions mediated by a public good transiently increase cooperativity in growing *Pseudomonas putida* metapopulations

Felix Becker<sup>1</sup>, Karl Wienand<sup>2</sup>, Matthias Lechner<sup>2</sup>, Erwin Frey<sup>1,2</sup> & Heinrich Jung<sup>1</sup>

Bacterial communities have rich social lives. A well-established interaction involves the exchange of a public good in *Pseudomonas* populations, where the iron-scavenging compound pyoverdine, synthesized by some cells, is shared with the rest. Pyoverdine thus mediates interactions between producers and non-producers and can constitute a public good. This interaction is often used to test game theoretical predictions on the “social dilemma” of producers. Such an approach, however, underestimates the impact of specific properties of the public good, for example consequences of its accumulation in the environment. Here, we experimentally quantify costs and benefits of pyoverdine production in a specific environment, and build a model of population dynamics that explicitly accounts for the changing significance of accumulating pyoverdine as chemical mediator of social interactions. The model predicts that, in an ensemble of growing populations (metapopulation) with different initial producer fractions (and consequently pyoverdine contents), the global producer fraction initially increases. Because the benefit of pyoverdine declines at saturating concentrations, the increase need only be transient. Confirmed by experiments on metapopulations, our results show how a changing benefit of a public good can shape social interactions in a bacterial population.

Bacteria have complex social lives: they communicate with each other and with other organisms, form tight communities in biofilms, exhibit division of labor, compete, and cooperate<sup>1–7</sup>. They also produce and exchange public goods. Public goods are chemical substances that are synthesized by some individuals (known as *producers* or *cooperators*) and are then shared evenly among the whole population, including cells that did not contribute to their production<sup>8–10</sup>. Such social interactions can also influence population dynamics, as exemplified in the context of metapopulations<sup>11–17</sup>. Metapopulations consist of several subpopulations. The subpopulations may grow independently for a time, then merge into a single pool that later splits again, restarting the cycle. This ecological system, which mimics some bacterial life-cycles<sup>18,19</sup>, also dramatically impacts the population's internal dynamics. To mathematically analyze the effects of social interactions, they can be framed in terms of game theoretical models<sup>20–24</sup> –for instance, the prisoner's dilemma, in the case of the exchange of public goods<sup>25–28</sup> –or formulated in terms of inclusive fitness models<sup>29–31</sup>. These approaches underestimate the impact on the social interaction of specific properties and mechanisms of action of the public good in question, mostly to simplify the mathematical description. Previous investigations have shown that, for example, phenomena like public good diffusion<sup>32–34</sup>, interference of different public goods with each other<sup>35</sup>, the regulatory nature of public good production<sup>36</sup>, or its function in inter-species competition<sup>37</sup> may affect strain competition. The shortcomings of game-theoretical models in studying the evolution of cooperation can be overcome by systems biology modeling approaches<sup>34,38,39</sup>.

<sup>1</sup>Microbiology, Department Biology 1, Ludwig-Maximilians-Universität Munich, Grosshaderner Strasse 2-4, D-82152 Martinsried, Germany. <sup>2</sup>Arnold-Sommerfeld-Center for Theoretical Physics and Center for Nanoscience, Ludwig-Maximilians-Universität, Theresienstrasse 37, D-80333, Munich, Germany. Felix Becker and Karl Wienand contributed equally to this work. Correspondence and requests for materials should be addressed to E.F. (email: [frey@lmu.de](mailto:frey@lmu.de)) or H.J. (email: [hjung@lmu.de](mailto:hjung@lmu.de))

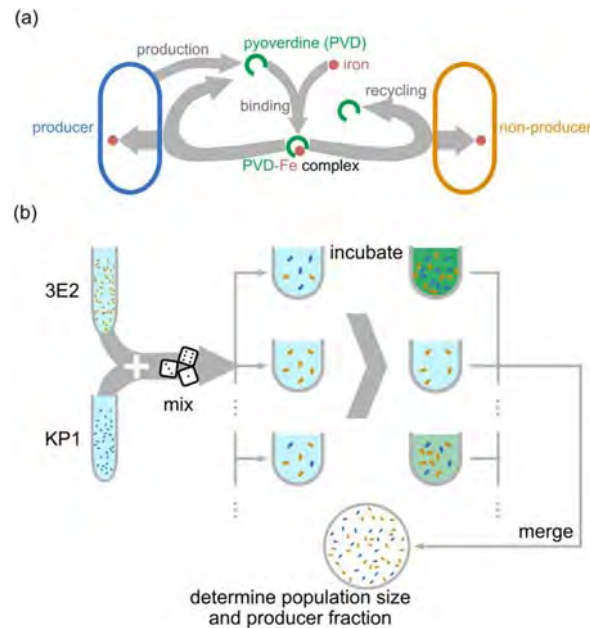


**Figure 1.** Outline of PVD-mediated interactions and experimental setting. **(a)** Outline of the social interaction. Producers (blue) secrete pyoverdine (PVD, green) into the environment, where it binds iron (red). The resulting Fe-PVD complex is transported into the periplasm of both producers and non-producers. Iron is reduced and incorporated into cells, while PVD is transported back into the environment to scavenge additional ferric ions<sup>44–46</sup>. **(b)** Metapopulation growth setting. We initiate a metapopulation by mixing producers and non-producers in random proportions and inoculating the individual populations, which grow independently. At given time points  $t$ , we take samples from each population, and merge them to determine the average population size and the global producer fraction of the metapopulation.

In this work, we directly quantify a social interaction mediated by a public good. Thus, we adopt a systems biology approach, rather than a more reductive game-theoretical one. We focus on the dissemination of iron-scavenging pyoverdine (PVD) in a metapopulation of fluorescent *Pseudomonas putida*, and study how its biological function determines the population dynamics.

In this well-established, native model system, cells secrete PVD into the environment to facilitate iron uptake when the metal becomes scarce<sup>29,40–44</sup>. PVD binds to ferric iron and is then actively transported into the periplasm. There, the iron is reduced, released and transported across the plasma membrane, while PVD is secreted back into the environment<sup>44–46</sup>. Figure 1 outlines the PVD-mediated interaction between producer and non-producer cells and the metapopulation set-up we use to study its effects on population dynamics.

In the following, we show, both experimentally and in computer simulations, that the global fraction of producer cells across a metapopulation increases during growth, but only transiently. This effect hinges on the specifics of PVD biochemistry, which elude a game-theoretical analysis. Thus, our study shows that the specific features of the public good considered are the key determinant of the outcome of the social interaction. Our experiments employ a well-defined system, with a constitutive producer and a non-producer strain. The simulations use a mathematical model based on quantitative measurements of PVD's costs and benefits, as well as its behavior as an accumulating public good. For appropriate values of the parameters, the theoretical results match those of experiments with *P. putida* metapopulations.

## Results

**Characterization of the model system.** To investigate the social role of public goods, we chose the soil bacterium *P. putida* KT2440 as a model system. This is a well-defined system in which, as sketched in Fig. 1a, a single public good mediates all cell-cell interactions. *P. putida* KT2440 synthesizes a single type of siderophore – a pyoverdine (PVD) molecule<sup>47</sup> – and does not produce 2-heptyl-3-hydroxy-4-quinolone or other known quorum-sensing molecules that might otherwise interfere with the social interaction<sup>48–50</sup>.

Wild-type *P. putida* KT2440 controls PVD production through a complex regulatory network. As shown in Fig. 2a, the central element of the network is the ferric uptake regulator (Fur) protein, which binds iron and, among other things, down-regulates expression of the iron starvation sigma factor *pfr*<sup>51–53</sup>, which in turn directs the transcription of PVD synthesis genes. As a consequence, siderophore production continually adapts to the availability of iron<sup>47,52</sup>. This regulation, however, obscures the costs of PVD production, as it also affects other processes. We therefore circumvented it by generating a *P. putida* strain, called KP1, which constitutively produces

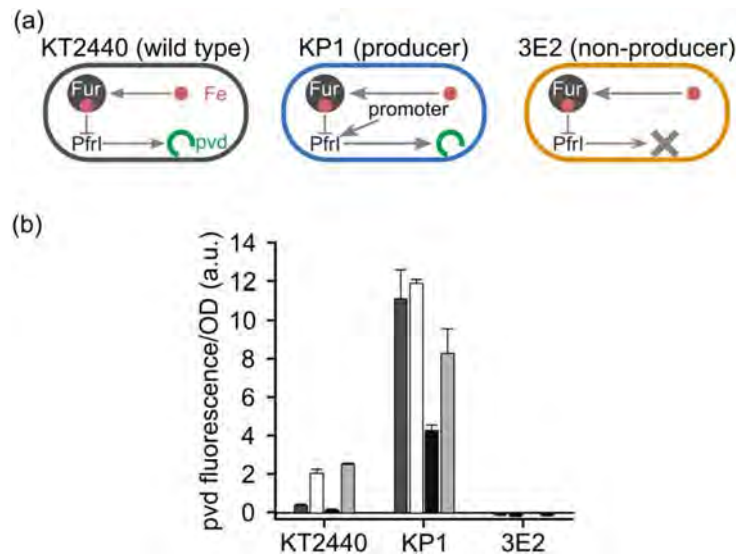


**Figure 2.** Characterization of the strains. (a) Sketch of each strain's regulatory system. In the wild-type *P. putida* KT2440 (gray), the ferric uptake regulator Fur binds iron and represses the expression of the *pfrI* gene necessary for PVD synthesis. The constitutive producer strain KP1 (blue) carries an additional copy of the *pfrI* gene controlled by a constitutive promoter. The non-producer strain 3E2 (orange) has an inactivated non-ribosomal peptide synthetase gene, which prevents PVD synthesis. (b) Average PVD production per cell by the wild-type and strains KP1 and 3E2 after 8 h of cultivation. The darker the columns, the more abundant is the iron in the medium. Dark gray columns represent moderate iron availability conditions (KB medium without additions); white columns represent extreme iron limitation (KB/1 mM DP); black columns represent iron-replete conditions (KB/100  $\mu$ M FeCl<sub>3</sub>); light gray columns represent iron-limiting conditions (KB/100  $\mu$ M FeCl<sub>3</sub>/1 mM DP). KP1 produces PVD under all conditions (albeit with different yields), 3E2 never produces the siderophore, and the wild-type adapts its rate of synthesis to iron availability.

PVD. KP1 carries a copy of the *pfrI* gene controlled by the constitutive promoter P<sub>A1/04/03</sub><sup>54</sup> at the *attTn7* site in the KT2440 genome. As the non-producer, we used strain 3E2, which carries an inactivated non-ribosomal peptide synthetase gene (pp4220) that inhibits PVD synthesis<sup>47</sup>. The two strains were otherwise isogenic.

We characterized producer (KP1) and non-producer (3E2) strains by measuring their average per-cell PVD production under different iron availabilities, and comparing the results with those for the wild type (strain KT2440). We cultivated all three strains, separately, in KB medium and KB supplemented with 100  $\mu$ M FeCl<sub>3</sub> (for short, KB/100  $\mu$ M FeCl<sub>3</sub>), as well as in the same two media supplemented with the chelator dipyriddy (DP, 1 mM) to reduce iron availability. Using atom absorption spectroscopy, we determined an iron concentration in KB of about 8  $\mu$ M. Figure 2b shows the average amount of PVD produced per cell after 8 h of growth (close to the end of exponential growth). The wild type partially represses production of PVD under moderate iron availability (KB, dark gray bars), and ceases synthesis altogether under high iron availability (KB/100  $\mu$ M FeCl<sub>3</sub>, black bars). Addition of DP reduces iron availability and stimulates PVD production in both media (Fig. 2b, white bars: KB/1 mM DP, light gray bars: KB). In contrast, KP1 produces large amounts of PVD under all tested growth conditions, and thus represents a constitutive PVD producer. The yield depends on conditions, probably because the regulated copy of *pfrI* is still present in the genome. 3E2, finally, never synthesizes PVD, regardless of the conditions, and is a true non-producer, as previously reported<sup>47</sup>.

**Quantifying the social role of pyoverdine.** Having established how each strain behaves, we quantified the impact of PVD on population dynamics. Specifically, we wanted to determine the metabolic load of PVD production, its impact on growth, its stability, and how evenly it is shared with other cells.

We assessed the impact of PVD production on growth by comparing the growth rates of strains KP1 and 3E2 under iron-rich conditions (KB). As shown in Fig. 2b, neither 3E2 nor the wild-type produces substantial amounts of PVD under these conditions, and the solid symbols in Fig. 3a show that both strains grow at about the same rate. KP1, on the other hand, produces PVD and grows more slowly. The data in Supplementary Table S1 allow us to quantify this difference in growth rate. Depending on the conditions, KP1's growth rate is 3–10% lower than that of strain 3E2. For example, the difference is minimized (1.03-fold) when the medium is replaced (in a 24-well plate format) every hour, whereas the largest difference (1.10-fold) is observed in batch cultures (96-well plate format). This suggests that factors other than iron level *per se*, such as nutrients and oxygen availability, modify the metabolic impact of PVD production.

The empty symbols in Fig. 3a illustrate the growth of the strains under extreme iron limitation (KB/1 mM DP). In these conditions, PVD is indispensable for iron uptake, and only producing strains – KP1 and the wild-type – can grow at all. Less restrictive conditions (KB/100  $\mu$ M FeCl<sub>3</sub> and KB/100  $\mu$ M FeCl<sub>3</sub>/1 mM DP) produce

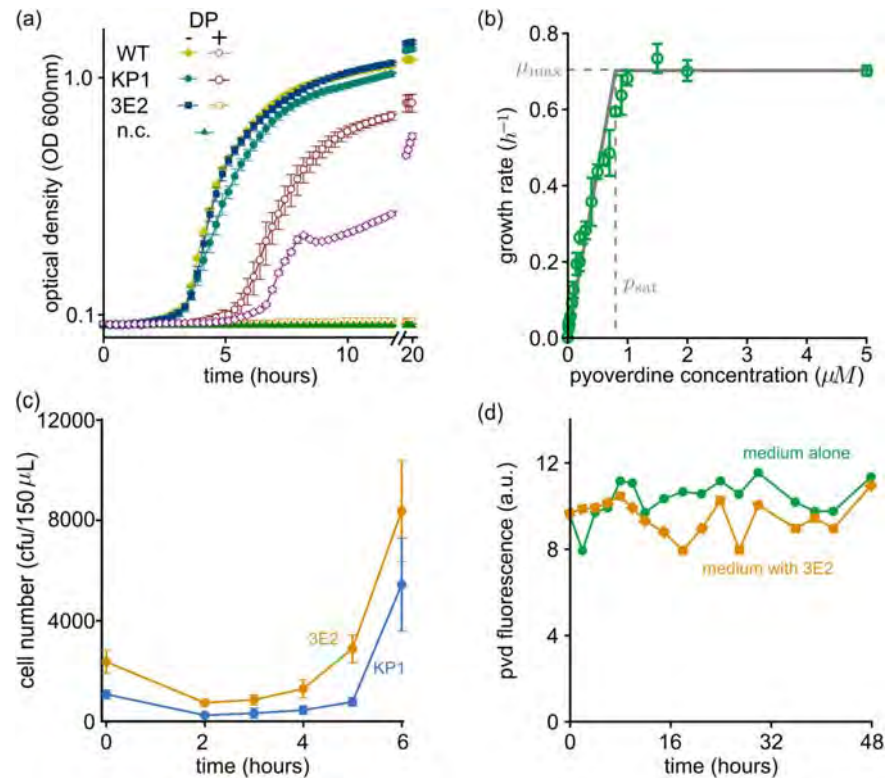


**Figure 3.** Characterization of the social impact of pyoverdine (PVD) in terms of costs (a), benefits (b), degree of sharing among cells (c) and stability (d). (a) In an environment with available iron (KB, solid symbols), non-producer cells (strain 3E2) grows as fast as the wild-type (WT), and faster than the producer (strain KP1). Under extreme iron limitation (KB /1 mM DP, empty symbols), PVD is needed for growth: KP1 and WT grow, whereas 3E2 does not (mean values and standard deviations were calculated from six measurements). (b) Green dots represent the growth rate  $\mu$  of 3E2 cultures, measured under extreme iron limitation (KB/1 mM DP) in the presence of the indicated concentrations of added PVD (error bars are standard deviation over four replicates). The solid gray line represents the growth rate calculated using equation (2) (maximal growth rate  $\mu_{\text{max}}$  and the saturation concentration  $p_{\text{sat}}$  fitted to the experimental data:  $\mu_{\text{max}} = 0.878$ ,  $p_{\text{sat}} = 0.8$ ). (c) Early growth of KP1–3E2 co-cultures (initial fraction of KP1 = 0.33) under extreme iron limitation (KB/1 mM DP). Shown are mean and SD of eight independent experiments. Since 3E2 needs PVD to grow (see panel b), this result indicates that PVD is shared between the strains. (d) Stability of PVD (2  $\mu\text{M}$ ) in KB medium and in the presence of the non-producer 3E2. The fluorescence emission was recorded at 460 nm (excitation 400 nm).

qualitatively similar results (see Supplementary Fig. S1). 3E2, if cultivated alone, cannot grow unless the medium is supplemented with PVD isolated from a producer culture. Figure 3b shows the maximal growth rate of 3E2 under these conditions as a function of the concentration of added PVD. For values lower than about 1  $\mu\text{M}$ , the growth rate increases almost linearly with PVD concentration, then sharply levels off. Higher PVD concentrations do not further stimulate growth – which is consistent with observations of iron saturation in other bacterial systems<sup>55,56</sup>.

This saturating behavior, we argue, stems directly from PVD's ability to bind iron and make it available to cells. Because PVD has an extremely high affinity for iron [ $10^{24} \text{M}^{-1}$  for  $\text{Fe}^{3+}$  at pH 7<sup>57</sup>], we can assume that each PVD molecule immediately binds an iron ion. Therefore, the PVD concentration  $p$  is equivalent to that of PVD-Fe complexes, and represents the concentration of iron accessible to cells (this may not hold if the level of PVD exceeds that of the iron available, but we expect this extreme case to arise only after the exponential growth phase in our setting, if ever). Each cell, then, incorporates iron ions at a constant rate  $k \cdot p$  which is proportional to the PVD concentration  $p$ . Moreover, cells try to maintain a constant internal iron concentration  $Fe_{\text{in}}$  and reproduce at a PVD-dependent rate  $\mu(p)$  when growth is limited by iron availability. If we also assume that the cell volume just before division is twice the volume  $V(0)$  of a newborn cell, we find that the growth rate is proportional to  $p$  (see Supplementary Note):

$$\mu(p) = \frac{k}{Fe_{\text{in}} V(0)} p. \quad (1)$$

For PVD concentrations above  $1 \mu\text{M}$ , however, some other factor limits growth. Cells cannot further increase  $\mu(p)$ , regardless of the PVD concentration, and the benefit of PVD saturates. In summary, there is a limit PVD concentration  $p_{\text{sat}}$  ( $\sim 1 \mu\text{M}$ ), below which the growth rate is proportional to the PVD concentration, following equation (1). Above  $p_{\text{sat}}$ , the growth rate is a constant  $\mu_{\text{max}}$ , whose value depends on the culture conditions. In mathematical terms,

$$\mu(p) = \mu_{\text{max}} \min\left(\frac{p}{p_{\text{sat}}}, 1\right) = \begin{cases} \frac{\mu_{\text{max}}}{p_{\text{sat}}}p, & \text{if } p < p_{\text{sat}} \\ \mu_{\text{max}}, & \text{if } p \geq p_{\text{sat}}. \end{cases} \quad (2)$$

The gray curve in Fig. 3b shows the function described in equation (2). Fitting the values for the parameters  $p_{\text{sat}}$  and  $\mu_{\text{max}}$ , the curve closely resembles the experimental results, validating our argument.

A central question in determining the social role of PVD is whether cells share the molecule with other cells, and thus also its benefit, or keep it to themselves. In other words, to what extent is PVD a *public good*? Fig. 3c shows the early stages of growth of a mixed population of KP1 and 3E2 (initial fraction of KP1 = 0.33) under extreme iron limitation (KB/1 mM DP). After a lag phase of about 2 h, both strains begin to grow. Since 3E2 needs PVD to grow in these conditions (see above and Supplementary Fig. S1), we conclude that both strains receive the benefit at the same time, and neither has preferential access to it. In our experiments, then, PVD behaves as a truly public good. Consequently, populations that start with a higher producer fraction  $x_0$  have more PVD available, and grow faster than populations with low  $x_0$  values (as shown in Supplementary Figs S1 and S2).

PVD is also very stable. Figure 3d shows the fluorescence yield of PVD over 48 h in KB medium alone (green line). The value fluctuates around a constant average, indicating that PVD does not spontaneously degrade – at least not appreciably – within the time scales of our experiments. The orange line in Fig. 3d represents a similar measurement, but in the presence of non-producer cells. In this case also, fluorescence does not appreciably decay, so cells do not seem to consume PVD during the interaction. This also means that, provided producers are present, the public good accumulates in the environment once its synthesis has been triggered.

Taken together, these observations characterize the social interaction as follows: (i) Constitutive producers grow more slowly than non-producers (given equal PVD availability); (ii) PVD acts as a public good, which is homogeneously shared among cells; (iii) once produced, PVD persists: it is chemically and functionally stable, and cells recycle it rather than consuming it; (iv) the public good drives the population dynamics, since PVD is necessary for access to the iron required for growth.

**Modeling social and growth dynamics.** Based on the experimental results presented in the previous section, we formulated a set of equations to describe the development of a single, well-mixed population of  $c$  producers and  $f$  non-producers. The population dynamics follows a logistic growth, where the function  $\mu(p)$  from equation (2) determines the per-capita growth rate. For our experimental setup, we estimate cells to incorporate only a minimal fraction of the available iron ( $< 3\%$ , see Supplementary Note), so the assumptions of equation (2) hold (and some other resource determines the carrying capacity  $K$ ). Although KP1 synthesizes PVD at condition-dependent rates, we adopt a simplified description and model synthesis as occurring at a constant rate  $\sigma$ . The produced PVD does not decay but accumulates in the medium. Finally, the costs of PVD synthesis slow down the growth of producers by a factor  $1 - s$  (where  $s < 1$ ), compared to non-producers. All in all, assuming the interaction between cells and PVD is fast, the dynamics can be summarized in the following equations:

$$\begin{aligned} \frac{dc}{dt} &= c\mu(p)(1-s)\left(1 - \frac{c+f}{K}\right), \\ \frac{df}{dt} &= f\mu(p)\left(1 - \frac{c+f}{K}\right), \\ \frac{dp}{dt} &= \sigma c. \end{aligned} \quad (3)$$

This set of equations mathematically describes the experimental facts, in terms of measurable quantities. It is also different from a traditional game theoretical formulation, which would require us to somehow define a payoff function.

To better highlight the key factors of the population dynamics, we rescale the variables in equations (3). First, we measure population size in terms of the fraction of resources used up, i.e.,  $n = (c+f)/K$ . This definition means that  $K$  determines the scale of population sizes, while  $n$  takes values between 0 and 1: as  $n$  approaches 1, the resources become depleted, and cells enter a dormant state<sup>14</sup>. Second, we consider the fraction  $x = c/(c+f)$  of producers within each population, rather than their absolute number. Third, we measure the amount of PVD in units of the saturation concentration,  $v = p/p_{\text{sat}}$  (and define  $\mu(v) = \min(v, 1)$ ). Finally, measuring time in units of the minimal doubling time  $1/\mu_{\text{max}}$ , equations (3) become

$$\begin{aligned} \frac{dn}{dt} &= n(1-n)(1-sx)\mu(v), \\ \frac{dx}{dt} &= -sx(1-x)(1-n)\mu(v), \\ \frac{dv}{dt} &= \alpha nx, \end{aligned} \quad (4)$$

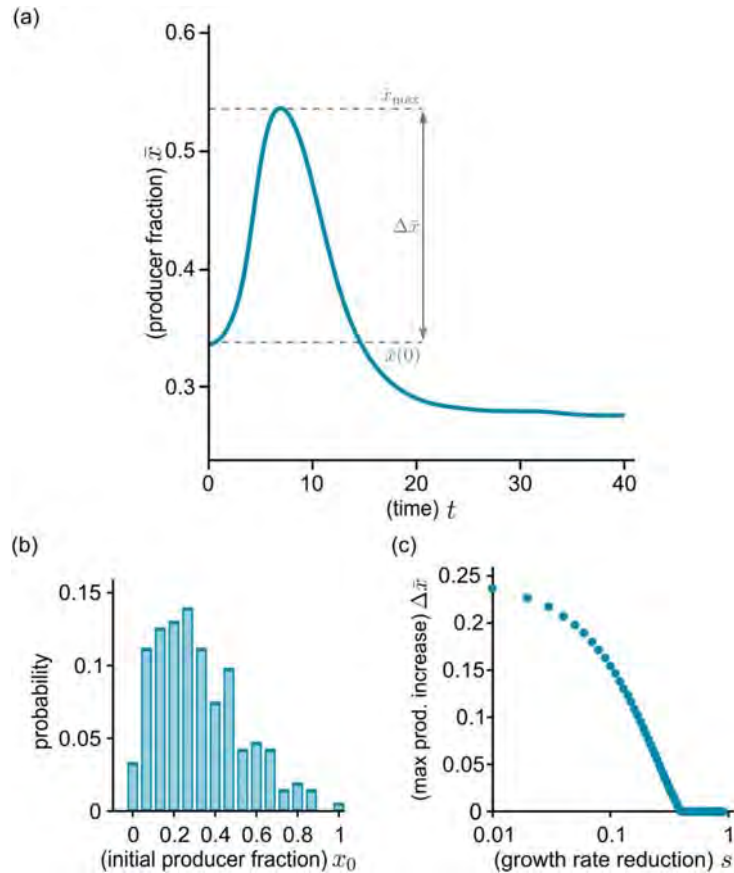


**Figure 4.** Simulation results for the growth of a metapopulation. The time course of the global producer fraction  $\bar{x}$  (a) is computed by numerically solving equations (4) for a given distribution of stochastic initial compositions (b) (parameter values:  $\alpha = 200$ ,  $s = 0.05$ , initial size  $n_0 = 10^{-3}$ ). The producer fraction initially increases as populations with more producers begin to expand earlier (see also Supplementary Movie S1). After reaching a maximum value  $\bar{x}_{\max}$ , the global producer fraction decreases. (c) The maximal magnitude of the increase  $\Delta\bar{x} = \bar{x}_{\max} - \bar{x}(0)$  decreases with stronger growth reduction  $s$  ( $s$  between 0.01 and 0.9, other parameters identical to panel (a): for low  $s$  it is comparable to the initial producer fraction, while very low producer growth precludes any increase at all).

where  $\alpha = \frac{\sigma K}{p_{\text{sat}} \mu_{\text{max}}}$  is a dimensionless parameter. This parameter represents the rate at which PVD benefit saturation sets in. Keeping other factors constant, the benefit saturates sooner if production is faster (higher  $\sigma$ ) and/or the number of total producers increases (higher  $K$  and thus larger populations). Conversely, if the saturating PVD concentration is higher (higher  $p_{\text{sat}}$ ), or cell reproduction is faster (higher  $\mu_{\text{max}}$ ), populations can reach higher densities before the benefit saturates. Generally speaking, the lower  $\alpha$ , the more advantageous producers are for their population. For  $\alpha \rightarrow 0$  for example, the reproduction time scale is shorter than that of public good production. Therefore, the relatively scarce PVD strictly limits growth, PVD saturation occurs only after many generations, and producer-rich populations outgrow producer-poor communities for longer. At the other extreme,  $\alpha \rightarrow \infty$  means that cells produce PVD much faster than they grow. In this case, a handful of producers suffices to quickly reach saturation levels of PVD. Whether they include few or many producers, all populations grow at the same rate, which negates the advantage of higher producer fractions.

We can also use equations (4) to describe a metapopulation of  $M$  independent populations. To simulate this scenario, we solve equations (4) numerically for an ensemble of stochastic initial conditions (using  $M = 10^4$ ). We generate a stochastic distribution of initial producer fractions  $x_0$  – depicted in Fig. 4b – as implemented in the experiments (see Fig. 5a and Materials and Methods). Because the experiments described here deal with relatively large populations (starting with around  $10^3$ – $10^4$  individuals, and expanding to between  $10^6$  and  $10^7$  cells), stochasticity in the initial size is low, and we initialize all populations in the simulated ensemble with the same size  $n_0 = 10^{-3}$ . Once the populations are formed, the choice of  $s$  and  $\alpha$  completely determines the population dynamics.

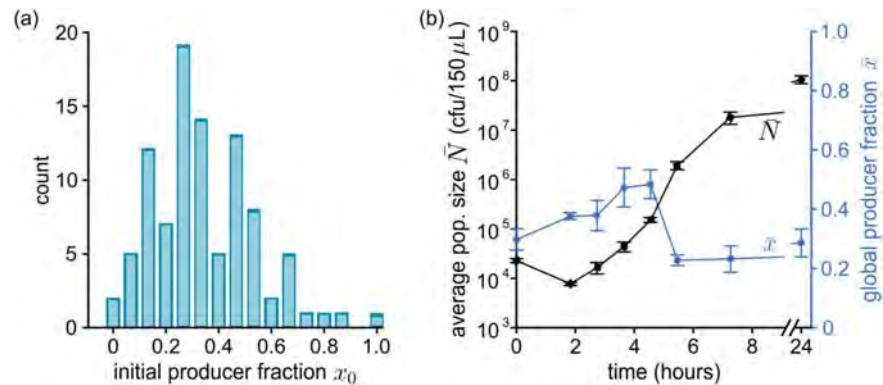


**Figure 5.** Experimental results for the growth of a mixed metapopulation. **(a)** Sample distribution of initial producer fractions in a 96-well plate. **(b)** Time course of the development of the total cell number  $\bar{N}(t)$  and global producer fraction  $\bar{x}(t)$  for a metapopulation grown under extreme iron limitation (KB/1 mM DP) in a 96-well plate shaken at 30 °C. At given time intervals, samples are taken from the wells, merged:  $\bar{N}(t)$  is determined by counting cfu and  $\bar{x}(t)$  is assessed based on the (green) color of colonies. Error bars are the result of three to five determinations of the respective parameter at the given time point. After a lag phase, populations begin to grow exponentially. During this phase, the global producer fraction transiently increases, dips sharply, then stabilizes to its final value.

During the simulations, we record the average size  $\bar{n} = \frac{1}{M} \sum_{i=1}^M n_i$  and the global producer fraction  $\bar{x}$  across the metapopulation

$$\bar{x} = \frac{\sum_i c_i}{\sum_i (c_i + f_i)}, \quad (5)$$

where  $n_i$  and  $x_i$  are the size and producer fraction of each population  $i$ , respectively. Note that this *global* fraction of public-good producers (i.e., the percentage of producer cells in the metapopulation) follows a different trajectory from the *local* one  $x_i$  (the fraction of producers actually present in each of the component subpopulations). Specifically, while the latter always decreases – because producers grow more slowly than non-producers – the former can, in some cases, increase.

How  $\bar{x}$  changes in time within a metapopulation, according to equations (4) (with  $\alpha = 200$ ,  $s = 0.05$ ,  $\pi = 10^{-3}$  is shown in Fig. 4a, and compositions sampled from the distribution in Fig. 4b, with average  $\bar{x}(0) \simeq 0.33$ ); Supplementary Movie S1 shows the same data, together with the evolution of the joint distribution of sizes  $n_i$  and compositions  $x_i$ . During early stages of growth, the more producers a population has, the quicker it accrues PVD, and the faster it grows. Populations with higher producer fractions rapidly increase their share in the metapopulation, driving up the global producer fraction  $\bar{x}$ . As time passes, populations with fewer producers also accumulate enough PVD to grow significantly (while the few with no producers never grow). Meanwhile, producer-rich populations have depleted their resources and end growth. As a result, the rate of increase of  $\bar{x}$  first slows, then reaches a maximum  $\bar{x}_{\max}$  and decreases again. Finally, once all populations have entered the dormant state, the global producer fraction stabilizes. Its ultimate value depends on the production cost  $s$  and, because all populations grow to the same size, it is lower or equal to the initial  $\bar{x}(0)$ .

The overall time course of  $\bar{x}$  and  $\bar{n}$  depends crucially on the choice of parameters, which reflect the features of the bacterial strains, as well as the cultivation conditions. Figure 4c, for example, shows how changing the growth reduction  $s$  affects the magnitude of the increase in global producer fraction  $\Delta\bar{x} = \bar{x}_{\max} - \bar{x}(0)$  (for  $\alpha = 200$  and the initial conditions shown in Fig. 4b). It is intuitively clear that a slower producer growth would yield a smaller increase. As the figure shows, we can find a region of extreme reduction ( $s > 0.4$ , which is unlikely to appear in natural systems), which cannot be offset by the benefit from the public good, thus producing no increase whatsoever in producer fraction. For lower values (roughly between 0.1 and 0.4),  $\Delta\bar{x}$  is positive, and increases as  $s$  is lowered. Finally, for low  $s$  (below 0.1),  $\Delta\bar{x}$  increases further, reaching values comparable with  $\bar{x}(0)$ , implying that the global producer fraction  $\bar{x}$  almost doubles during growth, albeit transiently. The specific values of  $s$  at which different results occur depend on the choice of  $\alpha$  and of the  $x_0$  distribution. Nevertheless, the qualitative behavior of  $\Delta\bar{x}$  remains the same.

The model thus provides insights into this public-good-mediated social interaction, and implies that it leads to a transient, but potentially very significant, increase in producer fraction. In the following section, we show that these predictions are in good agreement with experiments on competitive growth of mixed populations of producers and non-producers.

**Comparison between experimental and theoretical results.** We grew mixed populations composed of producers KP1 and non-producers 3E2 under extreme iron limitation (KB/1 mM DP), in which PVD is indispensable for iron uptake and growth (see Supplementary Fig. S1). The metapopulation consisted of a 96-well plate

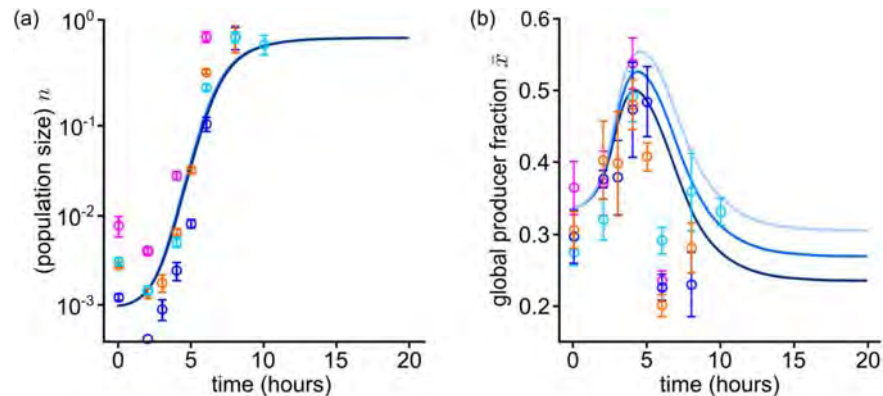


**Figure 6.** Comparison of simulation and experimental results for the population size (a) and global producer fraction (b) in a metapopulation. Solid lines represent numerical solutions of equations (4) for different values of the growth rate reduction  $s$ , and in (b) darker shades indicate higher values ( $s \in \{0.03, 0.05, 0.07\}$ ). Dots of different colors indicate the results of different independent experimental runs. Error bars are the result of three to five determinations of the respective parameter at the given time point in one experiment. The population size  $n$  is rescaled to the final yield (or carrying capacity). The stochastic initial compositions are sampled from the distribution in Fig. 4b. For appropriate values of the parameters (determined from fitting of the growth curve in (a)), theoretical and experimental result agree.

(so the metapopulation size is  $M = 96$ ), and each well was inoculated with about  $10^4$  cells. Producers and non-producers in each well were mixed in stochastic proportions, sampled from the distributions shown in Figs 4b and 5a, which were derived from the weighted average of three dice rolls (see Materials and Methods). These initial conditions mimic the characteristic variability of small populations. The mean initial producer fraction was  $\bar{x}(0) \simeq 0.33$ . As outlined in Fig. 1b, at given time points  $t$ , samples were taken from each well, merged, and their average cell number  $\bar{N}(t) = \frac{1}{M} \sum_{i=1}^M c_i + f_i$  and mean global producer fraction  $\bar{x}(t)$  were determined. Figure 5 shows the results of a representative experiment. On average, populations start growing after a lag phase of about 2 h and enter stationary phase after around 8 h. The global producer fraction  $\bar{x}$  initially increases, up to a maximum  $\bar{x}_{\max} \simeq 0.5$ . After sharply dipping to  $\bar{x}_{\min} \simeq 0.2$ , it levels off to values around 0.2–0.3, and remains constant for at least 24 h. These results qualitatively agree with those obtained by solving equations (4) for an analogous metapopulation (see previous section and Fig. 4).

The only qualitative departure from the simulation results is that  $\bar{x}$  drops towards the end of growth phase ( $t \simeq 6$  h) in the experiments. Notably, however, this also corresponds to an acceleration in population growth. Most probably, this stems from a change in the metabolic state of cells, which is not captured by the simplified description encoded in the equations (4).

We can also directly compare theoretical and experimental results. As initial conditions for the simulations, we sample the values of  $x_0$  from the same distribution as in the experiments, and set  $\bar{n}_0 = 10^{-3}$ , which we estimated by dividing the mean minimum size from experiments (taken at the end of the lag phase, so as to eliminate the slight population decay) by the final yield. To set  $s$ , we considered that KP1 grows at a rate that is between 1.03 and 1.10 times lower than that for 3E2 (as determined previously), which corresponds to a range for  $s$  of between 0.03 and 0.09. Since the rate of approach to saturation  $\alpha$  reflects several complex processes, we opted to fit it.

The data from four separate experiments (colored dots) and simulations for three possible values of  $s$  and an appropriate saturation rate,  $\alpha = 200$  (solid lines) are shown in Fig. 6. To meaningfully compare the two sets of data, we also need to fix the global time scale of simulations, which is done by fitting the slope of the exponential phase in Fig. 6a. The increase in the global producer fraction observed in simulations agrees very well with experiment (Fig. 6b):  $\bar{x}$  grows to a maximum  $\bar{x}_{\max} \simeq 0.5$  over similar periods, then decreases, and stabilizes to similar values.

Besides the aforementioned end-of-growth discrepancy – which seems to be due to behaviors well beyond the scope of our simplified mathematical description – experimental and theoretical results match.

## Discussion

In this work, we showed that social interactions mediated by a public good result in a transient increase in the global fraction of producers in a growing bacterial metapopulation. By combining theoretical modeling and experiments, we were able to quantitatively describe an exchange interaction involving a public good in a bacterial metapopulation.

We selected as our model system the native production of the iron-chelating siderophore pyoverdine (PVD) in *P. putida* KT2440 under iron limitation<sup>41,47</sup>. We characterized a constitutive producer (KP1) and a non-producer strain (3E2), and determined the growth rate reduction due to producing PVD. Under the chosen conditions, PVD is essential for iron acquisition and growth. We demonstrated that populations that produce more PVD grow faster than those with less (under otherwise identical conditions), though the magnitude of the benefit

progressively diminishes as PVD accumulates, and eventually vanishes when the available iron ceases to limit growth. Based on these experimental facts, we constructed a set of differential equations that describes the growth of mixed populations of PVD producers and non-producers. Solving these equations for a large metapopulation, we found that, at first, the more producers (and thus more PVD) are present in the sub-populations, the faster they grow. This generates a positive covariance between composition and growth rate, which drives the global producer fraction up, in accordance with the Price equation<sup>15,17,58</sup>. As PVD accumulates, however, the benefit to cells eventually saturates, reducing the advantage enjoyed by these producer-rich populations; meanwhile, populations containing fewer producers begin to grow and ultimately catch up with the initially faster ones. Therefore, the increase in the global fraction of producers is transient, both in simulations and in experiments.

Previous experimental studies related similar phenomena to the so-called Simpson's paradox<sup>11,12</sup>. However, they considered an artificial bacterial system, in which both the need for the public good and its production mechanism had been designed specifically for the experiments. In contrast, we employed a native system and quantified its social interactions, particularly the function and biochemical properties of the public good. Our analysis also shows that, without mechanisms to sustain it, the Simpson-related increase can only be transient. This conclusion is also compatible with previous qualitative predictions<sup>13–16</sup>, based on game theory models with implicit public goods. However, in contrast to our experiments, these studies predict that the producer fraction should peak at the end, instead of the mid-point of exponential growth. This indicates that simple cost-benefit considerations do not suffice to describe the social interaction. Inclusive fitness models have been used to describe an analogous scenario in wild-type *P. aeruginosa*, reaching qualitative conclusions compatible with our results<sup>29,30</sup>. Similarly to game-theoretical approaches, however, they remain mainly conceptual<sup>59</sup>. Our systems biology approach, instead, provides a simple description, with testable quantitative predictions, as well as important insights into the social interaction.

In metapopulation settings, diffusion, dispersal, and mobility affect public good interactions<sup>30,60</sup>. Besides these factors, our results highlight the potential role of the timing of dispersal. Some studies already pointed to dispersal timing, by considering a metapopulation that periodically splits into groups and merging these again to reform the pool. After several cycles, the metapopulation might develop stable coexistence of the strains<sup>13–16</sup>, or even have the producers fixate<sup>11,12</sup>. Testing this process, however, requires Poisson dilution conditions which implicate very low initial densities of producer cells. As a consequence, large fractions of cells die under iron-limiting conditions before physiologically effective PVD concentrations are reached. Therefore, a repetitive scenario of group formation and merging is experimentally not feasible for our well mixed cultivation conditions. In principle, introduction of a non-selective growth phase may rescue such a scenario<sup>61</sup>.

An interesting next step will be to include regulatory aspects in our system. Like many other bacteria, the wild-type *P. putida* KT2440 continually senses changes in environmental conditions, and uses this information to tune production of the public good<sup>62–64</sup>. By employing constitutive producer strains, we shifted the focus more on the social role of PVD itself, while replicating a potential earlier stage of evolution (if PVD production evolved before regulation). Our model also indicates that a cost-saving strategy such as down-regulation of PVD production as a consequence of PVD accumulation is not sufficient to prevent the long-term decline of the global fraction of producers, because all populations with producers eventually accumulate the same PVD concentration. So accounting for regulation, which has been shown to also impact growth<sup>65</sup>, will also necessarily involve elaborate production curves<sup>63</sup> and cost-saving strategies<sup>66</sup>. Ultimately, adaptive production raises complex questions about how cells shape the ecological and environmental conditions in which they interact<sup>67</sup>.

Another possible extension would be to allow privatized use of the public good. Privatized use of siderophores, in particular, has been shown to introduce fascinating social dynamics into intra- and inter-species competition<sup>35,68–70</sup>. Limited diffusion and private use have important social consequences<sup>32,33</sup>. Indeed, several studies have intensely debated under what conditions the secreted siderophores actually behave as public goods<sup>42,71–73</sup>. In our conditions, however, populations seem to behave as well-mixed, with negligible privatization.

Taken together, our work uses a simplified setting to highlight the determinant role of public goods in social interactions and population dynamics. For example, we showed the profound consequences of the public good's accumulation and saturating benefits, which simple game-theoretical considerations would fail to describe. Our approach could clearly be extended to investigate the fundamental principles underlying different interactions and bacterial systems. Thereby it should stimulate more mechanistic analyses of bacterial social interactions and their impact on population development.

## Materials and Methods

**Strains and growth conditions.** *Escherichia coli* DH5 $\alpha$  [F- $\phi$ 80d *lacZ*  $\Delta$ M15  $\Delta$ (*lacZYA-argF*) U169 *deoR* *recA1* *endA1* *hsd* R17(rk $-$ , mk $+$ ) *phoA* *supE44*  $\lambda$ -*thi-1* *gyrA96* *relA1*] was used as the carrier for plasmids. *Pseudomonas putida* KT2440 and the derived strain 3E2 (non-producer)<sup>47</sup> were employed as PVD producer (wild-type) and non-producer, respectively. *E. coli* strains were grown in lysogeny broth (LB) at 37 °C, and *P. putida* strains were grown at 30 °C in King's medium B (KB)<sup>74</sup>. KB medium was supplemented with 100  $\mu$ M FeCl<sub>3</sub> and/or 1 mM of the iron chelator 2,2'-dipyridyl (DP) where indicated. Solid media were LB or KB with 1.5% agar.

**Generation of the constitutive PVD producer strain KP1.** A *P. putida* strain that constitutively produces PVD was generated by placing a copy of the *pfrI* gene under the control of the constitutive promoter P<sub>A1/04/03</sub><sup>54</sup>. For this purpose, P<sub>A1/04/03</sub> and the *pfrI* gene were amplified by PCR from the plasmid mini*Tn7*(Gm) P<sub>A1/04/03</sub>ecfp-a<sup>75</sup> and the *P. putida* genome, respectively, cloned into plasmid pUC18R6K-mini-*Tn7*T-Gm, and inserted at the *attTn7* site in *P. putida* KT2440 following a mini-*Tn7* protocol for *Pseudomonas*<sup>76</sup>. The resulting *P. putida* strain KP1 was verified by PCR amplification of corresponding genome regions and sequencing. All oligonucleotide primers used for strain generations and verification are listed in Supplementary Table S2.

**Quantitative analysis of PVD production.** Pre-cultures of the respective strains were grown in iron-replete medium (KB/200  $\mu\text{M}$   $\text{FeCl}_3$ ) at 30 °C for 18 h. The pre-cultures were used to inoculate the appropriate media for the growth of the cultures used in experiments ( $N_0 = 10^7$  cells  $\text{mL}^{-1}$ ). Experiments were performed in 24-well plates (2 mL culture/well). The plates were shaken at 300 rpm at 30 °C. At given time points samples were taken and the optical density at 600 nm was measured. Subsequently, cells were removed by centrifugation, and the relative PVD content was determined by measuring the fluorescence emission at 460 nm (excitation 400 nm). PVD production was analyzed under iron limitation (KB/1 mM DP; KB/100  $\mu\text{M}$   $\text{FeCl}_3$ /1 mM DP) and iron replete conditions (KB; KB/100  $\mu\text{M}$   $\text{FeCl}_3$ ). Each individual experiment was performed with three parallel replicates. A minimum of three independent experiments were conducted per condition.

**Growth characteristics of strains under different environmental conditions.** Pre-cultures of the respective strains were grown in iron-replete medium as described above for the analysis of PVD production, and used to inoculate the appropriate media for growth of the cultures used in experiments ( $N_0 = 10^7$  cells  $\text{mL}^{-1}$ ). Experiments were performed in 96-well plates (150  $\mu\text{L}$  culture/well). The plates were shaken at 300 rpm at 30 °C. Growth was followed by measuring the optical density at 600 nm using a microplate reader (Infinite® M200 from Tecan Trading AG). The measurement was controlled and monitored with the i-control™ Software from Tecan Trading AG (30 °C, shaking at 280 rpm, 880 s per cycle, minimum 80 cycles). Each condition was implemented in six replicates per experiment, including medium blanks. For low cell numbers (e.g.,  $N_0 = 10^4$  cells  $150 \mu\text{L}^{-1}$ ), growth was analyzed by determining colony forming units (*cfu*) over time (threefold per time point). The specific growth rate  $\mu$  represents a quantitative measure of growth in the exponential phase and was calculated using the following equation:  $\mu = \frac{\ln(N_2 - N_1)}{t_2 - t_1}$ .

**Quantitative assessment of the benefit of PVD.** The benefit conferred by PVD was quantified under iron-limiting conditions (KB/1 mM DP) with the non-producer strain 3E2. PVD was isolated according to a previously described protocol<sup>17</sup> and added to the medium at concentrations of between 0 and 20  $\mu\text{M}$ . Growth was monitored via optical density measurement, and the specific growth rate  $\mu$  was calculated as described in the previous paragraph. Each individual experiment was performed with four parallel repeats per PVD concentration, and three independent experiments of this type were conducted per PVD concentration.

**Determination of PVD sharing in mixed culture.** Cells were grown in KB/1 mM DP (initial producer frequency  $\bar{x}(0) \approx 0.33$ ,  $N_0 = 10^4$  cells/ $150 \mu\text{L}$ , 96-well plate format) at 30 °C. Colony forming units (*cfu*) were determined at given time points (five replicates per time point), and producer and non-producer cells were discriminated by colony color and size. Three independent experiments were performed, each yielding similar results.

**Stability of PVD in KB medium with and without bacteria.** Medium without cells and medium containing about  $10^7$  cells  $\text{mL}^{-1}$  of the non-producer were supplemented with 2  $\mu\text{M}$  PVD and incubated at 30 °C for 48 h. At given time points samples were taken, and the relative PVD contents of medium and of the supernatant of medium with cells were determined by measuring the fluorescence emission of PVD at 460 nm (excitation 400 nm).

**Competitive growth experiments.** To analyze the impact of the initial producer frequencies  $x_0$  on growth, strains KP1 and 3E2 were mixed in KB/1 mM DP (96-well plate,  $N_0 = 10^4$  cells  $150 \mu\text{L}^{-1}$ ,  $x_0 \in \{0, 0.1, 0.2, 0.3, 0.5, 0.75, 1.0\}$ ). Total cell numbers were determined at the end of the lag phase and after 8 h of shaking at 30 °C by counting *cfu*. For each condition, a minimum of three individual experiments were performed. To analyze the development of the total cell number  $\bar{N}(t)$  and global producer frequency  $\bar{x}(t)$  in metapopulations, a random distribution of the initial producer frequency  $x_0$  was established by rolling three dices. The values of each triplet were weighted (lowest 2/3, middle 2/9 and highest 1/9) and rounded to yield sixteen different values from 0 to 15 that are equivalent to sixteen different initial producer frequencies  $x_0$  ranging from 0 to 1.0 and result in an initial average global cooperator fraction  $\bar{x}(0)$  of about 0.33. Cells were grown in KB/1 mM DP (96-well plate,  $N_0 = 10^4$  cells  $150 \mu\text{L}^{-1}$ ) at 30 °C while shaking at 300 rpm. At given time points aliquots of each well were merged and  $\bar{N}(t)$  was determined by counting *cfu*. The global producer frequency  $\bar{x}(t)$  was obtained based on differences in the color and size of the colonies of KP1 and 3E2 on KB agar plates (minimum three replicates per time point).

**Stochastic initial conditions and ensemble averages.** We generate all triplets of the integers between 0 and 5 to simulate the results of a sequence of (simultaneous) throws of three dice. Since the weights in the experimental procedure are assigned based on the order of the rolled values, we order the “rolled” values within each triplet from lowest to highest. This results in a table of all possible 3-dice rolls, which we can use directly to generate the initial conditions and simulate equations (4). To speed up calculations, however, we remove duplicate triplets: for example, 113, 131, 311 are different triplets before sorting, but are the same after. Once we remove the duplicate combinations, we assign the appropriate probability to them, i.e. the number of ways to produce them before sorting divided by the total number of triplets. With a minimal combinatorics, one can compute the total number of triplets ( $6^3 = 216$ ), and the multiplicities of triplets: those with three equal values have only one way to appear before sorting; those with two equal values have three; those with all different values have six.

To simulate the time evolution of  $n$  and  $x$ , we generate the initial composition  $x_0$  for each triplet, using the weighted average described above. After setting  $n_0$ ,  $\alpha$ , and  $s$ , the temporal evolution of the average  $\bar{x}$  and  $\bar{n}$  in ensembles of populations can be computed by solving equations (4) for each of the allowed values of  $x_0$  and weighting it using the relative probability, computed as described above.

**Data Availability.** The data that support the findings of this study are available from the corresponding authors upon reasonable request.

## References

- Ackermann, M. A functional perspective on phenotypic heterogeneity in microorganisms. *Nat Rev Microbiol* **13**, 497–508, <https://doi.org/10.1038/nrmicro3491> (2015).
- Germerodt, S. *et al.* Pervasive selection for cooperative cross-feeding in bacterial communities. *PLoS Comp Biol* **12**, e1004986, <https://doi.org/10.1371/journal.pcbi.1004986> (2016).
- Hawver, L. A., Jung, S. A. & Ng, W. L. Specificity and complexity in bacterial quorum-sensing systems. *FEMS Microbiol Rev* **40**, 738–752, <https://doi.org/10.1093/femsre/fuw014> (2016).
- Kolter, R. & Greenberg, E. P. Microbial sciences: the superficial life of microbes. *Nature* **441**, 300–302, <https://doi.org/10.1038/441300a> (2006).
- Papenfort, K. & Bassler, B. L. Quorum sensing signal-response systems in Gram-negative bacteria. *Nat Rev Microbiol* **14**, 576–588, <https://doi.org/10.1038/nrmicro.2016.89> (2016).
- Veening, J. W., Smits, W. K. & Kuipers, O. P. Bistability, epigenetics, and bet-hedging in bacteria. *Annu Rev Microbiol* **62**, 193–210, <https://doi.org/10.1146/annurev.micro.62.081307.163002> (2008).
- Keymer, J. E., Galajda, P., Lambert, G., Liao, D. & Austin, R. H. Computation of mutual fitness by competing bacteria. *Proc Natl Acad Sci USA* **105**, 20269–20273, <https://doi.org/10.1073/pnas.0810792105> (2008).
- Rainey, P. B. & Rainey, K. Evolution of cooperation and conflict in experimental bacterial populations. *Nature* **425**, 72–74, <https://doi.org/10.1038/nature01906> (2003).
- West, S. A., Diggel, S. P., Buckling, A., Gardner, A. & Griffins, A. S. The social lives of microbes. *Annu Rev Ecol Evol Syst* **38**, 53–77, <https://doi.org/10.1146/annurev.ecolsys.38.091206.095740> (2007).
- Menon, R. & Korolev, K. S. Public good diffusion limits microbial mutualism. *Phys Rev Lett* **114**, 168102, <https://doi.org/10.1103/PhysRevLett.114.168102> (2015).
- Chuang, J. S., Rivoire, O. & Leibler, S. Simpson's paradox in a synthetic microbial system. *Science* **323**, 272–275, <https://doi.org/10.1126/science.1166739> (2009).
- Chuang, J. S., Rivoire, O. & Leibler, S. Cooperation and Hamilton's rule in a simple synthetic microbial system. *Mol Syst Biol* **6**, 398, <https://doi.org/10.1038/msb.2010.57> (2010).
- Cremer, J., Melbinger, A. & Frey, E. Evolutionary and population dynamics: a coupled approach. *Phys Rev E, Stat Nonlinear Soft Matter Phys* **84**, 051921, <https://doi.org/10.1103/PhysRevE.84.051921> (2011).
- Cremer, J., Melbinger, A. & Frey, E. Growth dynamics and the evolution of cooperation in microbial populations. *Sci Rep* **2**, 281, <https://doi.org/10.1038/srep00281> (2012).
- Melbinger, A., Cremer, J. & Frey, E. Evolutionary game theory in growing populations. *Phys Rev Lett* **105**, 178101, <https://doi.org/10.1103/PhysRevLett.105.178101> (2010).
- Melbinger, A., Cremer, J. & Frey, E. The emergence of cooperation from a single mutant during microbial life cycles. *J R Soc Interface* **12**, <https://doi.org/10.1098/rsif.2015.0171> (2015).
- Price, G. R. Extension of covariance selection mathematics. *Ann Hum Genet* **35**, 485–490 (1972).
- Costerton, J. W. *et al.* Bacterial Biofilms in Nature and Disease. *Annu Rev Microbiol* **41**, 435–464 (1987).
- Xavier, J. B. Social interaction in synthetic and natural microbial communities. *Mol Syst Biol* **7**, 483, <https://doi.org/10.1038/msb.2011.16> (2011).
- Frey, E. Evolutionary game theory: Theoretical concepts and applications to microbial communities. *Physica A-Stat Mech Appl* **389**, 4265–4298, <https://doi.org/10.1016/j.physa.2010.02.047> (2010).
- Gore, J., Youk, H. & van Oudenaarden, A. Snowdrift game dynamics and facultative cheating in yeast. *Nature* **459**, 253–256, <https://doi.org/10.1038/nature07921> (2009).
- Hofbauer, J. & Sigmund, K. *Evolutionary Games and Population Dynamics*. (Cambridge University Press, 1998).
- Hofbauer, J. & Sigmund, K. Evolutionary game dynamics. *B Am Math Soc* **40**, 479–519, <https://doi.org/10.1090/S0273-0979-03-00988-1> (2003).
- Reichenbach, T., Mobilia, M. & Frey, E. Mobility promotes and jeopardizes biodiversity in rock-paper-scissors games. *Nature* **448**, 1046–1049, <https://doi.org/10.1038/nature06095> (2007).
- Axelrod, R. & Hamilton, W. D. The evolution of cooperation. *Science* **211**, 1390–1396 (1981).
- Damore, J. A. & Gore, J. Understanding microbial cooperation. *J Theor Biol* **299**, 31–41, <https://doi.org/10.1016/j.jtbi.2011.03.008> (2012).
- Frank, S. A. *Foundations of social evolution*. (Princeton University Press, 1998).
- Hamilton, W. D. The genetical evolution of social behaviour. I. *J Theor Biol* **7**, 1–16 (1964).
- Griffin, A. S., West, S. A. & Buckling, A. Cooperation and competition in pathogenic bacteria. *Nature* **430**, 1024–1027, <https://doi.org/10.1038/nature02744> (2004).
- Kümmerli, R., Gardner, A., West, S. A. & Griffin, A. S. Limited dispersal, budding dispersal, and cooperation: an experimental study. *Evolution* **63**, 939–949, <https://doi.org/10.1111/j.1558-5646.2008.00548.x> (2009).
- Nowak, M. A. Five rules for the evolution of cooperation. *Science* **314**, 1560–1563, <https://doi.org/10.1126/science.1133755> (2006).
- Julou, T. *et al.* Cell-cell contacts confine public goods diffusion inside *Pseudomonas aeruginosa* clonal microcolonies. *Proc Natl Acad Sci USA* **110**, 12577–12582, <https://doi.org/10.1073/pnas.1301428110> (2013).
- Kümmerli, R., Schiessl, K. T., Waldvogel, T., McNeill, K. & Ackermann, M. Habitat structure and the evolution of diffusible siderophores in bacteria. *Ecol Lett* **17**, 1536–1544, <https://doi.org/10.1111/ele.12371> (2014).
- Dobay, A., Bagheri, H. C., Messina, A., Kümmerli, R. & Rankin, D. J. Interaction effects of cell diffusion, cell density and public goods properties on the evolution of cooperation in digital microbes. *J Evol Biol* **27**, 1869–1877, <https://doi.org/10.1111/jeb.12437> (2014).
- Inglis, R. F., Biernaskie, J. M., Gardner, A. & Kümmerli, R. Presence of a loner strain maintains cooperation and diversity in well-mixed bacterial communities. *Proc Biol Sci* **283**, <https://doi.org/10.1098/rspb.2015.2682> (2016).
- MacLean, R. C., Fuentes-Hernandez, A., Greig, D., Hurst, L. D. & Gudelj, I. A mixture of “cheats” and “co-operators” can enable maximal group benefit. *PLoS Biol* **8**, e1000486, <https://doi.org/10.1371/journal.pbio.1000486> (2010).
- Niehus, R., Picot, A., Oliveira, N. M., Mitri, S. & Foster, K. R. The evolution of siderophore production as a competitive trait. *Evolution* **71**, 1443–1455, <https://doi.org/10.1111/evo.13230> (2017).
- Widder, S. *et al.* Challenges in microbial ecology: building predictive understanding of community function and dynamics. *ISME J* **10**, 2557–2568, <https://doi.org/10.1038/ismej.2016.45> (2016).
- Harcombe, W. R. *et al.* Metabolic resource allocation in individual microbes determines ecosystem interactions and spatial dynamics. *Cell Rep* **7**, 1104–1115, <https://doi.org/10.1016/j.celrep.2014.03.070> (2014).
- Buckling, A. *et al.* Siderophore-mediated cooperation and virulence in *Pseudomonas aeruginosa*. *FEMS Microbiol Ecol* **62**, 135–141, <https://doi.org/10.1111/j.1574-6941.2007.00388.x> (2007).
- Kümmerli, R., Jiricny, N., Clarke, L. S., West, S. A. & Griffin, A. S. Phenotypic plasticity of a cooperative behaviour in bacteria. *J Evol Biol* **22**, 589–598, <https://doi.org/10.1111/j.1420-9101.2008.01666.x> (2009).

42. Zhang, X. X. & Rainey, P. B. Exploring the sociobiology of pyoverdinin-producing *Pseudomonas*. *Evolution* **67**, 3161–3174, <https://doi.org/10.1111/evo.12183> (2013).
43. Visca, P., Imperi, F. & Lamont, I. L. Pyoverdine siderophores: from biogenesis to biosignificance. *Trends Microbiol* **15**, 22–30 (2007).
44. Imperi, F., Tiburzi, F. & Visca, P. Molecular basis of pyoverdine siderophore recycling in *Pseudomonas aeruginosa*. *Proc Natl Acad Sci USA* **106**, 20440–20445, <https://doi.org/10.1073/pnas.0908760106> (2009).
45. Gasser, V., Guillon, L., Cunrath, O. & Schalk, I. J. Cellular organization of siderophore biosynthesis in *Pseudomonas aeruginosa*: evidence for siderosomes. *J Inorg Biochem* **148**, 27–34, <https://doi.org/10.1016/j.jinorgbio.2015.01.017> (2015).
46. Hannauer, M., Barda, Y., Mislín, G. L. A., Shanzler, A. & Schalk, I. J. The ferrichrome uptake pathway in *Pseudomonas aeruginosa* involves an iron release mechanism with acylation of the siderophore and recycling of the modified desferrichrome. *J Bacteriol* **192**, 1212–1220, <https://doi.org/10.1128/Jb.01539-09> (2010).
47. Matthijs, S. *et al.* Siderophore-mediated iron acquisition in the entomopathogenic bacterium *Pseudomonas entomophila* L48 and its close relative *Pseudomonas putida* KT2440. *Biomaterials* **22**, 951–964, <https://doi.org/10.1007/s10534-009-9247-y> (2009).
48. Lee, J. & Zhang, L. The hierarchy quorum sensing network in *Pseudomonas aeruginosa*. *Protein Cell* **6**, 26–41, <https://doi.org/10.1007/s13238-014-0100-x> (2015).
49. Martins dos Santos, V. A. P., Heim, S., Moore, E. R., Stratz, M. & Timmis, K. N. Insights into the genomic basis of niche specificity of *Pseudomonas putida* KT2440. *Environ Microbiol* **6**, 1264–1286, <https://doi.org/10.1111/j.1462-2920.2004.00734.x> (2004).
50. Niewerth, H., Bergander, K., Chhabra, S. R., Williams, P. & Fetzner, S. Synthesis and biotransformation of 2-alkyl-4(1H)-quinolones by recombinant *Pseudomonas putida* KT2440. *Appl Microbiol Biotechnol* **91**, 1399–1408, <https://doi.org/10.1007/s00253-011-3378-0> (2011).
51. Cornelis, P., Matthijs, S. & Van Oeffelen, L. Iron uptake regulation in *Pseudomonas aeruginosa*. *Biomaterials* **22**, 15–22, <https://doi.org/10.1007/s10534-008-9193-0> (2009).
52. Swingle, B. *et al.* Characterization of the PvdS-regulated promoter motif in *Pseudomonas syringae* pv. *tomato* DC3000 reveals regulon members and insights regarding PvdS function in other pseudomonads. *Mol Microbiol* **68**, 871–889, <https://doi.org/10.1111/j.1365-2958.2008.06209.x> (2008).
53. Pasqua, M. *et al.* Ferric uptake regulator Fur is conditionally essential in *Pseudomonas aeruginosa*. *J Bacteriol* **199**, <https://doi.org/10.1128/JB.00472-17> (2017).
54. Lanzer, M. & Bujard, H. Promoters largely determine the efficiency of repressor action. *Proc Natl Acad Sci USA* **85**, 8973–8977 (1988).
55. Semsey, S. *et al.* Genetic regulation of fluxes: iron homeostasis of *Escherichia coli*. *Nucleic Acids Res* **34**, 4960–4967, <https://doi.org/10.1093/nar/gkl627> (2006).
56. Thulasiraman, P. *et al.* Selectivity of ferric enterobactin binding and cooperativity of transport in Gram-negative bacteria. *J Bacteriol* **180**, 6689–6696 (1998).
57. Meyer, J.-M. & Abdallah, M. A. The fluorescent pigment of *Pseudomonas fluorescens*: biosynthesis, purification and physicochemical properties. *J Gen Microbiol* **107**, 319–328 (1978).
58. Price, G. R. Selection and covariance. *Nature* **227**, 520–521 (1970).
59. Ghoul, M. *et al.* Pyoverdinin cheats fail to invade bacterial populations in stationary phase. *J Evol Biol* **29**, 1728–1736, <https://doi.org/10.1111/jeb.12904> (2016).
60. Gelimson, A., Cremer, J. & Frey, E. Mobility, fitness collection, and the breakdown of cooperation. *Phys Rev E* **87**, <https://doi.org/10.1103/PhysRevE.87.042711> (2013).
61. Wienand, K., Lechner, M., Becker, F., Jung, H. & Frey, E. Non-selective evolution of growing populations. *PLoS One* **10**, e0134300, <https://doi.org/10.1371/journal.pone.0134300> (2015).
62. Dandekar, A. A., Chugani, S. & Greenberg, E. P. Bacterial quorum sensing and metabolic incentives to cooperate. *Science* **338**, 264–266, <https://doi.org/10.1126/science.1227289> (2012).
63. Heilmann, S., Krishna, S. & Kerr, B. Why do bacteria regulate public goods by quorum sensing?—How the shapes of cost and benefit functions determine the form of optimal regulation. *Front Microbiol* **6**, 767, <https://doi.org/10.3389/fmicb.2015.00767> (2015).
64. Smalley, N. E., An, D., Parsek, M. R., Chandler, J. R. & Dandekar, A. A. Quorum sensing protects *Pseudomonas aeruginosa* against cheating by other species in a laboratory coculture model. *J Bacteriol* **197**, 3154–3159, <https://doi.org/10.1128/JB.00482-15> (2015).
65. Kiviet, D. J. *et al.* Stochasticity of metabolism and growth at the single-cell level. *Nature* **514**, 376–379, <https://doi.org/10.1038/nature13582> (2014).
66. Kümmerli, R. & Brown, S. P. Molecular and regulatory properties of a public good shape the evolution of cooperation. *Proc Natl Acad Sci USA* **107**, 18921–18926, <https://doi.org/10.1073/pnas.1011154107> (2010).
67. Bauer, M., Knebel, J., Lechner, M., Pickl, P. & Frey, E. Ecological feedback in quorum-sensing microbial populations can induce heterogeneous production of autoinducers. *Elife* **6**, <https://doi.org/10.7554/eLife.25773> (2017).
68. Jiricny, N. *et al.* Fitness correlates with the extent of cheating in a bacterium. *J Evol Biol* **23**, 738–747, <https://doi.org/10.1111/j.1420-9101.2010.01939.x> (2010).
69. Lee, W., van Baalen, M. & Jansen, V. A. Siderophore production and the evolution of investment in a public good: An adaptive dynamics approach to kin selection. *J Theor Biol* **388**, 61–71, <https://doi.org/10.1016/j.jtbi.2015.09.038> (2016).
70. Pande, S. *et al.* Privatization of cooperative benefits stabilizes mutualistic cross-feeding interactions in spatially structured environments. *ISME J* **10**, 1413–1423, <https://doi.org/10.1038/ismej.2015.212> (2016).
71. Kümmerli, R. & Ross-Gillespie, A. Explaining the sociobiology of pyoverdinin-producing *Pseudomonas*: a comment on Zhang and Rainey (2013). *Evolution* **68**, 3337–3343, <https://doi.org/10.1111/evo.12311> (2014).
72. Ghoul, M., West, S. A., Diggle, S. P. & Griffin, A. S. An experimental test of whether cheating is context dependent. *J Evol Biol* **27**, 551–556, <https://doi.org/10.1111/jeb.12319> (2014).
73. Rainey, P. B., Desprat, N., Driscoll, W. W. & Zhang, X. X. Microbes are not bound by sociobiology: response to Kümmerli and Ross-Gillespie (2013). *Evolution* **68**, 3344–3355, <https://doi.org/10.1111/evo.12508> (2014).
74. King, E. O., Ward, M. K. & Rainey, D. E. Two simple media for the demonstration of pyocyanin and fluorescein. *J Lab Clin Med* **44**, 301–307 (1954).
75. Lamberts, L., Sternberg, C. & Molin, S. Mini-Tn7 transposons for site-specific tagging of bacteria with fluorescent proteins. *Environ Microbiol* **6**, 726–732 (2004).
76. Choi, K. H. & Schweizer, H. P. mini-Tn7 insertion in bacteria with single attTn7 sites: example *Pseudomonas aeruginosa*. *Nat Prot* **1**, 153–161, <https://doi.org/10.1038/nprot.2006.24> (2006).
77. Meyer, J. M. *et al.* Siderotyping of fluorescent pseudomonads: characterization of pyoverdines of *Pseudomonas fluorescens* and *Pseudomonas putida* strains from Antarctica. *Microbiology* **144**, 3119–3126, <https://doi.org/10.1099/00221287-144-11-3119> (1998).

### Acknowledgements

This work was supported by the Deutsche Forschungsgemeinschaft through grant SPP1617 (JU 333/5–1, 2 and FR 850/11–1, 2). We thank Michelle Eder (HJ lab) for excellent technical assistance. *P. putida* strain 3E2 was kindly provided by P. Cornelis (Vrije Universiteit Brussels, Belgium).

### Author Contributions

Designed and performed the experiments: F.B., H.J.; designed and performed theoretical analysis: K.W., M.L., E.F.; analyzed the experimental and computational data: F.B., K.W., M.L., E.F., H.J. Wrote the paper: K.W., M.L., E.F., F.B., H.J.

### Additional Information

**Supplementary information** accompanies this paper at <https://doi.org/10.1038/s41598-018-22306-9>.

**Competing Interests:** The authors declare no competing interests.

**Publisher's note:** Springer Nature remains neutral with regard to jurisdictional claims in published maps and institutional affiliations.



**Open Access** This article is licensed under a Creative Commons Attribution 4.0 International License, which permits use, sharing, adaptation, distribution and reproduction in any medium or format, as long as you give appropriate credit to the original author(s) and the source, provide a link to the Creative Commons license, and indicate if changes were made. The images or other third party material in this article are included in the article's Creative Commons license, unless indicated otherwise in a credit line to the material. If material is not included in the article's Creative Commons license and your intended use is not permitted by statutory regulation or exceeds the permitted use, you will need to obtain permission directly from the copyright holder. To view a copy of this license, visit <http://creativecommons.org/licenses/by/4.0/>.

© The Author(s) 2018

## Interactions mediated by a public good transiently increase cooperativity in growing *Pseudomonas putida* metapopulations

Felix Becker,<sup>a</sup> Karl Wienand,<sup>b</sup> Matthias Lechner,<sup>b</sup> Erwin Frey,<sup>b,\*</sup> Heinrich Jung<sup>a,\*</sup>

<sup>a</sup>Microbiology, Department Biology 1, Ludwig-Maximilians-Universität Munich, Grosshaderner Strasse 2-4, Martinsried, Germany; <sup>b</sup>Arnold-Sommerfeld-Center for Theoretical Physics and Center for Nanoscience, Ludwig-Maximilians-Universität, Theresienstrasse 37, D-80333 Munich, Germany

\*Correspondence to: Heinrich Jung, [hjung@lmu.de](mailto:hjung@lmu.de) (HJ) and Erwin Frey [frey@lmu.de](mailto:frey@lmu.de) (EF). FB and KW contributed equally to this work.

## Supplementary Information

### Notes

#### Derivation of the growth rate $\mu(p)$

Assume a cell is born with an internal iron concentration  $Fe_{in}(0)$  and a volume  $V(0)$ . Let  $p$  be the concentration of PVD-Fe complexes (which we take to be the same as that of PVD; see text). Each cell, then, incorporates iron ions at a constant rate  $kp$  that is proportional to the concentration of PVD. So at time  $t$  after its birth, the cell has accumulated  $kpt$  iron ions. Its internal iron concentration  $Fe_{in}(t)$ , then, is  $Fe_{in}(0)V(0)$  (that is, the number of iron atoms at birth), plus the iron it has collected, all divided by the volume birth  $V(t)$  it has reached:

$$Fe_{in}(t) = \frac{Fe_{in}(0)V(0)+kpt}{V(t)} .$$

Because cells try to maintain iron concentration homeostasis, we can consider  $Fe_{in}$  to be constant. Moreover, as long as iron is the limiting factor for growth, the growth rate  $\mu(p)$  depends only on the PVD concentration.

On average, cells divide at time  $t_D = 1/\mu(p)$ , given that growth is logistic. Moreover, at the moment of division, the cell has attained twice the volume of its future daughters:  $V(t_D) = 2V(0)$ . With these substitutions in the above equation, and minimal algebra, we

obtain equation (2).

### Estimation of iron incorporated into cells

The iron content of a bacterial cell ranges from  $\sim 10^5$  to  $10^6$  atoms per cell (*Abdul-Tehrani et al., 1999, Andrews et al., 2003a*). In our experimental setup, cells reach a maximum density of  $2 \times 10^7$  cells per 150  $\mu\text{L}$  at the end of the exponential growth phase accumulating in total  $2 \times 10^{12}$  to  $2 \times 10^{13}$  iron atoms. We determined the iron concentration of our KB preparation by atomic absorption spectroscopy and found a concentration of  $\sim 8 \mu\text{M}$  (corresponding to  $\sim 7.2 \times 10^{14}$  iron atoms per 150  $\mu\text{L}$  KB medium). Using these numbers we calculated that  $\sim 0.28$  to  $2.8\%$  of the total iron of KB is incorporated into cells by the end of the exponential growth phase.

### References

- 1 Abdul-Tehrani, H. et al. (1999). Ferritin mutants of *Escherichia coli* are iron deficient and growth impaired, and *fur* mutants are iron deficient. *J Bacteriol* **181**, 1415-1428
- 2 Andrews, S. C., Robinson, A. K. & Rodriguez-Quinones, F. (2003). Bacterial iron homeostasis. *FEMS Microbiol Rev* **27**, 215-237

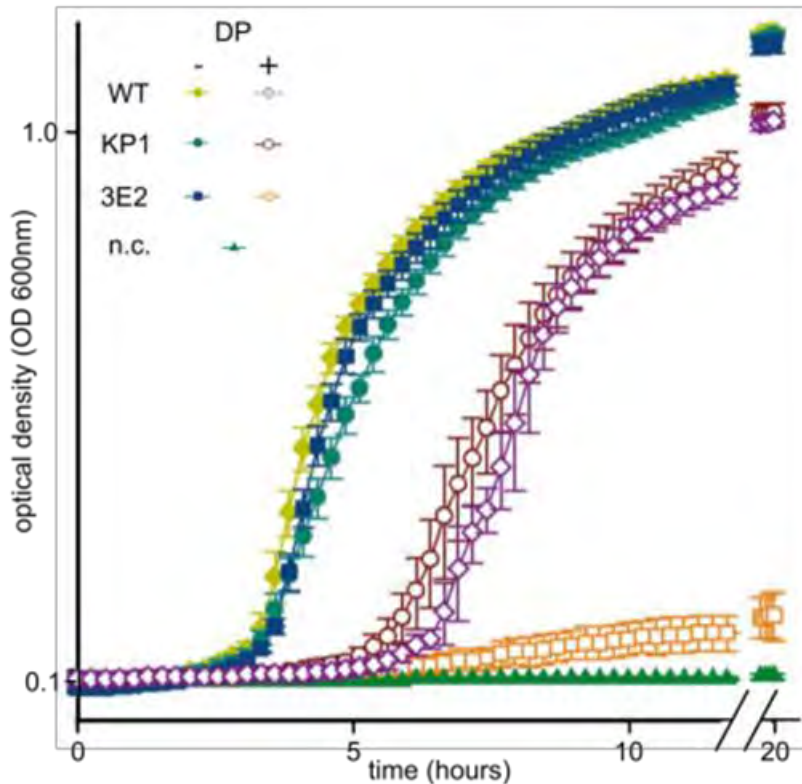


**Figure S1.** Growth of *P. putida* KT2440 and the derived strains KP1 and 3E2 under iron replete and limiting conditions. Cells were grown in KB supplemented with iron (KB/100  $\mu\text{M}$   $\text{FeCl}_3$ , full symbols) and in KB with iron chelator DP (KB/100  $\mu\text{M}$   $\text{FeCl}_3$ /1 mM DP, empty symbols). When iron is more available, PVD is not needed for growth, 3E2 and WT grow about at the same rate, and KP1 grows slower. Under iron limitation, producing strains (KP1 and WT) benefit from production and grow much faster than non-producing 3E2. The experiment was performed as described in the legend of Fig. 3a.

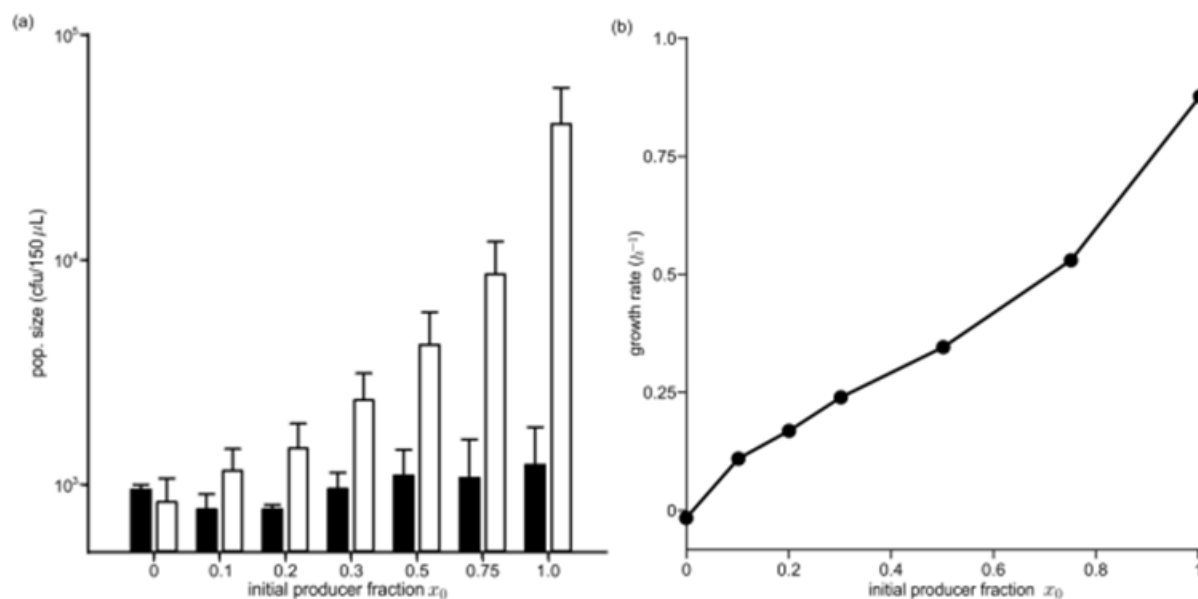


**Figure S2.** Impact of the initial producer fraction  $x_0$  on the growth of mixed populations under iron limiting conditions. **(a)** Impact of the initial producer fraction  $x_0$  on the growth yield. Strains KP1 and 3E2 were grown in mixed culture under iron-limiting conditions (KB/1 mM DP,  $N_0$  about  $10^3$  cells/150  $\mu$ L, 96-well plate format) with the given initial producer frequencies  $x_0$ . Total cell numbers were determined by counting *cfu* at the beginning of the experiment (black columns) and after 8 h of incubation (white columns). For each condition, minimum three individual experiments were performed. **(b)** Impact of the initial producer fraction  $x_0$  on the specific growth rate  $\mu$ . Mixed cultures of strains KP1 and 3E2 with  $x_0$  values between 0 (=100% 3E2) and 1 (=100% KP1) were incubated in shaking 96-well microtiter plates at 30°C ( $N_0 = 10^7$  cells mL<sup>-1</sup>). Growth was analyzed by measuring the optical density at 600 nm using a Tecan microplate reader.  $\mu$  was determined for each condition from the exponential phase of the resulting growth curves. All growth parameters represent the means of five growth experiments. Deviations were <10% of the mean value.

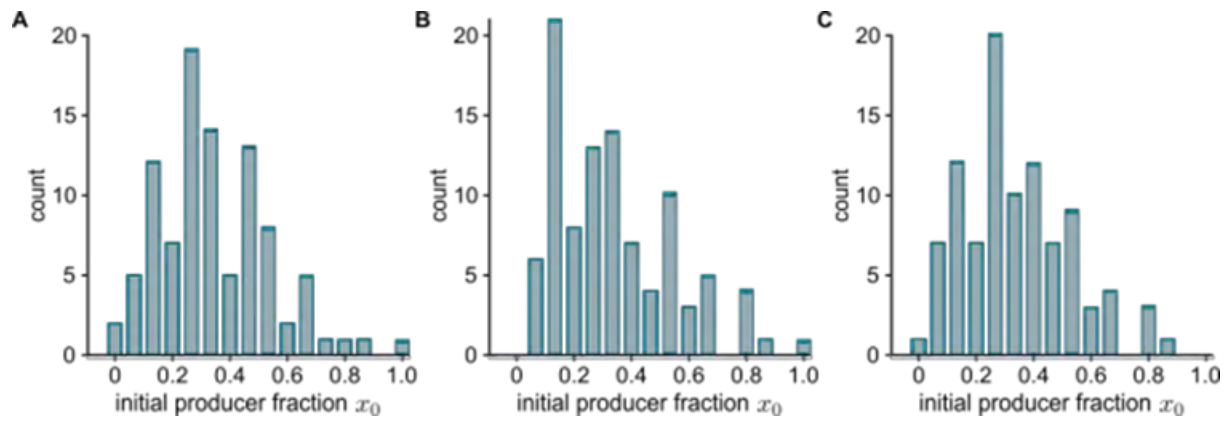


**Figure S3.** Distribution of initial compositions  $x_0$  in three replicates of the experiment. Although specific values differ, the overall features of the distribution remains the same. Most populations start mixed, with  $x_0$  between 0.1 and 0.5. When at all present, populations with all producers or no producers are very rare.

**Table S1.** Specific growth rate of *P. putida* KT2440 (WT), the non-producer (3E2), and the constitutive PVD producer (KP1) under iron-rich and iron-limiting conditions.

Growth medium	$\mu_{WT}$ ( $h^{-1}$ )	$\mu_{3E2}$ ( $h^{-1}$ )	$\mu_{KP1}$ ( $h^{-1}$ )	$\mu_{3E2}/\mu_{KP1}$
KB <sup>a</sup>	0.797 ± 0.047	0.786 ± 0.034	0.732 ± 0.22	1.074
KB/100 $\mu$ M FeCl <sub>3</sub> <sup>a</sup>	0.766 ± 0.013	0.759 ± 0.054	0.701 ± 0.027	1.082
KB/DP <sup>a</sup>	0.389 ± 0.178	0.004 ± 0.001	0.576 ± 0.011	0.007
KB/100 $\mu$ M FeCl <sub>3</sub> /DP <sup>a</sup>	0.615 ± 0.055	0.025 ± 0.007	0.582 ± 0.061	0.043
KB/100 $\mu$ M FeCl <sub>3</sub> <sup>b</sup>	1.237 ± 0.056	1.238 ± 0.065	1.201 ± 0.064	1.031
KB/100 $\mu$ M FeCl <sub>3</sub> <sup>c</sup>	n.d.	1.182 ± 0.099	1.077 ± 0.060	1.097

<sup>a</sup>The specific growth rate  $\mu$  was calculated from the growth curves shown in Fig. 3a and Fig. S1. Cells were grown in shaking 96-well microtiter plates at 30°C ( $N_0 = 10^7$  cells mL<sup>-1</sup>). Growth was analyzed by measuring the optical density at 600 nm using a Tecan microplate reader. Mean and SD values were calculated from fifteen growth experiments. The large error of  $\mu_{WT}$  in KB/DP was attributed to cell aggregation interfering with a reliable detection of optical densities (cp. also Fig. 3a).

<sup>b</sup>Cells were grown in shaking 24-well microtiter plates at 30°C ( $N_0 = 10^7$  cells mL<sup>-1</sup>). Every hour 50% of the culture was replaced with fresh medium. Growth was analyzed by measuring the optical density at 600 nm using a 1-mL cuvette (d=1 cm). Mean and SD values were calculated from nine growth experiments.

<sup>c</sup>Cells were grown in shaking 96-well microtiter plates at 30°C ( $N_0 = 10^4$  cells mL<sup>-1</sup>). Growth was analyzed by determination of colony forming units, *cfu*. Mean and SD values were calculated from five growth experiments.

**Table S2.** Oligonucleotides used in this investigation

Name	Sequence (5'...3')
<b>Generation of <i>P. putida</i> KP1</b>	
<i>P</i> <sub>A1_04_03</sub> bw kpn	AAATAGGGGGGTACCCGCACATTTCCC
<i>P</i> <sub>A1_04_03</sub> mod2	TTCCGCCATGCTTAATTTCTCCTCTTT
<i>pfrI</i> start mod2	AAATTAAGCATGGCGGAACAACACTATCC
<i>pfrI</i> end mod2	TGCGGCGTTGGATCCGCTGCGAGTTATTGGCCG
<b>Sequencing insert on plasmid</b>	
mini Tn7 reverse MCS	TTGCATTACAGTTTACGAACCGAAC
<b>Sequencing Tn7 insertion on genome</b>	
checkdown primer trans	GTCTTATTACGTGGCCGTGC
Primer TN7R as	CCACGCCCCTCTTTAATACG
tn7left s	TTTGTCATTTTAAATTTTCG
checkup primer trans	GCAGGAGCCGATGAGACAGA

**Movie S1.** Temporal evolution of  $\bar{x}$  in a metapopulation. The evolution of  $\bar{x}$  was obtained by solving equations (4) together with the evolution of the joint distribution of sizes  $n_i$  and compositions  $x_i$ .

**Concluding Discussion**

## CHAPTER IV

### 4. Concluding Discussion

This thesis examines the population dynamics of bacterial co-cultures consisting of *P. putida* pyoverdine producers (cooperators) and non-producers (defectors). For this purpose a metapopulation approach with subpopulations having a stochastic distribution of cooperator fraction and cell number was used. In Chapter II the dynamics under non-selective conditions (iron rich) were analyzed. Here, a conservation of the cooperator fraction was observed in all subpopulations. The cooperative behavior of this system under iron limiting conditions was investigated in Chapter III. Here, pyoverdine acted as a public good, and conditions leading to cooperative behavior in accordance to Simpson's paradox were identified. Furthermore, the cost and benefit of cooperative behavior in this public good system and the impact of environmental conditions on selection were examined. Finally, the central role of pyoverdine dynamics - a threshold and a saturation concentration for growth stimulation - on mediating social interactions was clarified.

#### 4.1. Important features for the metapopulation studies

This thesis focuses on population dynamics of metapopulations consisting of many subpopulations. In Chapter II, the metapopulation setup was used to determine population dynamics under non-selective conditions with stochastic distributions of initial cell numbers and initial cooperator fractions. A co-culture of cooperators and defectors was Poisson diluted and split into subpopulations with very low initial cell numbers of around 10 cells per well.

In Chapter III, public good-mediated social interactions (see **Fig. I.3**) were investigated with a multi-level (inside subpopulations and among subpopulations) selection approach (see **Fig I.4** about Simpson's paradox). Therefore, for the development of cooperativity, a stochastic distribution of initial cooperator fractions of a metapopulation as well as an evenly shared and stable public good are indispensable. For the stochastic distribution of initial cooperator fractions, a similar metapopulation setup as in Chapter II was used, but with higher initial cell densities. In previous research, cooperative behavior according to Simpson's paradox was not observed in populations with siderophores as a public good in static growth conditions supporting spatial structures, where public good was not evenly shared in the subpopulations (*Penn et al., 2012*). Therefore, it is important to have well mixed conditions to avoid

differences in local pyoverdine concentrations, so that the public good is evenly shared within one subpopulation and all cells benefit equally from iron acquisition by pyoverdine. Furthermore, pyoverdine plays a central role as a public good for social interactions under selective conditions (*Buckling et al., 2007*). Therefore, it is important that it is stable over the experimental dimensions, which was shown in Chapter III (see **Fig. 3d** of Chapter III).

In general, the metapopulations in Chapter II and Chapter III fulfilled the important requirements for their purposes: the metapopulation in Chapter II had stochastic distributions of initial cell numbers and cooperator fractions and was well-shaken; the metapopulation in Chapter III had the opportunity to develop cooperative behavior according to Simpson's paradox by having stochastic distributions of initial cooperator fractions in subpopulations, well-shaken cultures and a stable public good (similar as previously described by *Chuang et al., 2009*).

#### 4.2. Non-selective growth of the metapopulation

In Chapter II the non-selective growth of the metapopulation was investigated by letting cells grow under iron rich conditions and comparing this situation with a Pólya urn model. Under iron rich conditions, the pyoverdine production of the *P. putida* wildtype cooperator was completely shut off (see **Fig. 2b** of Chapter III). Since cooperators did not invest in pyoverdine production under iron rich conditions, there was no fitness difference between cooperators and defectors and both strains showed the same growth rate in monoculture (see **Table S1** of Chapter III).

Under these conditions, exponentially growing bacterial populations could preserve the stochastic distribution of the cooperator fraction until the end of the growth period (see **Fig. 4** of Chapter II). In this case, the distribution of the cooperator fraction relies on the initial cell number and cooperator fraction of the metapopulation (exemplary initial condition see **Fig. 3** of Chapter II). With decreasing initial cell number in the metapopulation, the stochastic distribution of cooperator fractions of the subpopulations broadens, and at very low cell numbers there is a large number of subpopulations containing either defector or cooperator cells. Furthermore, the peak of the stochastic distribution of the cooperator fractions of all subpopulations fraction has similar value as the cooperator fraction of the metapopulation (see **Fig. 4** of Chapter II). This observation is supported by a Pólya urn model simulating the exponential growth of a metapopulation (*Eggenberger & Pólya, 1923*). In this model, the

stochastic distribution of cooperator fractions broadens during the first generations of exponential growth, but then “freezes” to a steady state (see **Fig. 2** of Chapter II). Both in model and experiments, the cooperator fraction of the metapopulation remains constant over time. The experimental initial and final distributions of cooperator fractions are also similar to the predicted values of the Pólya urn model (see **Fig. 3** and **Fig. 4** of Chapter II).

The results differ from previous models of the probability of fixation in populations due to non-selective evolution (*Kimura, 1955, Otto & Whitlock, 1997*). These models examine non-selective evolutionary effects as genetic drift in populations with constant population size, whose composition changes via stochastic birth and death events in each generation. Thus, the proportion between birth and death events lead to genetic drift and the fraction of one strain can increase over generations and possibly take over the population (fixation) (*Kimura, 1955, Otto & Whitlock, 1997*). There are several differences to the Pólya urn model in Chapter II. First, in Chapter II populations increased in size rather than remaining constant. Second, because of the exponential growth, death events were neglected. Furthermore, the subpopulations in Chapter II did not fixate to either cooperators or defectors; instead, non-selective growth stabilized the stochastic distribution. Only in the first generations a broadening of the distribution of cooperator fractions was observed due to genetic drift (Chapter II). Afterwards, the cooperator fractions of the subpopulations stay constant over time and do not fixate. Hence, non-selective evolution of growing populations as in Chapter II has the potential to lead to the stable coexistence of cooperators and defectors over the long-term.

### **4.3. The importance of initial cell number**

For the metapopulation studies in Chapter II, Poisson dilution conditions were used to obtain very low cell densities with stochastic distributions of initial cell numbers and cooperator fractions between subpopulations (see **Fig. 3** of Chapter II), similar to *Chuang et al. (Chuang et al., 2009)* (see **Chapter I.1.5.** regarding a synthetic microbial system mediating antibiotic resistance via AHL molecules). Stochastic distribution is also one of the prerequisites for possible bacterial cooperative population dynamics behavior following Simpson’s paradox, which was the focus of Chapter III (*Blyth, 1972, Chuang et al., 2009*). However at low cell densities, the pyoverdine production levels are too low in the microbial system of this thesis and do not have a significant effect. In order to obtain a growth benefit from pyoverdine production, more than 0.1  $\mu\text{M}$  pyoverdine must be produced in a subpopulation (see **Fig. 3b**

in Chapter III). With low cell densities, the resulting pyoverdine concentrations after exponential growth would be below this threshold concentration. This means that for the cooperativity experiments in Chapter III, Poisson dilution conditions are difficult to use, because the cells would probably die due to the obtained low cell densities.

Higher initial cell concentrations and stochastic distribution of the initial cooperator fraction of subpopulations can solve this problem; these conditions can be obtained by introducing a non-selective growth phase with low initial cell numbers before the iron limiting growth. This non-selective growth can also be used to design population dynamics experiments with all the necessary preferences for developing cooperativity in accordance with Simpson's paradox (see **Fig I.4**). Another option for solving this problem would be the addition of isolated pyoverdine with a concentration equal to the threshold concentration (0.1  $\mu\text{M}$ ) to the Poisson diluted culture at the beginning of the selective growth phase. In Chapter III, a constitutive cooperator was used (see subchapter 4.4) to simplify theoretical modeling and avoid phenotypic heterogeneity of cooperators. Here, a non-selective growth phase would be impossible, because growth under iron rich conditions would lead to a decrease of the cooperator fraction in co-cultures due to constitutive pyoverdine production. Therefore, an experimental procedure with high initial cell densities and random initial cooperator fractions was established using a simulated rolling of three dices to determine initial cooperator fractions. Furthermore, high initial cell densities promise higher production levels of pyoverdine and bigger growth differences between subpopulations with high initial cooperator fractions to those with low initial cooperator fractions.

#### **4.4. Choice of constitutive cooperator to simplify social interactions mediated by pyoverdine**

As mentioned in the last subchapter, a constitutive pyoverdine cooperator was used for the cooperativity experiments under selective conditions in Chapter III in order to simplify the population dynamics and development of corresponding theoretical models.

As a public good, pyoverdine helps cooperator cells to sense the social environment and acts as a signaling molecule via a feedback mechanism (*Weigert & Kummerli, 2017*). The wildtype pyoverdine cooperator regulates pyoverdine production in response to iron concentration (see **Fig. 2b** of Chapter III) so that the relative fitness of defectors to wildtype cooperators depends strongly on environmental conditions, in this case on the iron

concentration (*Ghoul et al., 2014, Kummerli et al., 2009c*). In extreme cases, cooperator cells shut down pyoverdine production completely and grow at the same rate as “defector” cells. Furthermore, pyoverdine production is dependent on other factors: the growth phase, for example, there is no pyoverdine production in the stationary phase; or cell density, where higher cell densities lead to the faster decrease of production levels. This makes it even harder to predict and model cooperative behaviors with a wildtype pyoverdine cooperator (*Ghoul et al., 2016, Kummerli et al., 2009c*).

Therefore, a constitutive cooperator was used in Chapter III to simplify the population dynamics. The experiments in Chapter III show that the constitutive cooperator produces comparable pyoverdine amounts under iron limiting and iron rich conditions, but the wildtype cooperator does not produce any pyoverdine if iron is not limited (see **Fig. 2b** and **Fig. 3a** of Chapter III). Thus, pyoverdine production of constitutive cooperators under iron rich conditions also has an impact on the growth rate. Constitutive cooperators grow slower than wildtype cooperators (**Fig. S1** of Chapter III), which means that pyoverdine production under iron rich conditions is also a good way to measure quantitatively an approximated value for the cost of the cooperative act. Therefore, the growth rate differences between the constitutive cooperator and defector were measured, which would be impossible with a wildtype cooperator due to the regulation of pyoverdine biosynthesis. Additionally, constitutive pyoverdine production may also lead to a more significant growth advantage for subpopulations with high fraction of cooperators compared to subpopulations with a high fraction of defectors. This is an important prerequisite for the metapopulation study in Chapter III. In total, these results support the choice of a constitutive cooperator in Chapter III.

Another problem could be the phenotypic heterogeneity of pyoverdine production levels at the single cell level. In pure wildtype cooperator cultures, this could lead to wide ranges in cellular pyoverdine production levels of wildtype cooperator cells inside one subpopulation, which is similar to heterogeneous gene expression in mono-species biofilms (*Dumas & Kummerli, 2012, Flemming et al., 2016, Ross-Gillespie et al., 2015*). Here, stochastic gene expression and interactions between cells, for example via cell-cell contact or the feedback mechanism of pyoverdine, are seen as some of the main mechanisms leading to heterogeneity (*Ackermann, 2015*). Without this heterogeneity as in Chapter III with a constitutive cooperator, the modeling is easier and the effect of pyoverdine as public good is clearer to analyze.

In general, a constitutive pyoverdine cooperator simplifies the modeling of cooperative behavior and avoids phenotypic heterogeneity and regulation of pyoverdine production, which can lead to complete downregulation of pyoverdine production.

#### 4.5. Selective growth and the development of cooperative interactions

In Chapter III, the development of cooperativity was examined, which in this case is defined as an increase of the global cooperator fraction  $\bar{x}$ . In a systems biology approach, the social interactions mediated by the public good pyoverdine were examined under selective conditions with strict iron limitation. Under these conditions pyoverdine is indispensable for growth, which was shown with monoculture experiments where defectors could not grow at all under strict iron limitation (see **Fig. 3a** of Chapter III). The pyoverdine production levels per cell were also determined in both iron-limiting and iron rich conditions of both constitutive cooperator and defector (see **Fig. 2b** of Chapter III). There, the constitutive cooperator produces pyoverdine in all conditions, whereas the defector not at all. By quantitatively determining the growth rate difference between monocultures of the constitutive cooperator and defector under iron rich conditions, an estimation for the cost of cooperation was obtained (see **Tab. S1** of Chapter III). This metabolic cost leads to an intra-population selection, where defectors have a growth advantage against cooperators in one population. Furthermore in co-culture experiments under iron limitation, it was proven that pyoverdine is not privatized in the experimental setup of Chapter III, because cooperators and defectors start to grow at the same time point (see **Fig. 3c** of Chapter III). Additionally, with co-culture experiments under iron limitation with different initial cooperator fractions, it was proven that higher initial cooperator fractions led to faster growth (**Fig. S2** of Chapter III). This shows that there is also an inter-population selection, which means that populations with higher initial cooperator fractions have a growth advantage. In metapopulations, there is a multi-level selection of both intra-population and inter-population selection and in order to develop cooperativity, the inter-population selection needs to dominate. Furthermore, with growth rate measurements of defector cultures applied with differing initial extracellular pyoverdine concentrations, the benefit of cooperative behavior was quantified (see **Fig. 3b** of Chapter III). Here, the growth rate of the defector culture increases linearly with increasing extracellular pyoverdine concentration for pyoverdine concentration above the threshold concentration of about 0.1  $\mu\text{M}$ . However, this beneficial effect saturates with pyoverdine concentration over a value of around 0.8 to 1  $\mu\text{M}$ . This experimental result also showed that

there is a growth advantage of more cooperative subpopulations as in **Fig. S2** of Chapter III (more cooperative subpopulations have higher initial cooperator fractions and produce more pyoverdine compared to subpopulations with low cooperator fractions), but that this growth advantage does not stay constant over the exponential growth period: At the beginning of the exponential growth phase, subpopulations with higher initial cooperator fractions have a high growth advantage over subpopulations with lower initial cooperator fractions, because they produce more pyoverdine. However, this advantage decreases over time because subpopulations with high cooperator fractions reach pyoverdine concentrations where the benefit saturates. This dynamic behavior of benefit in dependence to pyoverdine concentration highlights the central role of pyoverdine's specific properties in mediating social interactions.

The experimentally determined basic properties, e.g., cost, pyoverdine concentration dependent benefit and pyoverdine production rate per cell in the previous paragraph were implemented into a theoretical model, which then predicts a transient increase of the global cooperator fraction  $\bar{x}$  in the metapopulation (see **Fig. 4a** of Chapter III). This increase is only transient, because of the abovementioned saturation effect. In the model, the inter-population selection is dominant at the beginning of the exponential growth phase and  $\bar{x}$  increases. But, because the selection advantage of defectors in subpopulations during the exponential growth phase remains constant, the intra-population selection becomes more and more dominant, the increase of  $\bar{x}$  peaks and then decreases until the metapopulation reaches the stationary growth phase, where  $\bar{x}$  stays constant. The transient increase of  $\bar{x}$  in the metapopulation model was similar to the previously-developed theoretical models based on the repetitive prisoner's dilemma, which simulates multi-level selection in public good systems as in Chapter III (*Melbinger et al., 2010, Cremer et al., 2011*). However, the repetitive prisoner's dilemma models predict the peak of transient increase at the end of the exponential growth phase, whereas for the model in Chapter III the peak was in the middle of exponential growth. This difference arises because previously-described models consider only the cost and benefit of the cooperative act as constant values, while the newly-developed model from Chapter III also considers properties of the public good pyoverdine, i.e. the threshold concentration and saturation behavior as mentioned above, and its impact on the benefit (*Melbinger et al., 2010, Cremer et al., 2011*). Another difference between the two models is that in the previous model the stochastic distribution of initial cooperator fraction was the only decisive factor for the

development of cooperativity (*Melbinger et al., 2010, Cremer et al., 2011*). So, the transient increase only occurs at low initial cell concentrations, where smaller initial cell concentrations broaden the stochastic distribution of initial cooperator fraction and lead to a greater transient increase of  $\bar{x}$  (*Melbinger et al., 2010, Cremer et al., 2011*). In Chapter III, the pyoverdine concentrations were identified as another important factor. At low cell densities, populations did not benefit from pyoverdine production, because its accumulated concentration was below a threshold concentration. Therefore, a high initial cell number was needed to obtain conditions, where the population would benefit from pyoverdine production by accumulating sufficient pyoverdine concentrations.

The findings of the model were experimentally proven via metapopulation studies with high initial cell numbers and a stochastic distribution of initial cooperator fraction in 96 subpopulations (see **Fig. 5a** of Chapter III). As a result, a statistically relevant transient increase in  $\bar{x}$  between the experiments was obtained (see **Fig. 5b** of Chapter III), which was similar to the theoretical model of Chapter III (see **Fig. 6** of Chapter III). In contrast to previous experimental studies from *Chuang et al.* with metapopulations (see **Chapter I.1.5.** observing a synthetic microbial system mediating antibiotic resistance via AHL molecules), the increase of  $\bar{x}$  in Chapter III is transient and not stable.

The studies of population dynamics in metapopulations can be extended to multiple life cycles, as was done in the experiments of *Chuang et al.* Multiple life cycles is understood as having multiple growth phases, which start with the dilution of merged cultures into fresh medium and regrouping into subpopulations. This is in contrast to population dynamics studies in this thesis, where only one life cycle was observed and high initial cell numbers were used. To obtain such a multiple life cycles scenario, bottlenecks are created by using Poisson dilution conditions. But, as in Chapter III, the cell densities would be then too low and cells would probably die because the threshold concentration of pyoverdine in the subpopulations would not be reached in one life cycle. Multiple life cycles with regrouping after Poisson dilution are not suitable for the system used in Chapter III. Presumably, for the experiments of Chapter III, the start of a new life cycle at the time point of maximum transient increase of  $\bar{x}$  would lead to a maintenance of cooperativity, which would then lead to an increase of  $\bar{x}$  or the complete takeover of cooperators after multiple life cycles. This scenario is supported by a theoretical model dealing with multiple life cycles in metapopulations and the impact of the duration of life cycles on maintaining cooperativity. In

this model, short life cycles lead to coexistence or complete cooperative metapopulations (Cremer *et al.*, 2012). Here, the “population-growth” mechanism is effective, meaning that inter-population selection is dominant and subpopulations with higher cooperators fraction grow faster. In this model, a long life cycle, meaning the start of a new life cycle at the end of an exponential growth phase or during a stationary growth phase, favors the “population-fixation” mechanism, where subpopulations fixate to completely cooperative or defective (Cremer *et al.*, 2012). There, completely cooperative subpopulations reach higher cell densities than purely defective ones, but with an increasing length of life cycles more and more subpopulations fixate to purely defective due to intra-population selection. This then can lead to a decrease of cooperators after each life cycle.

In sum, a systems biology approach was developed which had experimentally testable quantitative predictions, which in turn provided valuable insights into social interaction mediated by public goods. In particular, the central role of public goods, as illustrated by pyoverdine in Chapter III was shown and how its dynamics mediate complex social interactions. In the metapopulation of Chapter III, a transient increase of  $\bar{x}$  occurred in both experimental results and the theoretical model. Unlike other public good systems, a multiple life cycle approach using population bottlenecks was not suitable because there is no growth stimulation by pyoverdine at low cell densities.

#### **4.6. Impact of environmental conditions on public good mediated interactions**

The outcome of social interactions relies on several factors. Differences in environmental conditions, e.g. nutrition (determined by the choice of media) or diffusion, can have a significant impact on the development of cooperativity.

##### **4.6.1. Choice of media can lead to critical limitations, changes in cost of cooperative behavior and private usage of public goods**

The choice of media, which determines the nutrition, is one of these critical criteria. In the past few years there have been controversial discussions which media can lead to a cooperative behavior (Kummerli & Ross-Gillespie, 2014, Rainey *et al.*, 2014, Zhang & Rainey, 2013). The central question is in which media is the iron limitation sufficient that pyoverdine can act as a public good. Under some conditions, private usage of pyoverdine by cooperators was observed (Zhang & Rainey, 2013). For the experimental conditions in Chapter III,

pyoverdine can be regarded as a public good due to high initial cell densities, resulting in high pyoverdine concentrations, and the simultaneous start of the growth of cooperators and defectors in co-cultures (see **Fig. 3c** of Chapter III). Furthermore, a higher availability of iron or pyoverdine in the media can alter the cost of cooperation, in this case the pyoverdine production, which then also has an impact on cooperative interactions.

In the experiments described in Chapter II, the so-called CAA medium with additionally supplied iron was used (see Materials & Methods in Chapter II). Due to its very low iron concentrations, the CAA medium is regarded as the standard for cooperativity studies with siderophores as a public good (*Kummerli & Ross-Gillespie, 2014*). In Chapter II, readily reproducible results for the non-selective evolution experiments under iron rich conditions were obtained using CAA medium supplied with 200  $\mu\text{M}$  iron chloride. In contrast, under strict iron limiting conditions, provided by CAA medium with the addition of the iron chelator *apo*-transferrin along with sodium-hydrocarbonate, the results were different among experimental repetitions of metapopulation studies with same initial conditions and showed a very random profile with no statistical relevance (data not shown). Here, not only iron limitation but also additional limitations, of carbon or nitrogen for example, seemed to occur, affecting pyoverdine production and cell growth and leading to side effects on the development of social interactions. In systems with pyoverdine as a public good, carbon limitation leads to higher pyoverdine production cost for cooperators, because it is a building block for pyoverdine biosynthesis (*Sexton & Schuster, 2017*). This limitation affects cooperativity by significantly increasing the defector fraction, whereas phosphorus limitation has no impact on the cooperative interactions (*Sexton & Schuster, 2017*). Additionally, pseudomonads produce proteases, which presumably degrade the iron chelator *apo*-transferrin indicated by a growth boost at time points during late exponential growth phase (*Jin et al., 2018*). This degradation also shifts iron limiting into iron rich conditions. Furthermore, it was shown that nutrient-rich environments maintain cooperation (*Connelly et al., 2017*). Furthermore,

Therefore, for the population dynamics studies in Chapter III, the so-called King's B (KB) medium, which is richer in nutrients than the CAA medium, was used (see Materials & Methods in Chapter III); this medium was also part of the controversial discussion mentioned above (*Kummerli & Ross-Gillespie, 2014, Rainey et al., 2014, Zhang & Rainey, 2013*). However, twice as high chelator concentrations (1 mM) as compared to *Zhang & Rainey* was

used in the population dynamics studies in Chapter III, producing strict iron limiting conditions, which restrict the growth of pure defector cultures. Under the conditions in Chapter III there was no private usage of pyoverdine, and the population dynamics experiments showed a statistically relevant transient increase among the experiments, as mentioned in the previous subchapter.

Another important factor for cooperative behavior is the cost of cooperation - in this thesis the metabolic costs for pyoverdine production - which depends on the choice of media composition. It was shown in a system with a cooperator regulating pyoverdine production that decreasing the necessity for pyoverdine production led to a more stable cooperative behavior, because the cost of cooperation was decreased (*Dumas & Kummerli, 2012*). In contrast to the system mentioned above, the system in Chapter III has a constitutive pyoverdine cooperator, where a decreased necessity for pyoverdine production via either higher iron availability or pyoverdine supplemented at the beginning of the experiment, would not significantly decrease pyoverdine production. The cost for cooperation will stay instead constant. But, higher iron availability or supplemented pyoverdine would decrease the selective pressure by decreasing the dependence of defectors and cooperators on the pyoverdine production of cooperators. Higher available iron concentrations would make it possible to take up iron via diffusion. Additionally, high initial extracellular pyoverdine would give cells a growth stimulation effect from the beginning of the experiment. Although both cooperators and defectors have a growth benefit from less selective conditions, this benefit is presumably more beneficial for defectors, because cooperators still have metabolic costs for pyoverdine production. Under less selective conditions inter-population selection will become weaker; meaning that the growth advantage of subpopulations with high initial cooperator fractions compared to subpopulations with low ones will decrease. However, the cost of cooperation will stay the same and so will the intra-population selection, i.e. defectors grow faster than cooperators in co-cultures. In sum, intra-population selection becomes dominant over inter-population selection, which could lead to the extinction of cooperators.

### **4.6.2. The role of diffusion in social interactions mediated by public goods**

Another aspect of cooperative behavior is to what extent diffusion has an impact on cooperative interactions. In the experiments of Chapter III, social interactions under well-mixed conditions were examined. Of course, social behaviors are completely different in non-structured (well-mixed) or spatial structured (static) cultures. These differences definitely

change diffusion of both nutrients and public goods, and therefore have an enormous impact on both growth and public good interactions in the culture (Allison, 2005, Zhang & Rainey, 2013). Additionally, experimental conditions such as the viscosity of the medium can have an impact on diffusion and thus on the interactions of public goods, e.g. by favoring private over public use (Kummerli *et al.*, 2009b). Environmental stress caused by antimicrobial compounds or photons can also have an outcome on the private usage of pyoverdine in order to protect cooperators against reactive oxygen species (Jin *et al.*, 2018). Here, the pyoverdine is kept in the periplasmic space of cooperators during the time period of environmental stress and this leads to maintenance of cooperative behavior (Jin *et al.*, 2018). This kind of privatization is not abundant in the experiments in Chapter III, because none of these additional environmental stresses are prevalent.

Non-selective growth was measured under several experimental setups: cultures in 96 well plates were incubated in either a well plate incubator or a well plate reader and serial diluted cultures in 24 well plates were incubated in a well plate incubator. When comparing the results from the various setups, differences were observed in the growth rates of the strains and the selection advantage of defectors (see **Table S1** in Chapter III). These differences may be due to modified diffusion, aeration regimes and/or mixing characteristics among the various cultivation systems. The highest growth rates were obtained by shaking the 24 well plates with serial dilution of the culture with new medium every hour. On the one hand, the serial dilution setup decreases the chances of limitation of nutrients, as mentioned in subchapter 4.6.1, and oxygen, because the dilution step keeps the level of dissolved oxygen high. On the other hand, the architecture of the 24 well plates, for example the surface-to-volume ratio or mixing characteristic, might result in more thorough mixing and aeration than that of the 96 well plates. In the 96 well plates experiments, significant differences also occurred between experiments depending on how growth was measured: whether with automatic measurements of the optical density in a well plate reader or a manual determination of the *cfu* (colony forming units). The measurement of *cfu* counts only active cells, whereas the measurement of optical density counts active and dead cells. Of course, these different measuring methods produce differences in results. But it is also probable that these differences are additionally caused by differing shaking and aeration regimes between the well plate incubator and the well plate reader.

Other studies show that in a low diffusion regime, the social behavior mediated by signaling molecules, such as the public good pyoverdine with its feedback mechanism is highly influenced by experimental conditions (Youk & Lim, 2014). This is in large extent due to the difference between local and global product concentration, as also observed in a system dealing with extracellular proteases and the availability of peptides (Bachmann *et al.*, 2011, Youk & Lim, 2014). The concentration difference and the volume of the local concentration area depend on mixing characteristics and cell density, where higher densities decrease differences between local and global concentration (Youk & Lim, 2014). In Chapter III, small differences between local and global pyoverdine concentrations in the subpopulations cannot be completely ruled out. But, these differences should have only a minor impact on the population dynamics studies because of the high initial cell concentrations and the shaking of the culture. This is supported by the fact that cooperators and defectors start growing at the same time point in co-cultures under iron limitation (see **Fig. 3c** in Chapter III).

In general, because cooperative behaviors are so complex, as evidenced by the changing cost and benefit of the cooperative act, they can be impacted by many environmental conditions, including nutrition, aeration and diffusion (Allison, 2005, Chuang *et al.*, 2010, Connelly *et al.*, 2017, Sexton & Schuster, 2017, Youk & Lim, 2014). Iron limitation is the key reason for the development of social interactions mediated by pyoverdine, but the choice of medium may also lead to unwanted side effects. For this reason, a nutrient-rich medium with strict iron limitation was chosen in Chapter III. Furthermore, higher availability of neither iron nor pyoverdine would decrease the pyoverdine production cost in the system of Chapter III, because a constitutive cooperator was used. Regarding mixing and diffusion, pyoverdine can be seen as an equally-distributed public good due to the simultaneous onset of growth start of both cooperators and defectors in co-cultures.

#### **4.7. Pyoverdine-mediated social interactions in nature and their practical usage**

An important question addressed by lab experiments is to what extent they can provide insights into processes in natural environments and how these can lead to practical usage. Here, the preferences of the lab system are compared with natural conditions of systems with siderophore producing pseudomonads. Afterwards, exemplary usages of pyoverdine as industrial product were discussed based on their significance on natural processes.

#### 4.7.1. Significance of lab result for natural conditions

In order to mimic ecological processes, the experiments in this thesis used a ferric ( $\text{Fe}^{3+}$ ) iron source ( $\text{FeCl}_3$ ), the most prevalent form of iron found in nature due to the oxidation of ferrous iron ( $\text{Fe}^{2+}$ ) under aerobic conditions, along with the pyoverdine production of *P. putida* a system which also occurs in nature, where it plays a role as a public good in cooperative interactions. Furthermore, the evolution of pyoverdine defectors exists under natural conditions, and cooperative interactions between cooperators and defectors, both in nature and in lab conditions, are similar to the experiments in this thesis, e.g. by the splitting of the cultures into many subpopulations or liquid cultures (Bruce *et al.*, 2017, Butaite *et al.*, 2017). In contrast, bacteria in nature live mainly in complex and spatial structures, which could significantly reduce the dispersal of public goods (Julou *et al.*, 2013). Examples of environments with siderophores as a public good are communities in soil or freshwater, and cystic fibrosis patients (Bruce *et al.*, 2017, Butaite *et al.*, 2017, Harrison *et al.*, 2017). In particular, the results of this thesis could be applied to natural freshwater environments that show the greatest similarity e.g. those having a liquid and unstructured environment with a high possibility of developing a metapopulation.

In nature, evolution produces mostly partially-deficient public good defectors, and these have a higher chance of outcompeting cooperators due to fewer side effects (Dumas & Kummerli, 2012). This has also been confirmed with experiments, where the relative fitness of defectors compared to the constitutive cooperator was measured. Here, the partially-deficient defector used in Chapter II and III was chosen because it had the highest relative fitness and a much higher relative fitness than the engineered knock-out mutants (results not shown).

#### 4.7.2. Practical usage of pyoverdine mediated cooperative interactions

Cooperativity studies could lead to a practical usage of pyoverdine, because of its abovementioned significance in nature. Because pyoverdine plays a central role in virulence as a virulence factor in *P. aeruginosa* by scavenging iron in the host, a Trojan horse strategy with engineered cheater strains harboring a drug susceptibility can be used (Brown *et al.*, 2009, Little *et al.*, 2018). Here, these cheaters should at first outcompete the pathogenic strains, for example siderophore-producing *P. aeruginosa* cells, and afterwards be inactivated via medical treatment, but this strategy is limited to specific environmental conditions of strict iron limitation where cooperation would be very costly (Brown *et al.*, 2009, Dumas &

*Kummerli, 2012*). However, the evaluation of virulence in dependence on pyoverdine availability showed non-trivial virulence effects for the host, where a decrease of pyoverdine levels was not enough for a sufficient therapy (*Weigert et al., 2017*). Due to the fact that pyoverdine together with other public and private goods are regulated via quorum sensing in pathogenic pseudomonads, perhaps effective anti-virulence drugs can be developed by targeting the quorum-sensing mechanism (*Schuster et al., 2017*).

Finally, siderophores not only play the key role in iron acquisition, but also prevent the uptake of toxic metals, which leads to the preservation of the intracellular metal composition of pseudomonads (*Cunrath et al., 2016*). They are important not only for growth under iron limitation and virulence, but also for survival under environmental conditions with high concentrations of toxic metals, which can be bound by pyoverdine.

In sum, the experiments in this thesis have taken natural conditions into account by using a natural-occurring iron source, a metabolic pathway mediating cooperative interactions in nature, conditions similar to freshwater environments and a partially-deficient public good defector. This has provided useful insights into cooperativity under natural conditions, but of course these can be further improved with experiments mimicking natural conditions even better. Furthermore, outcomes of cooperativity studies can be employed in the development of anti-virulence drugs, and specific properties of pyoverdine can be used to develop binders of toxic metals in the environment.

### **4.8. Outlook**

It was shown in Chapter II of this thesis that under non-selective and well mixed conditions, the cooperator fractions of a metapopulation consisting of co-cultures of wildtype cooperators and defectors is conserved in subpopulations and it do not fixate to only cooperator or defector subpopulations. Furthermore, in Chapter III, conditions under selective pressure were identified where well mixed co-cultures of constitutive pyoverdine cooperators and defectors with random initial cooperator fractions in all subpopulations of a metapopulation led to a transient increase of the global cooperator fraction  $\bar{x}$ . However, there are some questions unanswered for this cooperative system with the public good pyoverdine.

Cooperative behavior of microbes relies significantly on the environmental conditions of their habitat. For selective growth of metapopulations under well mixed conditions, it would be interesting to test various environmental conditions, for example different levels of iron

limitation, to examine the environmental dependence of public good dynamics and its impact on cooperative behavior. Additionally, more natural conditions could be simulated by using minimal media without iron chelators so that pyoverdine would need to scavenge precipitated insoluble iron.

In Chapter III, a constitutive pyoverdine cooperator was used: however, in nature the level of pyoverdine production is regulated in the wildtype cooperator. Since it is completely downregulated at time points when enough iron and pyoverdine are prevalent, it could lead to a stable long-term increase of  $\bar{x}$  in metapopulation experiments (*Kummerli & Brown, 2010*). A further option to fully understand cooperative behavior in nature would be to screen and use natural isolates of cooperators and defectors for population dynamic studies and compare the outcomes with experiments done with lab strains. Additionally, the cooperative system could be extended by a third strain which could either produce an exclusive pyoverdine or produce pyoverdine regulated via quorum sensing. Moreover, a multiple life cycles approach could be employed to observe whether the outcomes of single life cycles remain stable over multiple repetitions.

It would be interesting to analyze how spatial structure, dispersal and segregation might affect public good dynamics and the development of cooperative behavior in response to local differences in environmental conditions and the “privatization” of pyoverdine. For example, for growing colonies, it is mainly the edges that are supplemented with nutrients due to low diffusion into the colony. Furthermore, the cell number of the inoculant can have a big impact on clustering and cooperative behavior. It would be important to examine whether low initial cell concentrations promote cooperation and segregation, because a study of early clonal patches originating from few cells showed that cooperators mostly have other cooperators as neighbors so that they can benefit from each other (*Nadell et al., 2016*). Additionally, if these colonies were examined under the microscope setting, new insights might be obtained into what extent more distant cells would benefit from pyoverdine and the impact this would have on cooperativity. Spatial structuring can also be determined in liquid non-shaking systems, where clusters can form. A multiple life cycles procedure could be applied by disturbing spatial growth via periodic shaking, which leads to bottlenecks by splitting clusters into small aggregates and initiating the growth of new clusters in the next life cycle. This could provide insights into how cooperation is maintained over longer time scales.

Phenotypic heterogeneity and phenotypic switching are two cost saving mechanisms by public good cooperators. It would be interesting to examine these phenomena with the wildtype pyoverdine cooperator (Avery, 2006, Veening *et al.*, 2008). Here, the dynamics of pyoverdine biosynthesis and its dependence on iron and pyoverdine availability should be examined in both well mixed and static cultures via (time-lapse) microscopy. In this way, production levels and heterogeneity can be analyzed in both pure cooperator and mixed cultures. These experiments could shed light on the bistability of cooperator production levels by having cooperator cells which produce either high levels of pyoverdine or no pyoverdine at all. This would represent a phenotypic specialization, which can stabilize cooperative behavior. Furthermore, fluctuating environments can be applied to look for phenotypic switching, i.e. shutting pyoverdine production on and off over observed time scale, of cooperator cells at the single cell level.

---

**REFERENCES OF CHAPTER I AND IV**

- Abdallah, M.A., (1991) Pyoverdins and pseudobactins. In: Handbook of Microbial Iron Chelates. G. Winkelmann (ed). CRC-Press, pp. 139-154.
- Ackerley, D.F., Caradoc-Davies, T.T., and Lamont, I.L. (2003) Substrate specificity of the nonribosomal peptide synthetase PvdD from *Pseudomonas aeruginosa*. *J Bacteriol* **185**: 2848-2855.
- Ackermann, M. (2015) A functional perspective on phenotypic heterogeneity in microorganisms. *Nat Rev Microbiol* **13**: 497-508.
- Albrecht-Gary, A.-M., Blanc, S., Rochel, N., Ocaktan, A.Z., and Abdallah, M.A. (1994) Bacterial Iron Transport: Coordination Properties of Pyoverdinin PaA, a Peptidic Siderophore of *Pseudomonas aeruginosa*. *Inorg Chem* **33**: 6391-6402.
- Allison, S.D. (2005) Cheaters, diffusion and nutrients constrain decomposition by microbial enzymes in spatially structured environments. *Ecology Letters* **8**: 626-635.
- Andrews, S.C., Robinson, A.K., and Rodriguez-Quinones, F. (2003) Bacterial iron homeostasis. *FEMS Microbiol Rev* **27**: 215-237.
- Ankenbauer, R.G. (1992) Cloning of the outer membrane high-affinity Fe(III)-pyochelin receptor of *Pseudomonas aeruginosa*. *J Bacteriol* **174**: 4401-4409.
- Archibald, F. (1983) *Lactobacillus plantarum*, an organism not requiring iron. *FEMS Microbiology Letters* **19**: 29-32.
- Audenaert, K., Pattery, T., Cornelis, P., and Hofte, M. (2002) Induction of systemic resistance to *Botrytis cinerea* in tomato by *Pseudomonas aeruginosa* 7NSK2: role of salicylic acid, pyochelin, and pyocyanin. *Molecular plant-microbe interactions : MPMI* **15**: 1147-1156.
- Avery, S.V. (2006) Microbial cell individuality and the underlying sources of heterogeneity. *Nat Rev Microbiol* **4**: 577-587.
- Axelrod, R., and Hamilton, W.D. (1981) The evolution of cooperation. *Science* **211**: 1390-1396.
- Bachmann, H., Molenaar, D., Kleerebezem, M., and van Hylckama Vlieg, J.E. (2011) High local substrate availability stabilizes a cooperative trait. *The ISME journal* **5**: 929-932.
- Baune, M., Qi, Y., Scholz, K., Volmer, D.A., and Hayen, H. (2017) Structural characterization of pyoverdines produced by *Pseudomonas putida* KT2440 and *Pseudomonas taiwanensis* VLB120. *Biomaterials* **30**: 589-597.
- Beare, P.A., For, R.J., Martin, L.W., and Lamont, I.L. (2003) Siderophore-mediated cell signalling in *Pseudomonas aeruginosa*: divergent pathways regulate virulence factor production and siderophore receptor synthesis. *Mol Microbiol* **47**: 195-207.
- Blyth, C.R. (1972) On Simpson's paradox and the sure-thing principle. *Journal of the American Statistical Association* **67**: 364-366.
- Bouvier, B., and Cezard, C. (2017) Impact of iron coordination isomerism on pyoverdinin recognition by the FpvA membrane transporter of *Pseudomonas aeruginosa*. *Physical chemistry chemical physics : PCCP* **19**: 29498-29507.
- Braun, V., and Hantke, K., (1991) Genetics of bacterial iron transport. In: Handbook of Microbial Iron Chelates. G. Winkelmann (ed). CRC-Press, pp. 107-138.
- Brillet, K., Journet, L., Celia, H., Paulus, L., Stahl, A., Pattus, F., and Cobessi, D. (2007) A beta strand lock exchange for signal transduction in TonB-dependent transducers on the basis of a common structural motif. *Structure (London, England : 1993)* **15**: 1383-1391.
- Brillet, K., Ruffenach, F., Adams, H., Journet, L., Gasser, V., Hoegy, F., Guillon, L., Hannauer, M., Page, A., and Schalk, I.J. (2012) An ABC Transporter with Two Periplasmic Binding Proteins Involved in Iron Acquisition in *Pseudomonas aeruginosa*. *ACS chemical biology*.
- Britigan, B.E., Rasmussen, G.T., and Cox, C.D. (1997) Augmentation of oxidant injury to human pulmonary epithelial cells by the *Pseudomonas aeruginosa* siderophore pyochelin. *Infect Immun* **65**: 1071-1076.
- Brockhurst, M.A. (2007) Population bottlenecks promote cooperation in bacterial biofilms. *PLoS One* **2**: e634.

- Brockhurst, M.A., Buckling, A., Racey, D., and Gardner, A. (2008) Resource supply and the evolution of public-goods cooperation in bacteria. *BMC Biol* **6**: 20.
- Brockhurst, M.A., Hochberg, M.E., Bell, T., and Buckling, A. (2006) Character displacement promotes cooperation in bacterial biofilms. *Curr Biol* **16**: 2030-2034.
- Brown, S.P., and Johnstone, R.A. (2001) Cooperation in the dark: signalling and collective action in quorum-sensing bacteria. *Proceedings. Biological sciences / The Royal Society* **268**: 961-965.
- Brown, S.P., West, S.A., Diggle, S.P., and Griffin, A.S. (2009) Social evolution in micro-organisms and a Trojan horse approach to medical intervention strategies. *Philos Trans R Soc Lond B Biol Sci* **364**: 3157-3168.
- Bruce, J.B., Cooper, G.A., Chabas, H., West, S.A., and Griffin, A.S. (2017) Cheating and resistance to cheating in natural populations of the bacterium *Pseudomonas fluorescens*. *Evolution* **71**: 2484-2495.
- Buckling, A., Harrison, F., Vos, M., Brockhurst, M.A., Gardner, A., West, S.A., and Griffin, A. (2007) Siderophore-mediated cooperation and virulence in *Pseudomonas aeruginosa*. *FEMS Microbiol Ecol* **62**: 135-141.
- Butaite, E., Baumgartner, M., Wyder, S., and Kummerli, R. (2017) Siderophore cheating and cheating resistance shape competition for iron in soil and freshwater *Pseudomonas* communities. *Nat Commun* **8**: 414.
- Cao, J., Woodhall, M.R., Alvarez, J., Cartron, M.L., and Andrews, S.C. (2007) EfeUOB (YcdNOB) is a tripartite, acid-induced and CpxAR-regulated, low-pH Fe<sup>2+</sup> transporter that is cryptic in *Escherichia coli* K-12 but functional in *E. coli* O157:H7. *Mol Microbiol* **65**: 857-875.
- Cezard, C., Farvacques, N., and Sonnet, P. (2015) Chemistry and biology of pyoverdines, *Pseudomonas* primary siderophores. *Curr Med Chem* **22**: 165-186.
- Chen, W.J., Kuo, T.Y., Hsieh, F.C., Chen, P.Y., Wang, C.S., Shih, Y.L., Lai, Y.M., Liu, J.R., Yang, Y.L., and Shih, M.C. (2016) Involvement of type VI secretion system in secretion of iron chelator pyoverdine in *Pseudomonas taiwanensis*. *Sci Rep* **6**: 32950.
- Chuang, J.S., Rivoire, O., and Leibler, S. (2009) Simpson's paradox in a synthetic microbial system. *Science* **323**: 272-275.
- Chuang, J.S., Rivoire, O., and Leibler, S. (2010) Cooperation and Hamilton's rule in a simple synthetic microbial system. *Mol Syst Biol* **6**: 398.
- Cobessi, D., Celia, H., Folschweiller, N., Schalk, I.J., Abdallah, M.A., and Pattus, F. (2005) The crystal structure of the pyoverdine outer membrane receptor FpvA from *Pseudomonas aeruginosa* at 3.6 angstroms resolution. *J Mol Biol* **347**: 121-134.
- Connelly, B.D., Bruger, E.L., McKinley, P.K., and Waters, C.M. (2017) Resource abundance and the critical transition to cooperation. *J Evol Biol* **30**: 750-761.
- Cornelis, P. (2010) Iron uptake and metabolism in pseudomonads. *Applied microbiology and biotechnology* **86**: 1637-1645.
- Cornelis, P., Hohnadel, D., and Meyer, J.M. (1989) Evidence for different pyoverdine-mediated iron uptake systems among *Pseudomonas aeruginosa* strains. *Infect Immun* **57**: 3491-3497.
- Cox, C.D. (1982) Effect of pyochelin on the virulence of *Pseudomonas aeruginosa*. *Infect Immun* **36**: 17-23.
- Cremer, J., Melbinger, A., and Frey, E. (2011) Evolutionary and population dynamics: a coupled approach. *Phys Rev E Stat Nonlin Soft Matter Phys* **84**: 051921.
- Cremer, J., Melbinger, A., and Frey, E. (2012) Growth dynamics and the evolution of cooperation in microbial populations. *Sci Rep* **2**: 281.
- Cremer, J., Reichenbach, T., and Frey, E. (2009) The edge of neutral evolution in social dilemmas. *New J. Phys.* **11**: 093029.
- Crespi, B.J. (2001) The evolution of social behavior in microorganisms. *Trends Ecol Evol* **16**: 178-183.
- Cunrath, O., Geoffroy, V.A., and Schalk, I.J. (2016) Metallome of *Pseudomonas aeruginosa*: a role for siderophores. *Environ Microbiol* **18**: 3258-3267.
- Daniels, R., Vanderleyden, J., and Michiels, J. (2004) Quorum sensing and swarming migration in bacteria. *FEMS Microbiol Rev* **28**: 261-289.

- Davies, D.G., and Geesey, G.G. (1995) Regulation of the alginate biosynthesis gene *algC* in *Pseudomonas aeruginosa* during biofilm development in continuous culture. *Appl Environ Microbiol* **61**: 860-867.
- Dean, C.R., and Poole, K. (1993) Expression of the ferric enterobactin receptor (PfeA) of *Pseudomonas aeruginosa*: involvement of a two-component regulatory system. *Mol Microbiol* **8**: 1095-1103.
- Deziel, E., Lepine, F., Milot, S., and Villemur, R. (2003) *rhlA* is required for the production of a novel biosurfactant promoting swarming motility in *Pseudomonas aeruginosa*: 3-(3-hydroxyalkanoxy)alkanoic acids (HAAs), the precursors of rhamnolipids. *Microbiology* **149**: 2005-2013.
- Diggle, S.P., Gardner, A., West, S.A., and Griffin, A.S. (2007) Evolutionary theory of bacterial quorum sensing: when is a signal not a signal? *Philos Trans R Soc Lond B Biol Sci* **362**: 1241-1249.
- Dos Santos, V.A., Heim, S., Moore, E.R., Stratz, M., and Timmis, K.N. (2004) Insights into the genomic basis of niche specificity of *Pseudomonas putida* KT2440. *Environ Microbiol* **6**: 1264-1286.
- Drake, E.J., and Gulick, A.M. (2011) Structural characterization and high-throughput screening of inhibitors of PvdQ, an NTN hydrolase involved in pyoverdine synthesis. *ACS chemical biology* **6**: 1277-1286.
- Draper, R.C., Martin, L.W., Beare, P.A., and Lamont, I.L. (2011) Differential proteolysis of sigma regulators controls cell-surface signalling in *Pseudomonas aeruginosa*. *Mol Microbiol* **82**: 1444-1453.
- Dugatkin, L.A., Perlin, M., Lucas, J.S., and Atlas, R. (2005) Group-beneficial traits, frequency-dependent selection and genotypic diversity: an antibiotic resistance paradigm. *Proceedings. Biological sciences / The Royal Society* **272**: 79-83.
- Dumas, Z., and Kummerli, R. (2012) Cost of cooperation rules selection for cheats in bacterial metapopulations. *J Evol Biol* **25**: 473-484.
- Dunny, G.M., Brickman, T.J., and Dworkin, M. (2008) Multicellular behavior in bacteria: communication, cooperation, competition and cheating. *Bioessays* **30**: 296-298.
- Edgar, R.J., Hampton, G.E., Garcia, G.P.C., Maher, M.J., Perugini, M.A., Ackerley, D.F., and Lamont, I.L. (2017) Integrated activities of two alternative sigma factors coordinate iron acquisition and uptake by *Pseudomonas aeruginosa*. *Mol Microbiol* **106**: 891-904.
- Edgar, R.J., Xu, X., Shirley, M., Konings, A.F., Martin, L.W., Ackerley, D.F., and Lamont, I.L. (2014) Interactions between an anti-sigma protein and two sigma factors that regulate the pyoverdine signaling pathway in *Pseudomonas aeruginosa*. *BMC microbiology* **14**: 287.
- Eggenberger, F., and Pólya, G. (1923) Über die Statistik verketteter Vorgänge. *ZAMM - Zeitschrift für Angewandte Mathematik und Mechanik* **3**: 279-289.
- Elena, S.F., and Lenski, R.E. (2003) Evolution experiments with microorganisms: the dynamics and genetic bases of adaptation. *Nat Rev Genet* **4**: 457-469.
- Elliott, R.P. (1958) Some Properties of Pyoverdine, the Water-soluble Fluorescent Pigment of the *Pseudomonads*. *Appl Microbiol* **6**: 241-246.
- Escolar, L., Perez-Martin, J., and de Lorenzo, V. (1999) Opening the iron box: transcriptional metalloregulation by the Fur protein. *J Bacteriol* **181**: 6223-6229.
- Flemming, H.C., Wingender, J., Szewzyk, U., Steinberg, P., Rice, S.A., and Kjelleberg, S. (2016) Biofilms: an emergent form of bacterial life. *Nat Rev Microbiol* **14**: 563-575.
- Foster, K.R., Shaulsky, G., Strassmann, J.E., Queller, D.C., and Thompson, C.R.L. (2004) Pleiotropy as a mechanism to stabilize cooperation. *Nature* **431**: 693-696.
- Foster, K.R., and Wenseleers, T. (2006) A general model for the evolution of mutualisms. *J Evol Biol* **19**: 1283-1293.
- Frank, S.A., (1998) *Foundations of social evolution*. Princeton University Press.
- Frost, G.E., and Rosenberg, H. (1973) The inducible citrate-dependent iron transport system in *Escherichia coli* K12. *Biochim Biophys Acta* **330**: 90-101.

- Gao, L., Guo, Z., Wang, Y., Wang, Y., Wang, K., Li, B., and Shen, L. (2018) The Two-Operon-Coded ABC Transporter Complex FpvWXYZCDEF is Required for *Pseudomonas aeruginosa* Growth and Virulence Under Iron-Limiting Conditions. *J Membr Biol* **251**: 91-104.
- Gardner, A., and West, S.A. (2006) Demography, altruism, and the benefits of budding. *J Evol Biol* **19**: 1707-1716.
- Gasser, V., Guillon, L., Cunrath, O., and Schalk, I.J. (2015) Cellular organization of siderophore biosynthesis in *Pseudomonas aeruginosa*: Evidence for siderosomes. *J Inorg Biochem* **148**: 27-34.
- Ghoul, M., West, S.A., Diggle, S.P., and Griffin, A.S. (2014) An experimental test of whether cheating is context dependent. *J Evol Biol* **27**: 551-556.
- Ghoul, M., West, S.A., McCorkell, F.A., Lee, Z.B., Bruce, J.B., and Griffin, A.S. (2016) Pyoverdine cheats fail to invade bacterial populations in stationary phase. *J Evol Biol* **29**: 1728-1736.
- Greenwald, J., Hoegy, F., Nader, M., Journet, L., Mislin, G.L., Graumann, P.L., and Schalk, I.J. (2007) Real time fluorescent resonance energy transfer visualization of ferric pyoverdine uptake in *Pseudomonas aeruginosa*. A role for ferrous iron. *J Biol Chem* **282**: 2987-2995.
- Greenwald, J., Nader, M., Celia, H., Gruffaz, C., Geoffroy, V., Meyer, J.M., Schalk, I.J., and Pattus, F. (2009) FpvA bound to non-cognate pyoverdines: molecular basis of siderophore recognition by an iron transporter. *Mol Microbiol* **72**: 1246-1259.
- Greig, D., and Travisano, M. (2004) The Prisoner's Dilemma and polymorphism in yeast SUC genes. *Proceedings. Biological sciences / The Royal Society* **271 Suppl 3**: S25-26.
- Griffin, A.S., West, S.A., and Buckling, A. (2004) Cooperation and competition in pathogenic bacteria. *Nature* **430**: 1024-1027.
- Griffiths, E. (1991) Iron and bacterial virulence ? a brief overview. *Biology of Metals* **4**: 7-13.
- Guerinot, M.L. (1994) Microbial iron transport. *Annu Rev Microbiol* **48**: 743-772.
- Guerinot, M.L., and Yi, Y. (1994) Iron: Nutritious, Noxious, and Not Readily Available. *Plant Physiology* **104**: 815-820.
- Hamilton, W.D. (1963) The Evolution of Altruistic Behavior. *Am Nat* **97**: 354-356.
- Hamilton, W.D. (1964a) The genetical evolution of social behaviour. I. *J Theor Biol* **7**: 17-52.
- Hamilton, W.D. (1964b) The genetical evolution of social behaviour. II. *J Theor Biol* **7**: 17-52.
- Hannauer, M., Braud, A., Hoegy, F., Ronot, P., Boos, A., and Schalk, I.J. (2012a) The PvdRT-OpmQ efflux pump controls the metal selectivity of the iron uptake pathway mediated by the siderophore pyoverdine in *Pseudomonas aeruginosa*. *Environ Microbiol* **14**: 1696-1708.
- Hannauer, M., Schafer, M., Hoegy, F., Gizzi, P., Wehrung, P., Mislin, G.L., Budzikiewicz, H., and Schalk, I.J. (2012b) Biosynthesis of the pyoverdine siderophore of *Pseudomonas aeruginosa* involves precursors with a myristic or a myristoleic acid chain. *FEBS Lett* **586**: 96-101.
- Hannauer, M., Yeterian, E., Martin, L.W., Lamont, I.L., and Schalk, I.J. (2010) An efflux pump is involved in secretion of newly synthesized siderophore by *Pseudomonas aeruginosa*. *FEBS Lett* **584**: 4751-4755.
- Hantke, K. (1981) Regulation of ferric iron transport in *Escherichia coli* K12: isolation of a constitutive mutant. *Mol Gen Genet* **182**: 288-292.
- Harrison, F., McNally, A., da Silva, A.C., Heeb, S., and Diggle, S.P. (2017) Optimised chronic infection models demonstrate that siderophore 'cheating' in *Pseudomonas aeruginosa* is context specific. *The ISME journal* **11**: 2492-2509.
- Hider, R.C., and Kong, X. (2010) Chemistry and biology of siderophores. *Nat Prod Rep* **27**: 637-657.
- Hooi, D.S., Bycroft, B.W., Chhabra, S.R., Williams, P., and Pritchard, D.I. (2004) Differential immune modulatory activity of *Pseudomonas aeruginosa* quorum-sensing signal molecules. *Infect Immun* **72**: 6463-6470.
- Inglis, R.F., Biernaskie, J.M., Gardner, A., and Kummerli, R. (2016) Presence of a loner strain maintains cooperation and diversity in well-mixed bacterial communities. *Proceedings. Biological sciences / The Royal Society* **283**.
- James, H.E., Beare, P.A., Martin, L.W., and Lamont, I.L. (2005) Mutational analysis of a bifunctional ferrisiderophore receptor and signal-transducing protein from *Pseudomonas aeruginosa*. *J Bacteriol* **187**: 4514-4520.

- Jin, Z., Li, J., Ni, L., Zhang, R., Xia, A., and Jin, F. (2018) Conditional privatization of a public siderophore enables *Pseudomonas aeruginosa* to resist cheater invasion. *Nat Commun* **9**: 1383.
- Joyner, D.C., and Lindow, S.E. (2000) Heterogeneity of iron bioavailability on plants assessed with a whole-cell GFP-based bacterial biosensor. *Microbiology* **146** ( Pt **10**): 2435-2445.
- Julou, T., Mora, T., Guillon, L., Croquette, V., Schalk, I.J., Bensimon, D., and Desprat, N. (2013) Cell-cell contacts confine public goods diffusion inside *Pseudomonas aeruginosa* clonal microcolonies. *Proc Natl Acad Sci U S A* **110**: 12577-12582.
- Kammler, M., Schon, C., and Hantke, K. (1993) Characterization of the ferrous iron uptake system of *Escherichia coli*. *J Bacteriol* **175**: 6212-6219.
- Keller, L., (1999) *Levels of selection in evolution*. Princeton University Press.
- Keller, L., and Surette, M.G. (2006) Communication in bacteria: an ecological and evolutionary perspective. *Nat Rev Microbiol* **4**: 249-258.
- Kerr, B., Neuhauser, C., Bohannan, B.J.M., and Dean, A.M. (2006) Local migration promotes competitive restraint in a host–pathogen 'tragedy of the commons'. *Nature* **442**: 75-78.
- Killingback, T., Bieri, J., and Flatt, T. (2006) Evolution in group-structured populations can resolve the tragedy of the commons. *Proceedings. Biological sciences / The Royal Society* **273**: 1477-1481.
- Kimura, M. (1955) Solution of a Process of Random Genetic Drift with a Continuous Model. *Proc Natl Acad Sci U S A* **41**: 144-150.
- Knebel, J., Kruger, T., Weber, M.F., and Frey, E. (2013) Coexistence and survival in conservative Lotka-Volterra networks. *Phys Rev Lett* **110**: 168106.
- Koster, W. (2001) ABC transporter-mediated uptake of iron, siderophores, heme and vitamin B12. *Res Microbiol* **152**: 291-301.
- Kreft, J.U. (2004) Conflicts of interest in biofilms. *Biofilms* **1**: 265-276.
- Kummerli, R., and Brown, S.P. (2010) Molecular and regulatory properties of a public good shape the evolution of cooperation. *Proc Natl Acad Sci U S A* **107**: 18921-18926.
- Kummerli, R., Gardner, A., West, S.A., and Griffin, A.S. (2009a) Limited dispersal, budding dispersal, and cooperation: an experimental study. *Evolution* **63**: 939-949.
- Kummerli, R., Griffin, A.S., West, S.A., Buckling, A., and Harrison, F. (2009b) Viscous medium promotes cooperation in the pathogenic bacterium *Pseudomonas aeruginosa*. *Proceedings. Biological sciences / The Royal Society* **276**: 3531-3538.
- Kummerli, R., Jiricny, N., Clarke, L.S., West, S.A., and Griffin, A.S. (2009c) Phenotypic plasticity of a cooperative behaviour in bacteria. *J Evol Biol* **22**: 589-598.
- Kummerli, R., and Ross-Gillespie, A. (2014) Explaining the sociobiology of pyoverdinin producing *Pseudomonas*: a comment on Zhang and Rainey (2013). *Evolution* **68**: 3337-3343.
- Kummerli, R., Santorelli, L.A., Granato, E.T., Dumas, Z., Dobay, A., Griffin, A.S., and West, S.A. (2015) Co-evolutionary dynamics between public good producers and cheats in the bacterium *Pseudomonas aeruginosa*. *J Evol Biol* **28**: 2264-2274.
- Lai, B.M., Yan, H.C., Wang, M.Z., Li, N., and Shen, D.S. (2018) A common evolutionary pathway for maintaining quorum sensing in *Pseudomonas aeruginosa*. *Journal of microbiology (Seoul, Korea)* **56**: 83-89.
- Lamont, I.L., Beare, P.A., Ochsner, U., Vasil, A.I., and Vasil, M.L. (2002) Siderophore-mediated signaling regulates virulence factor production in *Pseudomonas aeruginosa*. *Proc Natl Acad Sci U S A* **99**: 7072-7077.
- Lavrrar, J.L., Christoffersen, C.A., and McIntosh, M.A. (2002) Fur-DNA interactions at the bidirectional fepDGC-entS promoter region in *Escherichia coli*. *J Mol Biol* **322**: 983-995.
- Lazdunski, A.M., Ventre, I., and Sturgis, J.N. (2004) Regulatory circuits and communication in Gram-negative bacteria. *Nat Rev Microbiol* **2**: 581-592.
- Le Gac, M., and Doebeli, M. (2010) Environmental viscosity does not affect the evolution of cooperation during experimental evolution of colicogenic bacteria. *Evolution* **64**: 522-533.
- Lin, J., Zhang, W., Cheng, J., Yang, X., Zhu, K., Wang, Y., Wei, G., Qian, P.Y., Luo, Z.Q., and Shen, X. (2017) A *Pseudomonas* T6SS effector recruits PQS-containing outer membrane vesicles for iron acquisition. *Nat Commun* **8**: 14888.

- Little, A.S., Okkotsu, Y., Reinhart, A.A., Damron, F.H., Barbier, M., Barrett, B., Oglesby-Sherrouse, A.G., Goldberg, J.B., Cody, W.L., Schurr, M.J., Vasil, M.L., and Schurr, M.J. (2018) *Pseudomonas aeruginosa* AlgR Phosphorylation Status Differentially Regulates Pyocyanin and Pyoverdine Production. *MBio* **9**.
- Litwin, C.M., and Calderwood, S.B. (1993) Role of iron in regulation of virulence genes. *Clin Microbiol Rev* **6**: 137-149.
- Llamas, M.A., Imperi, F., Visca, P., and Lamont, I.L. (2014) Cell-surface signaling in *Pseudomonas*: stress responses, iron transport, and pathogenicity. *FEMS Microbiol Rev* **38**: 569-597.
- Luce, R.D., and Raiffa, H., (1957) *Games and Decisions: Introduction and Critical Survey*. Dover Publications.
- Marshall, B., Stintzi, A., Gilmour, C., Meyer, J.M., and Poole, K. (2009) Citrate-mediated iron uptake in *Pseudomonas aeruginosa*: involvement of the citrate-inducible FecA receptor and the FeoB ferrous iron transporter. *Microbiology* **155**: 305-315.
- Matthijs, S., Laus, G., Meyer, J.M., Abbaspour-Tehrani, K., Schafer, M., Budzikiewicz, H., and Cornelis, P. (2009) Siderophore-mediated iron acquisition in the entomopathogenic bacterium *Pseudomonas entomophila* L48 and its close relative *Pseudomonas putida* KT2440. *Biometals* **22**: 951-964.
- Matthijs, S., Tehrani, K.A., Laus, G., Jackson, R.W., Cooper, R.M., and Cornelis, P. (2007) Thioquinolobactin, a *Pseudomonas* siderophore with antifungal and anti-*Pythium* activity. *Environ Microbiol* **9**: 425-434.
- Melbinger, A., Cremer, J., and Frey, E. (2010) Evolutionary game theory in growing populations. *Phys Rev Lett* **105**: 178101.
- Melbinger, A., Cremer, J., and Frey, E. (2015) The emergence of cooperation from a single mutant during microbial life cycles. *J R Soc Interface* **12**: 20150171.
- Meyer, J.-M., Hallé, F., Hohnadel, D., Lemanceau, P., and Ratefiarivelo, H., (1987) Siderophores of *Pseudomonas* - biological properties. In: Iron transport in microbes, plants, and animals. G. Winkelmann, D. Van der Helm & J.B. Neilands (eds). VCH, pp.
- Meyer, J.M. (1992) Exogenous siderophore-mediated iron uptake in *Pseudomonas aeruginosa*: possible involvement of porin OprF in iron translocation. *Journal of general microbiology* **138**: 951-958.
- Meyer, J.M., Gruffaz, C., Raharinosy, V., Bezverbnaya, I., Schafer, M., and Budzikiewicz, H. (2008) Siderotyping of fluorescent *Pseudomonas*: molecular mass determination by mass spectrometry as a powerful pyoverdine siderotyping method. *Biometals* **21**: 259-271.
- Meyer, J.M., Stintzi, A., De Vos, D., Cornelis, P., Tappe, R., Taraz, K., and Budzikiewicz, H. (1997) Use of siderophores to type pseudomonads: the three *Pseudomonas aeruginosa* pyoverdine systems. *Microbiology* **143** ( Pt 1): 35-43.
- Moon, C.D., Zhang, X.X., Matthijs, S., Schafer, M., Budzikiewicz, H., and Rainey, P.B. (2008) Genomic, genetic and structural analysis of pyoverdine-mediated iron acquisition in the plant growth-promoting bacterium *Pseudomonas fluorescens* SBW25. *BMC microbiology* **8**: 7.
- Mossialos, D., Ochsner, U., Baysse, C., Chablain, P., Pirnay, J.P., Koedam, N., Budzikiewicz, H., Fernandez, D.U., Schafer, M., Ravel, J., and Cornelis, P. (2002) Identification of new, conserved, non-ribosomal peptide synthetases from fluorescent pseudomonads involved in the biosynthesis of the siderophore pyoverdine. *Mol Microbiol* **45**: 1673-1685.
- Nadal-Jimenez, P., Koch, G., Reis, C.R., Muntendam, R., Raj, H., Jeronimus-Stratingh, C.M., Cool, R.H., and Quax, W.J. (2014) PvdP is a tyrosinase that drives maturation of the pyoverdine chromophore in *Pseudomonas aeruginosa*. *J Bacteriol* **196**: 2681-2690.
- Nadell, C.D., Drescher, K., and Foster, K.R. (2016) Spatial structure, cooperation and competition in biofilms. *Nat Rev Microbiol* **14**: 589-600.
- Neilands, J.B. (1991) A brief history of iron metabolism. *Biol Met* **4**: 1-6.
- Nowak, M.A. (2006) Five rules for the evolution of cooperation. *Science* **314**: 1560-1563.
- Nowak, M.A., and May, R.M. (1992) Evolutionary games and spatial chaos. *Nature* **359**: 826-829.
- Otto, B.R., Verweij-van Vught, A.M., and MacLaren, D.M. (1992) Transferrins and heme-compounds as iron sources for pathogenic bacteria. *Crit Rev Microbiol* **18**: 217-233.

- Otto, S.P., and Whitlock, M.C. (1997) The probability of fixation in populations of changing size. *Genetics* **146**: 723-733.
- Parsek, M.R., and Greenberg, E.P. (2005) Sociomicrobiology: the connections between quorum sensing and biofilms. *Trends Microbiol* **13**: 27-33.
- Payne, S.M. (1988) Iron and virulence in the family Enterobacteriaceae. *Crit Rev Microbiol* **16**: 81-111.
- Payne, S.M. (1993) Iron acquisition in microbial pathogenesis. *Trends Microbiol* **1**: 66-69.
- Penn, A.S., Conibear, T.C., Watson, R.A., Kraaijeveld, A.R., and Webb, J.S. (2012) Can Simpson's paradox explain co-operation in *Pseudomonas aeruginosa* biofilms? *FEMS Immunol Med Microbiol* **65**: 226-235.
- Poole, K., Neshat, S., Krebes, K., and Heinrichs, D.E. (1993) Cloning and nucleotide sequence analysis of the ferripyoverdine receptor gene *fvpA* of *Pseudomonas aeruginosa*. *J Bacteriol* **175**: 4597-4604.
- Posey, J.E., and Gherardini, F.C. (2000) Lack of a role for iron in the Lyme disease pathogen. *Science* **288**: 1651-1653.
- Rainey, P.B., Buckling, A., Kassen, R., and Travisano, M. (2000) The emergence and maintenance of diversity: insights from experimental bacterial populations. *Trends Ecol Evol* **15**: 243-247.
- Rainey, P.B., Desprat, N., Driscoll, W.W., and Zhang, X.X. (2014) Microbes are not bound by sociobiology: response to Kummerli and Ross-Gillespie (2013). *Evolution* **68**: 3344-3355.
- Rainey, P.B., and Rainey, K. (2003) Evolution of cooperation and conflict in experimental bacterial populations. *Nature* **425**: 72-74.
- Ratledge, C., and Dover, L.G. (2000) Iron metabolism in pathogenic bacteria. *Annu Rev Microbiol* **54**: 881-941.
- Ravel, J., and Cornelis, P. (2003) Genomics of pyoverdine-mediated iron uptake in pseudomonads. *Trends Microbiol* **11**: 195-200.
- Reichenbach, T., and Frey, E. (2008) Instability of spatial patterns and its ambiguous impact on species diversity. *Phys Rev Lett* **101**: 058102.
- Reichenbach, T., Mobilia, M., and Frey, E. (2007a) Mobility promotes and jeopardizes biodiversity in rock-paper-scissors games. *Nature* **448**: 1046-1049.
- Reichenbach, T., Mobilia, M., and Frey, E. (2007b) Noise and correlations in a spatial population model with cyclic competition. *Phys Rev Lett* **99**: 238105.
- Reid, R.T., Live, D.H., Faulkner, D.J., and Butler, A. (1993) A siderophore from a marine bacterium with an exceptional ferric ion affinity constant. *Nature* **366**: 455-458.
- Riley, M.A., and Wertz, J.E. (2002) Bacteriocins: evolution, ecology, and application. *Annu Rev Microbiol* **56**: 117-137.
- Ringel, M.T., Drager, G., and Bruser, T. (2016) PvdN Enzyme Catalyzes a Periplasmic Pyoverdine Modification. *J Biol Chem* **291**: 23929-23938.
- Ringel, M.T., Drager, G., and Bruser, T. (2018) PvdO is required for the oxidation of dihydropyoverdine as the last step of fluorophore formation in *Pseudomonas fluorescens*. *J Biol Chem* **293**: 2330-2341.
- Ross-Gillespie, A., Dumas, Z., and Kummerli, R. (2015) Evolutionary dynamics of interlinked public goods traits: an experimental study of siderophore production in *Pseudomonas aeruginosa*. *J Evol Biol* **28**: 29-39.
- Ross-Gillespie, A., Gardner, A., West, S.A., and Griffin, A.S. (2007) Frequency dependence and cooperation: theory and a test with bacteria. *Am Nat* **170**: 331-342.
- Rousset, F., (2004) *Genetic Structure and Selection in Subdivided Populations*. Princeton University Press.
- Sachs, J.L., Mueller, U.G., Wilcox, T.P., and Bull, J.J. (2004) The evolution of cooperation. *Q Rev Biol* **79**: 135-160.
- Schalk, I.J., and Guillon, L. (2013) Pyoverdine biosynthesis and secretion in *Pseudomonas aeruginosa*: implications for metal homeostasis. *Environ Microbiol* **15**: 1661-1673.
- Schalk, I.J., Kyslik, P., Prome, D., van Dorsselaer, A., Poole, K., Abdallah, M.A., and Pattus, F. (1999) Copurification of the FpvA ferric pyoverdine receptor of *Pseudomonas aeruginosa* with its

- iron-free ligand: implications for siderophore-mediated iron transport. *Biochemistry* **38**: 9357-9365.
- Schuster, M., Sexton, D.J., and Hense, B.A. (2017) Why Quorum Sensing Controls Private Goods. *Front Microbiol* **8**: 885.
- Schwyn, B., and Neilands, J.B. (1987) Universal chemical assay for the detection and determination of siderophores. *Anal Biochem* **160**: 47-56.
- Sexton, D.J., and Schuster, M. (2017) Nutrient limitation determines the fitness of cheaters in bacterial siderophore cooperation. *Nat Commun* **8**: 230.
- Shen, J., Meldrum, A., and Poole, K. (2002) FpvA receptor involvement in pyoverdine biosynthesis in *Pseudomonas aeruginosa*. *J Bacteriol* **184**: 3268-3275.
- Shirley, M., and Lamont, I.L. (2009) Role of TonB1 in pyoverdine-mediated signaling in *Pseudomonas aeruginosa*. *J Bacteriol* **191**: 5634-5640.
- Sigel, S.P., and Payne, S.M. (1982) Effect of iron limitation on growth, siderophore production, and expression of outer membrane proteins of *Vibrio cholerae*. *J Bacteriol* **150**: 148-155.
- Simpson, E.H. (1951) The Interpretation of Interaction in Contingency Tables. *Journal of the Royal Statistical Society. Series B (Methodological)* **13**: 238-241.
- Smith, E.E., Sims, E.H., Spencer, D.H., Kaul, R., and Olson, M.V. (2005) Evidence for diversifying selection at the pyoverdine locus of *Pseudomonas aeruginosa*. *J Bacteriol* **187**: 2138-2147.
- Smith, J.M. (1964) Group Selection and Kin Selection. *Nature* **201**: 1145-1147.
- Stojiljkovic, I., Baumler, A.J., and Hantke, K. (1994) Fur regulon in gram-negative bacteria. Identification and characterization of new iron-regulated *Escherichia coli* genes by a fur titration assay. *J Mol Biol* **236**: 531-545.
- Stojiljkovic, I., Cobeljic, M., and Hantke, K. (1993) *Escherichia coli* K-12 ferrous iron uptake mutants are impaired in their ability to colonize the mouse intestine. *FEMS Microbiology Letters* **108**: 111-115.
- Sun, G.X., Zhou, W.Q., and Zhong, J.J. (2006) Organotin decomposition by pyochelin, secreted by *Pseudomonas aeruginosa* even in an iron-sufficient environment. *Appl Environ Microbiol* **72**: 6411-6413.
- Tateda, K., Ishii, Y., Horikawa, M., Matsumoto, T., Miyairi, S., Pechere, J.C., Standiford, T.J., Ishiguro, M., and Yamaguchi, K. (2003) The *Pseudomonas aeruginosa* autoinducer N-3-oxododecanoyl homoserine lactone accelerates apoptosis in macrophages and neutrophils. *Infect Immun* **71**: 5785-5793.
- Tiburzi, F., Imperi, F., and Visca, P. (2008) Intracellular levels and activity of PvdS, the major iron starvation sigma factor of *Pseudomonas aeruginosa*. *Mol Microbiol* **67**: 213-227.
- Travisano, M., and Velicer, G.J. (2004) Strategies of microbial cheater control. *Trends Microbiol* **12**: 72-78.
- Trivers, R.L. (1971) The Evolution of Reciprocal Altruism. *The Quarterly Review of Biology* **46**: 35-57.
- van Oeffelen, L., Cornelis, P., Van Delm, W., De Ridder, F., De Moor, B., and Moreau, Y. (2008) Detecting cis-regulatory binding sites for cooperatively binding proteins. *Nucleic Acids Res* **36**: e46.
- Vande Woestyne, M., Bruyneel, B., Mergeay, M., and Verstraete, W. (1991) The Fe(2+) Chelator Proferrorosamine A Is Essential for the Siderophore-Mediated Uptake of Iron by *Pseudomonas roseus fluorescens*. *Appl Environ Microbiol* **57**: 949-954.
- Veening, J.W., Stewart, E.J., Berngruber, T.W., Taddei, F., Kuipers, O.P., and Hamoen, L.W. (2008) Bet-hedging and epigenetic inheritance in bacterial cell development. *Proc Natl Acad Sci U S A* **105**: 4393-4398.
- Velicer, G.J. (2003) Social strife in the microbial world. *Trends Microbiol* **11**: 330-337.
- Velicer, G.J., Kroos, L., and Lenski, R.E. (2000) Developmental cheating in the social bacterium *Myxococcus xanthus*. *Nature* **404**: 598-601.
- Venturi, V., Otten, M., Korse, V., Brouwer, B., Leong, J., and Weisbeek, P. (1995a) Alginate regulatory and biosynthetic gene homologs in *Pseudomonas putida* WCS358: correlation with the siderophore regulatory gene pfrA. *Gene* **155**: 83-88.

- Venturi, V., Ottevanger, C., Bracke, M., and Weisbeek, P. (1995b) Iron regulation of siderophore biosynthesis and transport in *Pseudomonas putida* WCS358: involvement of a transcriptional activator and of the Fur protein. *Mol Microbiol* **15**: 1081-1093.
- Venturi, V., Ottevanger, C., Leong, J., and Weisbeek, P.J. (1993) Identification and characterization of a siderophore regulatory gene (*pfrA*) of *Pseudomonas putida* WCS358: homology to the alginate regulatory gene *aigQ* of *Pseudomonas aeruginosa*. *Mol Microbiol* **10**: 63-73.
- Vinayavekhin, N., and Saghatelian, A. (2009) Regulation of alkyl-dihydrothiazole-carboxylates (ATCs) by iron and the pyochelin gene cluster in *Pseudomonas aeruginosa*. *ACS chemical biology* **4**: 617-623.
- Visca, P., Colotti, G., Serino, L., Verzili, D., Orsi, N., and Chiancone, E. (1992) Metal regulation of siderophore synthesis in *Pseudomonas aeruginosa* and functional effects of siderophore-metal complexes. *Appl Environ Microbiol* **58**: 2886-2893.
- Visca, P., Imperi, F., and Lamont, I.L. (2007) Pyoverdine siderophores: from biogenesis to biosignificance. *Trends Microbiol* **15**: 22-30.
- Visca, P., Leoni, L., Wilson, M.J., and Lamont, I.L. (2002) Iron transport and regulation, cell signalling and genomics: lessons from *Escherichia coli* and *Pseudomonas*. *Mol Microbiol* **45**: 1177-1190.
- Wagner, C.H. (1982) Simpson's Paradox in Real Life. *The American Statistician* **36**: 46-48.
- Webb, J.S., Givskov, M., and Kjelleberg, S. (2003) Bacterial biofilms: prokaryotic adventures in multicellularity. *Curr Opin Microbiol* **6**: 578-585.
- Wei, H., and Aristilde, L. (2015) Structural characterization of multiple pyoverdines secreted by two *Pseudomonas* strains using liquid chromatography-high resolution tandem mass spectrometry with varying dissociation energies. *Anal Bioanal Chem* **407**: 4629-4638.
- Weigert, M., and Kummerli, R. (2017) The physical boundaries of public goods cooperation between surface-attached bacterial cells. *Proceedings. Biological sciences / The Royal Society* **284**.
- Weigert, M., Ross-Gillespie, A., Leinweber, A., Pessi, G., Brown, S.P., and Kummerli, R. (2017) Manipulating virulence factor availability can have complex consequences for infections. *Evol Appl* **10**: 91-101.
- West, S.A., and Buckling, A. (2003) Cooperation, virulence and siderophore production in bacterial parasites. *Proceedings. Biological sciences / The Royal Society* **270**: 37-44.
- West, S.A., and Cooper, G.A. (2016) Division of labour in microorganisms: an evolutionary perspective. *Nat Rev Microbiol* **14**: 716-723.
- West, S.A., Griffin, A.S., Gardner, A., and Diggle, S.P. (2006) Social evolution theory for microorganisms. *Nat Rev Microbiol* **4**: 597-607.
- Wilson, D.S. (1975) A theory of group selection. *Proc Natl Acad Sci U S A* **72**: 143-146.
- Wirth, C., Meyer-Klaucke, W., Pattus, F., and Cobessi, D. (2007) From the periplasmic signaling domain to the extracellular face of an outer membrane signal transducer of *Pseudomonas aeruginosa*: crystal structure of the ferric pyoverdine outer membrane receptor. *J Mol Biol* **368**: 398-406.
- Xavier, J.B. (2011) Social interaction in synthetic and natural microbial communities. *Mol Syst Biol* **7**: 483.
- Xavier, J.B., and Foster, K.R. (2007) Cooperation and conflict in microbial biofilms. *Proc Natl Acad Sci U S A* **104**: 876-881.
- Ye, L., Ballet, S., Hildebrand, F., Laus, G., Guillemyn, K., Raes, J., Matthijs, S., Martins, J., and Cornelis, P. (2013) A combinatorial approach to the structure elucidation of a pyoverdine siderophore produced by a *Pseudomonas putida* isolate and the use of pyoverdine as a taxonomic marker for typing *P. putida* subspecies. *Biometals* **26**: 561-575.
- Yeterian, E., Martin, L.W., Guillon, L., Journet, L., Lamont, I.L., and Schalk, I.J. (2010) Synthesis of the siderophore pyoverdine in *Pseudomonas aeruginosa* involves a periplasmic maturation. *Amino Acids* **38**: 1447-1459.
- Youk, H., and Lim, W.A. (2014) Secreting and sensing the same molecule allows cells to achieve versatile social behaviors. *Science* **343**: 1242782.
- Zhang, X.X., and Rainey, P.B. (2013) Exploring the sociobiology of pyoverdine-producing *Pseudomonas*. *Evolution* **67**: 3161-3174.

## Acknowledgments

It was a long, fruitful and challenging time until my thesis was finished. During this time, there are a lot of people who give me great support and help.

My first and sincere appreciation goes to my supervisor Prof. Dr. Heinrich Jung, for providing me the chance of studying and doing scientific research in his group. I am very thankful for all the nice projects and his continuous encouragement, help and support in all stages of my PhD.

I want to thank Prof. Dr. Erwin Frey, Dr. Karl Wienand and Dr. Matthias Lechner for the good cooperation in this multidisciplinary research project. The meetings were always helpful to learn a lot about theoretical modeling and to bring both biological experiments and theoretical models on one level. And it helped to successfully publish Chapters II and III.

Special thanks go to my thesis committee especially to Prof. Dr. Marc Bramkamp for being the second examiner of this thesis.

Also I gratefully thank the DFG for funding my PhD program and for being part of the excellent SPP1617.

A big thank to Prof. Dr. Heinrich Jung, Dr. Chong Becker and Chip Epstein for critical reading of this thesis. Without them, my thesis would have a much worse language and I am very grateful how much time you all sacrificed.

Next I want to thank the whole AG H. Jung and AG K. Jung, for the nice time together and the interesting scientific meetings every Friday!

Special thanks go to the working group of Heinrich Jung and its lab members. At first a thanks to all my students (Johannes, Julia, Sophia and Ana). You all supported my work excellently, were easily to supervise and the atmosphere in the lab was always great. Also a big thanks to all other lab members (Susi, Ara, Michelle and Kim) for the good atmosphere, the open heart if help is needed and the funny lunch time. The ton of office members (Poldi, Matthias, Elaine, Yang, Bruno, Wolfram, Ivica, Claudia, Lena, Kim and Susi) also a big thanks for the fun in the office. It was always fun to discuss football, cultural differences and nonsense. Last but not least all members of the AG H. Jung and AG K. Jung and people I may have forgotten. Thank you guys, I learnt a lot from all of you and I enjoyed the time with you. I appreciate the help and support from you and I will never forget the time in the lab with you.

Last but not least I want to thank my family, without them I would never have come as far. You are the most important people. I want to thank my parents and two brothers with their families for all the support. It is very sad, that you can only watch the rest of the thesis just from the sky, daddy. And thankful to the time in Munich I met my dear 饜后冲 and her nice friends (你是我的首要人). 我享受我们天天在一起的时间。我爱我的可爱, 漂亮, 亲爱, 勤奋 和小宝贝。我们待在一起永远永远。我亲亲和抱抱你亿万。对不起, 我是一欺凌树袋熊。我非常感谢你的一片盛意, 耐性, 依靠 和爱情。